

**FEATURE EXTRACTION AND CLASSIFICATION
OF ICTAL EEG USING INSTANTANEOUS
AMPLITUDE-FREQUENCY CONTOURS**

A THESIS

Submitted by

BIJU K. S.

Reg. No. 4460

for the award of the degree

of

DOCTOR OF PHILOSOPHY



**DIVISION OF ELECTRONICS ENGINEERING
SCHOOL OF ENGINEERING
COCHIN UNIVERSITY OF SCIENCE AND TECHNOLOGY, KOCHI**

NOVEMBER 2018



**SCHOOL OF ENGINEERING
COCHIN UNIVERSITY OF SCIENCE AND TECHNOLOGY
KOCHI, KERALA**

Dr. Jibukumar M. G.

Ph:+91 9497683331

Professor

email: jibukumar@cusat.ac.in

THESIS CERTIFICATE

This is to certify that the thesis entitled “**FEATURE EXTRACTION AND CLASSIFICATION OF ICTAL EEG USING INSTANTANEOUS AMPLITUDE-FREQUENCY CONTOURS**” submitted by **Mr. Biju K. S.** to the Cochin University of Science and Technology, Kochi for the award of the degree of Doctor of Philosophy is a bonafide record of research work carried out by him under my supervision and guidance at the Division of Electronics, School of Engineering, Cochin University of Science and Technology, Kochi. The contents of this thesis, in full or in parts, have not been submitted to any other University or Institute for the award of any degree or diploma.

I further certify that all the relevant corrections and modifications suggested by the audience during the pre-synopsis seminar and recommended by the Doctoral Committee have been incorporated in the thesis.

Kochi-682 022

Dr. Jibukumar M. G .

Date: 12/11/2018

(Research Guide)

DECLARATION

I hereby declare that the thesis entitled “**FEATURE EXTRACTION AND CLASSIFICATION OF ICTAL EEG USING INSTANTANEOUS AMPLITUDE-FREQUENCY CONTOURS** ” is a bonafide record of the research work carried out by me, under the supervision of Prof. Jibukumar M. G., Electronics and Communication Engineering Division, School of Engineering, Cochin University of Science and Technology, Kochi-22. I further declare that this work has not formed the basis for the award of any other degree, diploma, associateship, fellowship or any other title for recognition.

Kochi

12/11/2019

Biju K. S.

ACKNOWLEDGEMENT

To bring something into existence is truly the work of ALMIGHTY. First, I would like to thank **GOD ALMIGHTY** for giving me strength and confidence to complete the thesis. I take this opportunity to extend my heartfelt thanks to each person who helped me throughout the work.

I am extremely grateful to my guide Dr. Jibukumar M. G., Professor, Division of Electronics, for guiding me in this thesis work. From the conception of the novel idea behind this thesis to the successful completion of the work, his guidance and motivation had ever presented. He has been a wonderful listener to my research woes and his suggestions and advice have been time tested to be the best in most situations.

I would like to express my sincere gratitude towards Dr. Abdulla P., Professor, Division of Electronics and Doctoral committee member for his support and valuable advice. I would like to express my deep gratitude to Dr. George Mathew, Principal, School of Engineering and Dr. M. R. Radhakrishna Panicker, Principal (Former), School of Engineering for giving me the opportunity to submit this thesis as per the schedule.

I would also like to thank Dr. Beena K. S., Dean, Faculty of Engineering and Dr. P. S. Sreejith, Dean (Former) Faculty of Engineering, for valuable guidance, expert advice, suggestions and encouragement. I would like to thank all faculty members and staff of Division of Electronics Engineering, School of Engineering for their support and help during my research.

I am greatly indebted to Dr. C. Rajasekharan, Professor, Government Medical College, Thiruvananthapuram for the valuable support, advice and guidance for choosing the research topic of this thesis.

I would also like to express my sincere thanks to Prof. Cyriac M. Odackal, Research scholar who always showed a deep interest in my work. His comments, critiques and suggestions have helped considerably in the progress of my research. I am indebted to Prof. Girishkumar C., Faculty of Engineering & Computer Technology, AIMST University, Malaysia for his support and valuable advice.

I would like to thank Dr. S. Jayadev, Department of Commerce, Mahatma Gandhi College, Thiruvananthapuram and Dr. Sabu K., Department of Mechanical Engineering, College of Engineering, Thiruvananthapuram for helping the statistical analysis used in this work. I would like to put on record my sincere thanks to Prof. Sangeetha U., Dr. Abhilash Suryan, Dr. Binulal B. R., Prof. Harsha A., and Miss. Nivea Kesav their advice and encouragement throughout the work and in preparation of research articles.

I would like to acknowledge the help extended, Mr. Manoj Kumar K, Scientist-D (CS), INFLIBNET Centre, Gandhinagar for his timely support and suggestions.

Dr. Alexraj S. M, Mrs. Hara A. H. and Dr. Birenjith S. was my colleagues at Government Engineering College, Thiruvananthapuram have been highly accommodating and supportive of my research interests through these years.

I extended my sincere thanks to all my Co-researchers and Colleagues whose constructive criticism and comments have helped me shape this project.

I express special gratitude to my family member and friends, for their cooperation in all measures.

I am so grateful to each person who directly and indirectly helped me in completing the thesis work.

ABSTRACT

Electroencephalogram (EEG) is an important approach in clinical diagnosis and research on human brain activity. The EEG is extremely nonlinear and non-stationary signal. Empirical mode decomposition provides a simpler method for analyzing nonlinear and non-stationary data. The Hilbert-Huang transform provides a very good view of time-frequency-energy representation of signal. The characteristics of instantaneous amplitude function and instantaneous frequency function components of Hilbert-Huang transform gives a new insight of local information about EEG signal. The features extracted from the instantaneous amplitude functions and instantaneous frequency functions are used for effective ictal EEG classification. An ictal characterizes an EEG signal, during the acute epileptic seizure.

The EEG is decomposed into different frequency sub-bands of EEG using wavelet packet transform. The role of each sub-band frequency during the epileptic seizure is analyzed using the feature vectors. Using the empirical mode decomposition method, any non-stationary data is decomposed into a finite number of components, known as intrinsic mode functions (IMF). The effect of ictal classification with multiple features of the individual intrinsic mode functions of both amplitude and frequency contours is analyzed. Also the performance of the ictal classification of the individual features from multiple intrinsic mode functions is then computed. The discriminating capability of ictal EEG and healthy EEG was tested in artificial neural network and adaptive neuro-fuzzy inference system classifiers for three Cases. The classification performance is statistically compared with the analysis of variance test.

The different types of ictal classification can be performed in autoregressive modeling based spectral features and temporal features of

Hilbert-Huang transform twin components. The interictal, ictal and healthy EEG signals are classified in the four Cases by using artificial neural network.

Considering the nonlinear behaviour of the EEG signal, state space modeling of the IMFs of the EEG is carried out. Kalman filter is used to take the state estimations of each IMF. The features of state estimations are used for classify ictal EEG.

Thus, analysis of the characteristics of the instantaneous amplitude function and instantaneous frequency functions of EEG signal is a novel method for ictal classification. The first and second IMFs of instantaneous amplitude - frequency components show relevant information about the ictal EEG, which helps to classify ictal EEG. The proposed method is a simpler and meaningful way to analyze the EEG data compared to other methods.

Keywords: Artificial neural network, Adaptive neuro-fuzzy inference system, Autoregressive model, Empirical mode decomposition, Hilbert–Huang transform, Ictal EEG, Intrinsic mode functions, State space model.

CONTENTS

ACKNOWLEDGEMENTS	i
ABSTRACT.....	iii
TABLE OF CONTENTS	v
LIST OF TABLES	ix
LIST OF FIGURES	xi
ABBREVIATIONS	xv
NOTATIONS.....	xix
CHAPTER 1 INTRODUCTION.....	1
1.1 The Brain.....	1
1.2 The Neuron.....	2
1.3 Action Potential of Cell.....	3
1.4 Electroencephalogram.....	5
1.5 Epilepsy.....	8
1.6 Signal Processing on EEG	12
1.7 Motivation of the Thesis	14
1.8 Objective of the Thesis.....	15
1.9 Highlights of the Thesis	16
1.10 Organization of the Thesis	19
CHAPTER 2 LITERATURE REVIEW.....	21
2.1 Features Extraction.....	22
2.1.1 Time -Frequency Method.....	25
2.1.2 Nonlinear Method	27
2.1.3 Hybrid Techniques	32
2.1.4 Empirical Mode Decomposition Method	34
2.2 Classification.....	37
2.3 Description of the Database	40
2.4 Inferences	42

CHAPTER 3	ANALYSIS OF EPILEPTIC SEIZURE	
	USING WAVELET PACKET TRANSFORM	-----45
3.1	Introduction	-----45
3.2	Wavelet Packet Transform	-----46
3.3	Methodology	-----48
3.4	Feature Extraction	-----49
3.5	Classification	-----51
3.6	Results and Discussion	-----52
3.7	Inferences	-----64
CHAPTER 4	ICTAL EEG ANALYSIS USING HILBERT-	
	HUANG TRANSFORM	-----67
4.1	Introduction	-----67
4.2	The Sifting Process: Extracting the IMFS	-----69
4.2.1	Hilbert-Huang Transform	-----71
4.3	Methodology	-----73
4.4	Feature Extraction	-----74
4.5	Classification	-----76
4.5.1	Performance Evaluation	-----76
4.6	Results and Discussion	-----77
4.7	Inferences	-----91
CHAPTER 5	CLASSIFICATION OF ICTAL USING	
	MODELING BASED SPECTRAL AND TEMPORAL	
	COMPONONTS OF HILBERT-HUANG TRANSFORM	-----93
5.1	Introduction	-----93
5.1.1	Hilbert–Huang Transform	-----94
5.1.2	AR Model Spectra	-----94
5.2	Methodology	-----96
5.3	Feature Extraction	-----97
5.4	Classifier	-----99
5.5	Results and Discussion	-----100
5.6	Inferences	-----116

CHAPTER 6	ICTAL EEG CLASSIFICATION BASED ON STATE SPACE MODELING OF IMF SIGNAL	117
6.1	Introduction	117
6.2	Methodology	118
6.3	Estimation of State Space Model	118
6.4	Feature Extraction	122
6.5	Results and Discussion	124
6.7	Inferences	134
CHAPTER 7	CONCLUSION	135
7.1	Contribution of the Thesis	135
7.1.1	EEG analysis using wavelet packet transform for epileptic seizure detection	135
7.1.2	Energy-Entropy feature extraction of the instantaneous amplitude function and statistical features of the instantaneous frequency function for ictal EEG classification	136
7.1.3	Different types of ictal classification on spectral and temporal features of instantaneous amplitude -frequency components	137
7.1.4	Ictal EEG classification based on state space modeling of intrinsic mode function	138
7.2	Future Scope of Work	140
REFERENCES		
LIST OF PUBLICATIONS BASED ON THESIS		
CURRICULUM VITAE		

LIST OF TABLES

Table	Title	Page No
Table 3.1	Training error for 500 epoch of EEG sub-bands -----	56
Table 3.2	Comparison with other methods in wavelet features for EEG classification -----	61
Table 4.1	Basic equation of energy, entropy and statistical parameters -----	75
Table 4.2	Statistical analysis of different individual IMF features-----	85
Table 4.3	Statistical analysis of multiple features with individual IMFs----	86
Table 4.4	Statistical analysis of Individual features from multiple IMFs---	86
Table 4.5	Accuracy (%) for Case1: Single features for individual IMFs ---	88
Table 4.6	Sensitivity (%) for Case1: Single features for individual IMFs -----	88
Table 4.7	Specificity (%) for Case1: Single features for individual IMFs--	89
Table 4.8	Classification for Case 2: Multiple features with individual IMFs-----	89
Table 4.9	Classification for Case 3: Individual features from multiple IMFs -----	90
Table 4.10	Comparison with other ictal classification algorithms in the literature -----	91
Table 5.1	Spectral features and temporal features in this study -----	98
Table 5.2	Statistical analysis of one- way ANOVA in Case 1: normal-ictal EEG class -----	108
Table 5.3	Statistical analysis of one- way ANOVA in Case 2: normal-interictal EEG class -----	110
Table 5.4	Statistical analysis of one- way ANOVA in Case 3: interictal-ictal EEG class-----	111
Table 5.5	Performance measures of Spectral features of IA and temporal features of IF -----	114
Table 5.6	Performance measures of Spectral features of IA and temporal features of IA-----	114

Table 5.7	Comparison with other AR modeling of EEG signal in the literature using the EEG data set -----	115
Table 6.1	Relevant mathematical expressions of different features for computation -----	124
Table 6.2	Classifier performance for different features -----	129
Table 6.3	Classifier performance for different combination of features -----	132
Table 6.4	Comparison with other algorithms in the literature using the EEG data set -----	133

LIST OF FIGURES

Figure	Title	Page No
Fig. 1.1	Structure of neuron -----	2
Fig. 1.2	Action potential of a cell-----	4
Fig. 1.3	10–20 International EEG Electrode Placement-----	6
Fig. 1.4	Frequency rhythms of EEG signal-----	7
Fig. 1.5	Clinical classifications of seizures-----	10
Fig. 1.6	Preictal, ictal and interictal stages in EEG recording of a patient -----	11
Fig. 1.7	Basic block diagram for EEG signal processing and analysis -----	12
Fig. 3.1	Tree structure of Wavelet packet Transform-----	48
Fig. 3.2	Signal flow diagram of the epileptic detection system-----	49
Fig. 3.3	Healthy EEG and abnormal EEG Signal in the EEG database -----	53
Fig. 3.4	Feature extraction of delta band in the healthy EEG signal-----	54
Fig. 3.5	Feature extraction of delta band in the abnormal EEG signal -----	54
Fig. 3.6	Feature extraction of theta band in the healthy EEG signal-----	55
Fig. 3.7	Feature extraction of theta band in the abnormal EEG signal -----	55
Fig. 3.8	Training error of mean Teager energy on the delta band in ANFIS editor-----	57
Fig. 3.9	Training data and average testing error of mean Teager energy on the delta band-----	58

Fig. 3.10	Testing data and FIS output of mean Teager energy on the delta band -----	58
Fig. 3.11	Training data and average testing error of all features in the delta band-----	59
Fig. 3.12	Testing data and FIS output for all features in the delta band -----	60
Fig. 3.13	Different feature parameters of healthy and abnormal EEG in different EEG sub-bands of channel T7-P7 -----	62
Fig. 3.14	Different feature parameters of healthy and abnormal EEG in different EEG sub-bands of channel T8-P8 -----	62
Fig. 4.1	Envelop $x_{upper}(t)$ and $x_{lower}(t)$ -----	70
Fig. 4.2	Compute the mean of $x_{upper}(t)$ and $x_{lower}(t)$ -----	70
Fig. 4.3	Extract the first IMF -----	71
Fig. 4.4	Proposed Methodology-----	74
Fig. 4.5	IMFs of healthy EEG -----	79
Fig. 4.6	IMFs of ictal EEG-----	79
Fig. 4.7(a) & (b)	Hilbert–amplitude spectrum for healthy and ictal EEG -----	81
Fig. 4.8	Mean and standard deviation of feature from amplitude function -----	83
Fig. 4.9 (a)	Mean and standard deviation of interquartile range feature from frequency function -----	83
Fig. 4.9 (b)	Mean and standard deviation of mean absolute deviation feature from frequency function -----	83
Fig. 4.9 (c)	Mean and standard deviation of standard deviation feature from frequency function -----	84

Fig. 5.1	Illustrations of the proposed method for ictal classification based on spectral and temporal features of amplitude –frequency contour of HHT-----	96
Fig. 5.2 (a)	Plots of IF1 and IF2 of normal EEG -----	102
Fig. 5.2 (b)	Plots of IF1 and IF2 of interictal EEG-----	102
Fig. 5.2 (c)	Plots of IF1 and IF2 of ictal EEG -----	102
Fig. 5.3 (a)	Plots of IA1 and PSD signals of IA1 in normal EEG -----	103
Fig. 5.3 (b)	Plots of IA1 and PSD signals of IA1 in interictal EEG -----	104
Fig. 5.3 (c)	Plots of IA1 and PSD signals of IA1 in ictal EEG -----	104
Fig. 5.4 (a)	Plots of IA2 and PSD signals of IA2 in normal EEG -----	104
Fig. 5.4 (b)	Plots of IA2 and PSD signals of IA2 in interictal EEG -----	105
Fig. 5.4 (c)	Plots of IA2 and PSD signals of IA2 in ictal EEG -----	105
Fig. 5.5	Mean and standard deviation of (a) spectral peak (b) spectral mean energy (c) spectral Teager energy (d) spectral entropy -----	106
Fig. 5.6	Mean and standard deviation of (a) coefficient of variation (b) skewness (c) Kurtosis (d) interquartile range -----	107
Fig. 6.1	Functional diagram of the proposed -----	118
Fig. 6.2	Healthy EEG signal and its IMFs -----	125
Fig. 6.3	Epileptic EEG signal and its IMFs -----	125
Fig. 6.4	Mean Teager energy of state values of healthy datasets for different IMFs -----	127
Fig. 6.5	Mean Teager energy of state values of ictal datasets for different IMFs -----	127

Fig. 6.6	Confusion matrix and ROC curve of ANN classifier with Kurtosis-standard deviation features -----	130
Fig. 6.7	Confusion matrix and ROC curve of ANN classifier with Approximate entropy-Sample entropy features -----	131
Fig. 6.8	Confusion matrix and ROC curve of ANN classifier with Interquartile range - Mean absolute deviation features -----	131
Fig. 6.9	Confusion matrix and ROC curve of ANN classifier with Mean energy - Mean Teager energy features -----	132

ABBREVIATIONS

AEM	Antiepileptic medicine
ANFIS	Adaptive Neuro-Fuzzy Inference System
ANN	Artificial Neural Network
ANOVA	Analysis of Variance
ApEn	Approximate Entropy
AR	Autoregressive
BPNN	Back Propagation Neural Network
CHB	Children's Hospital Boston
Chb01	CHB EEG data set
CPR	Probabilities of Recurrence
CV	Coefficient Variation
CWT	Continuous Wavelet Transform
DWT	Discrete Wavelet Transforms
E	Energy
ECoG	Electrocorticography
EEG	Electroencephalogram
EMD	Empirical Mode Decomposition
En	Entropy
FFT	Fast Fourier Transform
FIS	Fuzzy Inference System
Fig.	Figure
FN	False Negative
FP	False Positive
FPR	False Positive Rate
F-Rank	Feature ranking
GUI	Graphical user interface
HHT	Hilbert - Huang Transform
HOS	Higher Order Statistics

HT	Hilbert Transform
Hz	Hertz
IA	Instantaneous Amplitude
IF	Instantaneous Frequency
IMF	Intrinsic Mode Functions
IQR	Inter Quartile Range
K_U	Kurtosis
LE	Lyapunov Exponent
MA	Mean Autocorrelation
MAD	Mean Absolute Deviation
ME	Mean Energy
MEG	Magneto Encephalography
MhGAP	Mental Health Gap Action Program
MIT	Massachusetts Institute of Technology
MTE	Mean Teager Energy
MVAR	Multivariate Autoregressive
PSD	Power Spectral Density
ROC	Receiver Operating Characteristics
RQA	Recurrence Quantification Analysis
S_{En}	Spectral Entropy
S_K	Skewness
S_{ME}	Spectral Mean Energy
S_P	Spectral Peak
SpEn	Sample Entropy
SSMC	Cauchy Observation Noise
STD	Standard Deviation
STE	Spectral Mean Teager Energy
SVD	Singular Value Decomposition
TFP	Time- Frequency Plane
TLE	Temporal Lobe Epilepsy

TN	True Negative
TP	True Positive
TPR	True Positive Rate
V	Variance
VMD	Variational Mode Decomposition
WHO	World Health Organization
WPT	Wavelet Packet Transform
WT	Wavelet Transform
acc	Accuracy
anfisedit	ANFIS tool
db	Daubechies Wavelet
edf	European data format
eds.	Editors
et al.	And others
fMRI	Functional Magnetic Resonance Imaging
iEEG	Intracranial EEG
max	Maximum
sen	Sensitivity
sig	Significant level
spe	Specificity
std	Standard deviation
trimf	Triangular function
w.r.t	With respect to

NOTATIONS

English Symbols

$A(i)$	AR coefficients
$z_k(t)$	Analytical function of $x_k(t)$
$\hat{e}_{b,p}$	Backward prediction error
Ca^+	Calcium
$A_i^m(r), B_i^m(r)$	Correlation integral
$x(k), x(n)$	Discrete signal
$E(X)$	Expectation of a random variable X
f	EEG frequency
P_k^-	Priori error covariance
P_k	Posteriori error covariance
$e(k)$	Error signal
$\hat{x}(k)$	Estimated signal
$\hat{e}_{f,p}$	Forward prediction error
$\hat{v}(t)$	Hilbert transform
$H(\omega, t)$	Hilbert Spectrum
K_k	Kalman gain
\hat{e}_p	Least-square error
$h(\omega)$	Marginal spectrum
\bar{x}	Mean of sample
z_k	Measurement data
ms	Millisecond
mV	Millivolt
u_k	Optional control
$c_k(t)$	IMF components
$a_k(t)$	Instantaneous amplitude of $x_k(t)$
$x_{lower}(t)$	Local minima
$x_{upper}(t)$	Local maxima

p_k	Probability of the datum being in bin k.
p_{xx}	Power spectral density
N	Population size
K^+	Potassium ions
\hat{y}_k^-	Priori state estimator
\hat{y}_k	Posteriori state estimator
p	Probability measures
$g(k), h(k)$	Quadrature mirror filters
Q_k	K^{th} quartile
$r_1(t)$	Residual signal
L	Sample length
n	Sample size
a	Scaling parameter
b	Shifting parameter
Na^+	Sodium ions
Q	State noise covariance
y_k	State of process
S_t	Temporal signal
T7-P7/ T8-P8	Temporal – parietal leads
$W_{j,k}^n$	Wavelet packet transform
w, v	White random variables

Greek Symbols

α	Alpha frequency band
β	Beta frequency band
δ	Delta frequency band
ω	Digital frequency
γ	Gamma frequency band
$\omega_k(t)$	Instantaneous frequency of $x_k(t)$

$\theta_k(t)$	Instantaneous phase of $x_k(t)$
μV	Microvolt
ε_k	Error due to white noise
Ωm	Resistivity
$\phi(t)$	Scaling function of WPT
$\varphi(t)$	Shifting function of WPT
σ	Standard deviation
τ	Time constant
σ^2	Variance
$\psi(t)$	Wavelet function

Miscellaneous Symbol

*	Linear convolution
---	--------------------

CHAPTER 1

INTRODUCTION

Biosignal processing and analysis is an emerging field of immense influence in modern medical diagnosis. In recent years, the Engineers have developed many algorithms and processing techniques in order to help medical practitioners in the evaluation of diagnosis in fast and accurate manner. New set of information is revealed by using these techniques and methodologies in biosignals, which are not easily observable in the raw data. This vital information is very useful for properly diagnosing the diseases.

1.1 THE BRAIN

The human body is one of the most perfect imaginable creations. It is controlled by the brain. The efficiency of the human body in achieving the assigned tasks is directly related to the capability of the human brain. The largest part of the brain is the cerebrum. The outermost layer is the cerebral cortex, which is integrated with large number of nervous functions. The posterior part of the cerebral cortex is dealing with the perception of the environment and anterior part is dealing with the execution of the decision-making in the brain (Kasper *et al.* 2015).

The cerebrum is divided into left hemispheres and the right hemisphere. Each cerebral hemisphere is divided into four major functional lobes, which are frontal, parietal, temporal and occipital lobes. Each lobe is concerned with sensation of vision, sound, smell, taste and touch, etc. The frontal lobes consist of primary motor cortex which controls the voluntary movements of specific body parts. The pre-frontal cortex deals with the mental processes such as intelligence, memory, judgement, etc. The temporal lobe consists of the auditory sensory area. The parietal lobes interpret size, shape, texture and touch sensation. The occipital lobe region realizes the vision

(Walker and Colledge, 2013). So whatever happened into the body will reflect in the functional lobes. This will help the diagnosis of many neurological disorders and other abnormal activities in the human body.

1.2 THE NEURON

The fundamental unit of the nervous system is the neuron. The neuron is a single nerve cell consisting of a cell body (soma). The nucleus, which is the heart of the cell contains hereditary information. The Figure 1.1 shows the structure of neuron. The several short input projections known as dendrites and long propagation channel called axons. The axon together with its myelin sheath covering forms the nerve fibres.

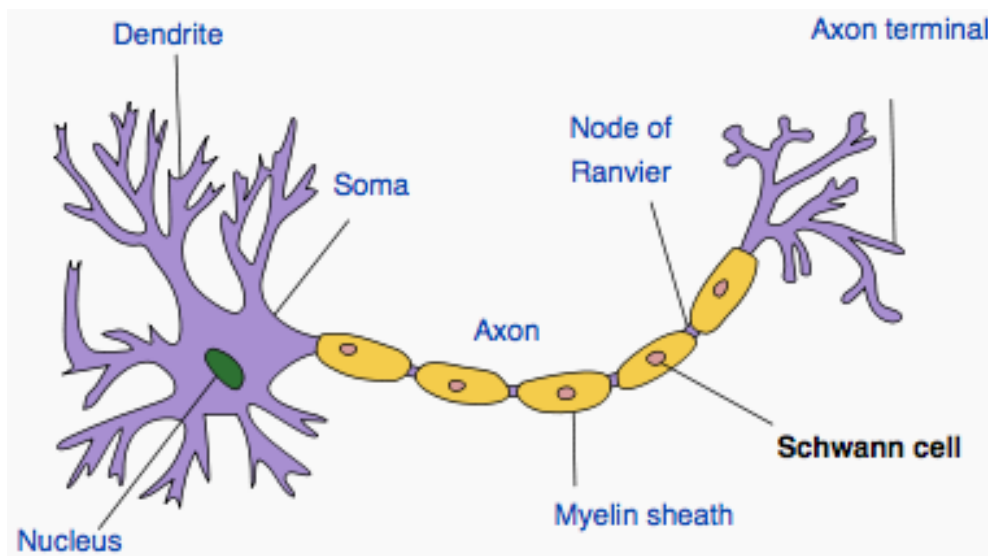


Fig.1.1 Structure of neuron

The dendrites are connected to either its axon or to the dendrites of other cells. It receives impulses from the nerves or relay the signal to other nerves. The nervous system is a complex system. It can be divided into the central nervous system, which is the master controller and peripheral nervous

system, which interconnect brain to every part of the body (Kasper *et al.* 2015).

1.3 ACTION POTENTIAL OF CELL

The information transmitted through a nerve is called action potential. The action potential is caused by an exchange of ions across the neuron membranes. The action potential is a temporary charge in the membrane, which is transmitted along the axon. Normally a potential of -70 to -60 mV is generated within the cell body with respect to extra cellular fluid, called resting potential. The Figure 1.2 illustrated the action potential of a cell.

When the dendrites of nerve cell receive a stimulus, the characteristic of cell membrane is changed. It allows the Na^+ ions, (which concentrate outside the cell) move into the cell from outside through voltage gated Na^+ channels. The K^+ ions, which concentrate inside the cell moves from inside to outside through the voltage gated K^+ channel. The rate of flow of Na^+ ions is faster as Na^+ channels open and close faster than K^+ channels. Now the equilibrium potential across the cell membrane becomes +30 mV. This potential generated is called an action potential. This process is called depolarization. The site of generation of the action potential is the initial segment in a spinal motor neuron and the initial node of receiver in a sensory neuron as these are the area with the highest concentration of Na^+ channel.

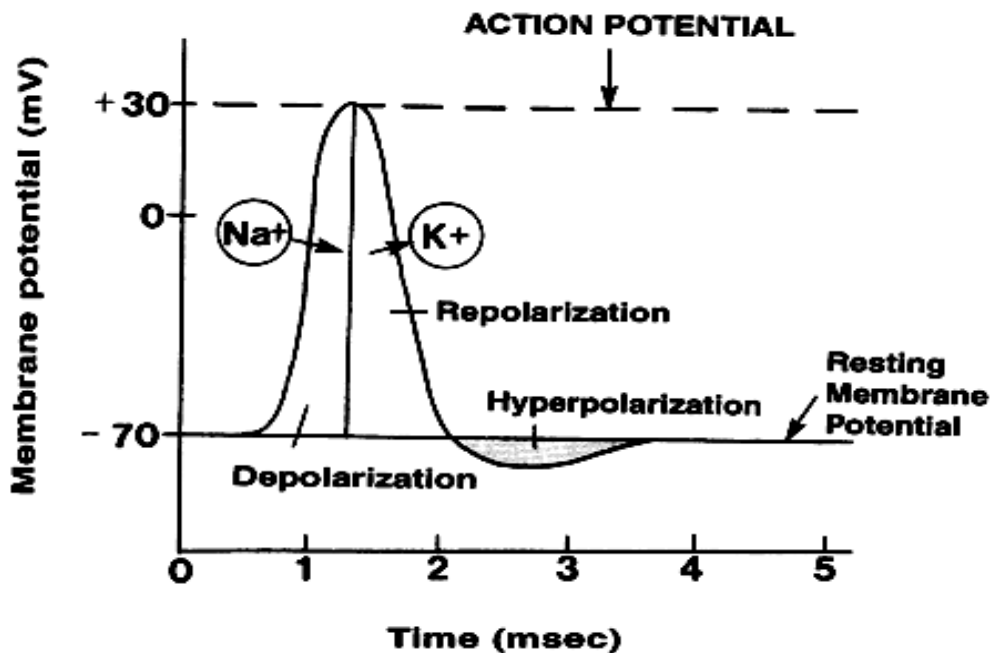


Fig. 1.2 Action potential of a cell

After an instant because of Na^+/K^+ ions pumping action, all the Na^+ ions inside are pumped out and K^+ ions are allowed to enter into the cell. This process is called repolarization. Now the cell returns to its resting potential. After hyperpolarization of Na^+/K^+ pump, membrane regains its resting state of -70mV potential. The duration during which the nerve does not respond to a second stimulus is called the refractory period. The absolute refractory period is during which no response occurs irrespective of strength of stimulus. This is from the firing level until the one-third completion of repolarisation. The relative refractory period is during which a response is produced if second stimulus is stronger than the first one. The relative refractory period is from one-third completion of repolarisation to the end of hyperpolarisation. The action potentials are initiated by many different types of stimuli, such as chemical, light, electricity, pressure, heat, touch, etc. But the nerves within the central nervous system (brain and spinal cord) are mostly stimulated by chemical activities at synapses.

1.4 ELECTROENCEPHALOGRAM

The electroencephalogram (EEG) has been the most commonly used biosignal for clinical evaluation of electrical activity of the brain. In 1924 Han Berger, a German psychiatrist and pioneer brain researcher succeeded in recording the human EEG (Tudor *et al.* 2005). The word electro means electrical activities, *encephalo* from Greek word *enkephalos*, *en* means in and *kephalte* means head (Collins, 2000). The EEG signal is inherently complicated due to their non-Gaussian, non-stationary, and often nonlinear nature. The study of this electrical current can provide information about various neurological disorders and other abnormalities in humans.

The EEG signal is recorded in two ways, non-invasive method and invasive method. In non-invasive method signal is recorded by placing electrodes on the scalp of the brain, called scalp EEG. The limitation of the scalp EEG is that the strength of EEG is very low in the order of 10-100 μV . This is because of the high skull-scalp resistance. Normally resistivity scale of scalp has 2.2 Ωm and skull has 177 Ωm . Even skull can attenuate biosignal to one hundred times than the skin tissue. Prior to that very weak amplitude of these biosignals are sensitive to different type of artifacts.

In invasive method of EEG recording, a needle electrode is penetrating to a certain depth or implanted strip of electrodes into the brain. This type of recording is called ECoG (Electrocorticography) or iEEG (intracranial EEG). In ECoG, signal strength is improved and clarity is more compared to scalp EEG because the microelectrode is penetrated into foci. The main limitations of iEEG are the positioning of needle electrode to the target in the brain. Normally iEEG is collected from a patient suffering from medically intractable epilepsy. So the availability of data of iEEG samples are very less (Lachaux *et al.* 2003).

The brain activities can also be recorded and analysed by magnetoencephalography (MEG) or functional magnetic resonance Imaging (fMRI) techniques. The accessibility to fMRI or MEG is limited and it is more expensive. Main drawback of MEG is that those who capture magnetics image should not wear any implantable materials. The magnetic resonance imaging only gives perception of the blood flow during the specific activity in the brain. However, fMRI gets better soft tissue imaging. The time resolution of fMRI image sequence is very low and many types of mental exertion, brain disorder and malfunction of brain are not identified in imaging, since level of oxygenated blood is low (Amaro and Barker, 2006). The spatial resolution depends on the number of turns of the coil in MEG. Hence, the scalp EEG is more commonly used in both clinical and research purposes.

The electrodes are distributed symmetrically around the scalp as shown in Figure 1.3. The Internationally accepted 10-20 electrode system for EEG provided a temporal and spectral summary of brain wave activities (Klem et al. 1999). Each electrode responds to the aggregate potential generated by many neurons in the area beneath it. In most clinical and research activities 19 electrodes including reference node (A1, A2) are used for EEG recording. Normally amplitude range of scalp EEG is between 10 μ V -100 μ V with a frequency band of 0.5Hz to 100 Hz (Alotaiby et al. 2014).

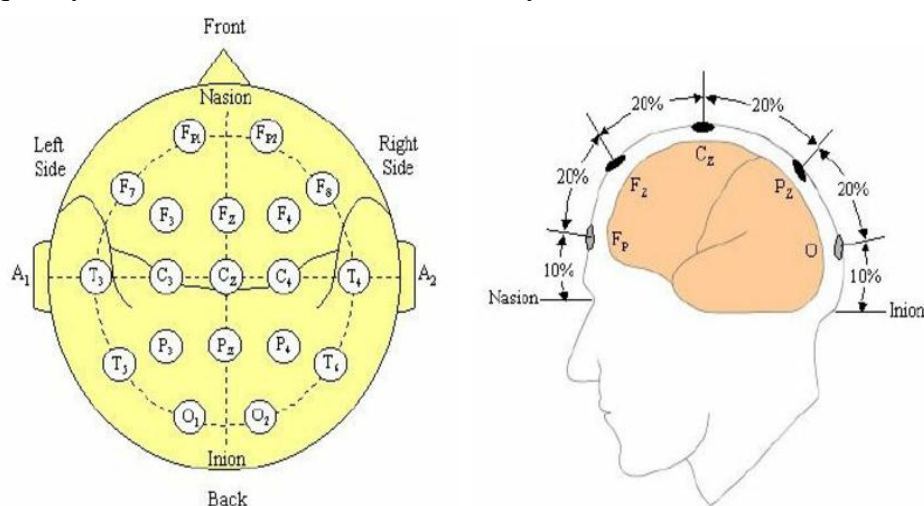


Fig. 1.3 10–20 EEG electrode placement system

Three major types of EEG channels that are being used (i) differential mode (ii) average mode and (iii) unipolar mode. The differential mode is commonly used, which are the differential of any two electrodes on the scalp. In average mode, a random electrode records the average of all nodes on the scalp. In a unipolar lead, any node is recording with respected to reference node.

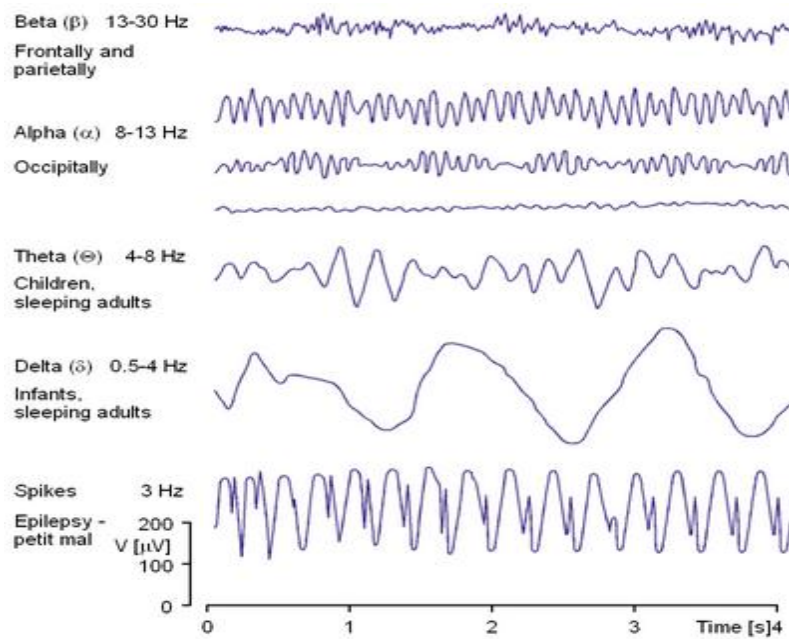


Fig. 1.4 Frequency rhythms of EEG signal (Jaakko, M. and Robert, 1995)

The EEG signal depends on the functionality of the brain. The EEG rhythms are different phenomena or events in the EEG. The commonly used EEG frequency (f) bands are normally classified into *delta* (δ), *theta* (θ), *alpha* (α), *beta* (β) and *gamma* (γ). The Figure 1.4 shows the frequency rhythms of EEG signals.

$$\text{delta } (\delta) : 0.5 \leq f < 4\text{Hz}$$

$$\text{theta } (\theta) : 4 \leq f < 8\text{Hz}$$

$$\text{alpha } (\alpha) : 8 \leq f < 13\text{Hz}$$

$$\text{beta } (\beta) : 13 \leq f < 30\text{Hz}$$

$$\text{gamma } (\gamma) : 30\text{Hz} < f$$

The brain signals are highly complex in nature. The characteristics of EEG signal are nonlinear and non-stationary. The EEG signals are strongly depending on the individual, age and mental state. The occurrence of the symptoms is also random in person by person. The brain reacts differently at different stages of time and hence the brain signals will be different accordingly. Hence it is difficult to get more information about the abnormalities or disorders of brain from raw EEG. But the detailed study of frequency rhythms of EEG signal are used to (i) help in detecting and localizing cerebral brain lesions, (ii) aid in studying epilepsy, (iii) used in diagnosing mental disorders, (iv) assist in studying sleep patterns and (v) allow observation and analysis of brain responses to sensory stimuli.

1.5 EPILEPSY

Epilepsy or Apasmara described in the hand book of the Ayurvedic, is defined as state of consciousness loss (Dash and Jounious, 1997). The word Epilepsy is originated from Greek word *epilambanein*, which has a meaning of ‘to attack’ or ‘to seize upon’ (Tudor *et al.* 2015). A seizure is defined as the occurrence of sign and/or symptoms due to abnormal excessive or hyper synchronous discharge from the neurons in the brain. Epilepsy is two or more unprovoked seizure episodes over duration of 24 hours (Walker and Colledge, 2013).

Approximately 1-2% of world population have epileptic disorder. Epilepsy is chronic non-contagious neurological disorder that affects people of all countries irrespective of age or gender (Megiddo *et al.*, 2016). In the Indian perceptible about 10 million epilepsy patients are there in the Indian subcontinent (Santhosh *et al.*, 2014). Many people in India who have an active epileptic disorder due to lack of knowledge and lack of access of health care facilities are away from the statistics. This phenomenon is called treatment gap in epilepsy. About 60% of epileptic disorders have an etiology. The rest

40%, also known as secondary epilepsy can be due to metabolic disturbances like hypoglycemia, alcohol withdrawal, trauma like severe head injury, brain tumour, infection such as meningitis, presence of toxins, brain damage due to lack of oxygen etc. (Kasper *et al.* 2015). The epilepsy is sometimes misleading as a migraine or a headache.

Clinically, seizure of different epilepsies varies. It occurs in an unprovoked manner and is usually unpredictable, which may last for about a few seconds to minutes. Common symptoms of all seizures are loss or impairment of consciousness. Typically epileptic seizures are strongly correlated with abnormal brain rhythms. The healthy brain activity is interrupted and a characteristic abnormal rhythm appears. This epileptic brain rhythm is considered as an important indicator for epilepsy and is used for further diagnosis. The characteristic of an epileptic seizure is determined based on the abnormal pattern of discharge in the region of the brain with underlying the condition or syndrome. The physiology of epilepsy can be explained by the imbalance between the excitatory and inhibitory neurotransmitters in the brain. There is a fall in the inhibitory neurotransmitters gamma-aminobutyric acid (GABA) which causes an increase in the influx of Ca^{2+} ions followed by Na^{+} ions into the nerve fibre which acts as the primary trigger for the seizure.

The epileptic seizures are clinically classified as generalized seizures and partial or focal seizures. The focal seizure originates as a paroxysmal discharge in a discrete area of the cerebral cortex (often the temporal lobes). Then it is subsequently spread to the rest of the brain, called focal seizure with secondary generalization via diencephalic activity pathways. The Figure 1.5 shows the clinical classification of seizures (Kasper *et al.* 2015). It may or may not impair consciousness. After that, the person may or may not feel a drowsing period, which lasts between 1-3 minutes. Individuals typically experience simple partial seizures for less than a minute, and are able to recall

events that occurred during the episode. The complex partial seizures are often preceded by an aura and include automatisms such as fumbling, lip smacking, picking cloth etc.

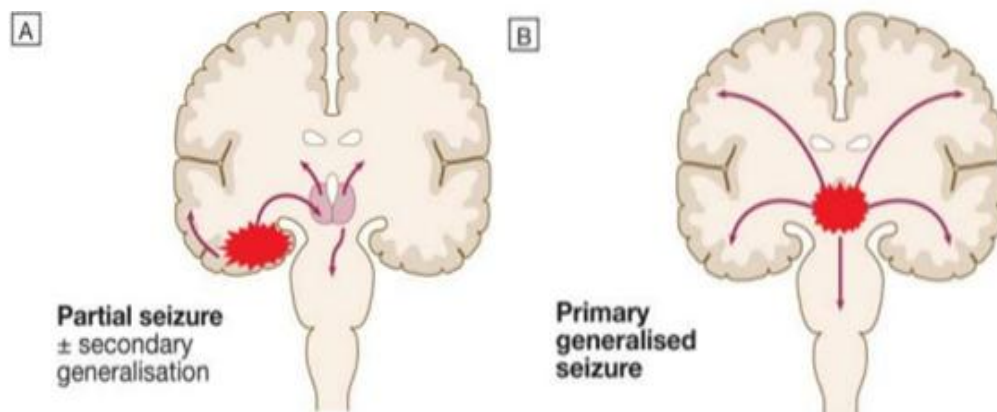


Fig. 1.5 Clinical classification of seizures

In a primary generalized seizure, the abnormal electrical discharge originates from the diencephalic activity system and spread simultaneously to all areas of the cortex. It may cause loss of consciousness and/or muscle contraction or stiffness. The generalized convulsive seizures are further classified into the tonic-clonic seizure, absence seizure and myoclonic seizure. This classification is based on the characterization of seizure that has occurred. Generalised tonic-clonic seizure is almost always accompanied by an aura which would be either olfactory (medial temporal lobe lesions) or auditory (lateral temporal lobe lesions) or sensory (occipital lobe) hallucinations. This is followed by an increase in tone of the body (tonic phase) and jerkiness of the body (clonic phase) accompanied by up rolling of eyes and frothing from the mouth.

Ictal is the characterization by due to an acute epileptic seizure (Mula and Monaco, 2011). The word 'ictal' originates from the Latin word *ictus*, meaning 'a blow' or 'sudden attack'. So an EEG signal during a seizure is called ictal. There are different classes of ictal. The symptoms preceded to seizure events are called preictal and symptoms followed by seizure events are

called post-ictal. The EEG signal in between two ictal events is called inter-ictal. The Figure 1.6 illustrates the different ictal stages in the EEG signal.

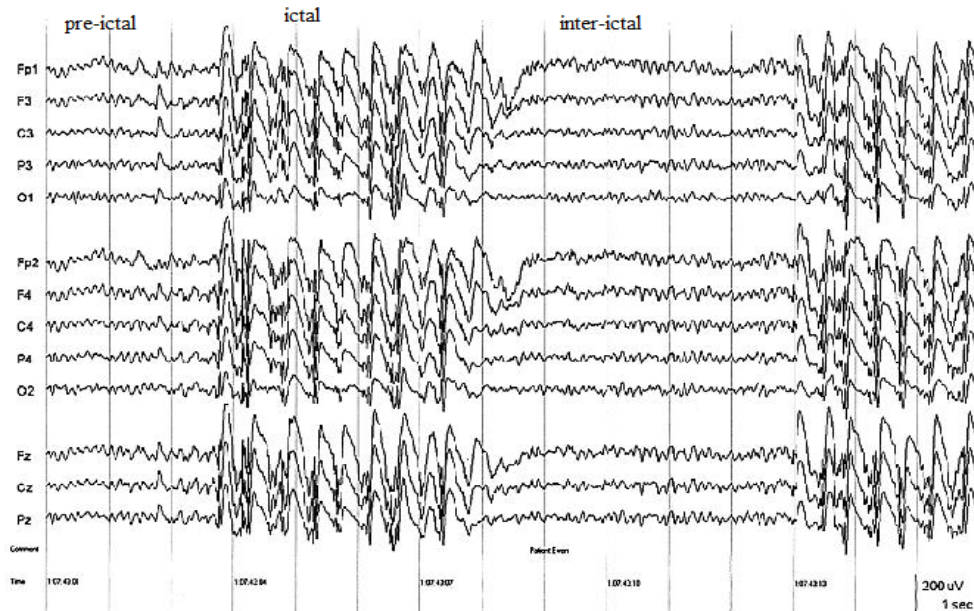


Fig. 1.6 Preictal, ictal and interictal stages in EEG recording of a patient (Casaubon *et al.* 2003)

Unique characterizations of complex wave patterns are observed in EEG during the epileptiform discharge. These wave patterns are sharp wave, spike wave slow wave or polyphase pattern of spike and slow wave (Janati *et al.* 2016). The duration of volatile sharp wave has 70 to 200ms, spike wave has less than 70ms and slow wave is greater than 20ms. The epileptiform discharge comprises a less than or equal to 3Hz, slow wave or a combination of sharp and slow wave. The 3Hz slow wave pattern has higher magnitude than the sharp wave pattern. The observation and characterization of these patterns will help in confirming the diagnosis of true seizure episodes.

The exposures to intermittent photonic stimulus, hyperventilation activity or auditory stimulus were used to increase the epileptiform discharge (Xue and Ritaccio, 2006). The epileptiform discharge consists of spike wave

and sharp wave, which are the the characteristics of epilepsy. The epileptiform discharge can be recorded and analysed using EEG.

1.6 SIGNAL PROCESSING OF EEG

For an EEG signal analysis, the local information is very important. Essentially, a post processing technique is used in EEG analysis. This local information is not only in the temporal domain, but also in the spatial domain. We cannot neglect or eliminate the crest and trough of each signal. Each crest and or trough of the brain wave implies some information about the brain. Therefore the EEG signal processing method is the key to determine whether the physiological or pathological information of EEG can be accurately reflected. Advanced signal processing techniques are required to efficiently detect and analyse the brain waves. A precise characterization of the abnormal EEG pattern can lead to a clearer view of many diseases. The Figure 1.7 shows block diagram for EEG signal processing and analysis.

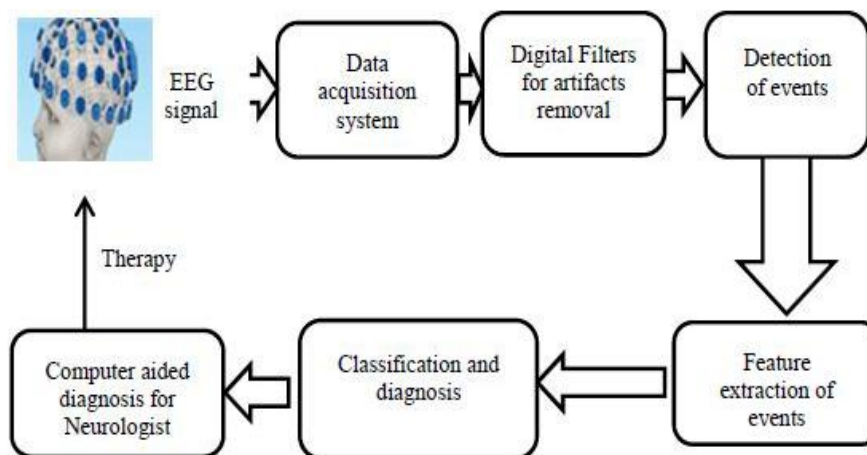


Fig. 1.7 Basic block diagram for EEG signal processing and analysis

The above block diagram shows the computer aided diagnosis or therapy based signal processing. The biosignal processing is used to extract valuable information from physiological data. The data will give the state of the art of the patients, which provide better diagnosis of diseases. In general the entire system

can be divided into digital data acquisition, signal processing unit and signal analysis section.

The physiological signal collected from the patient is converted into an electrical quantity with help of EEG electrode placed on scalp. The scalp recorded signal consists of mixture of brain signal with lots of noise. In the digital data acquisition system, the weak signal is properly amplified and signal conditioning circuit are incorporated to reduce the noise. Then the pre-processed signal is properly sampled and encoded into a digital signal using analog to digital converter. The EEG signal is very weak in the order of μV also bounded with artifacts. The artifacts are undesirable electrical potentials, which are generated by the other part of body along with the brain waves. The noise and artifacts are effectively suppressed in the digital domain by using different algorithms, which improve the interpretation of EEG signals.

A Neurodiagnostic technologist monitors the behaviour of the EEG signal and identified the abnormality of the signal. In the signal processing unit, the events are characterized or features have to be extracted into a set of parameters, which are the functions of state of the art of the brain. The feature parameters are the low dimension data capable of handling by the unsupervised learning techniques. The machine learning algorithms are employed for classifying the feature vectors according to the status of the events. This will help the Neurologist to catch deep insight of the diagnosis and prescribe better therapy to the patients. The advanced signal processing techniques are widely applied and proved to be beneficial in improving both clinical aspects and experimental studies for detection, perception, diagnosis and medication of vast neurological abnormality of the brain. The detailed explanation of advancements in EEG signal processing is explained in the next chapter. Advancements in biosignal processing improve the life expectancy of human beings.

1.7 MOTIVATION OF THE THESIS

All over the world, the epileptic patients suffer to get timely and right treatment. The Mental Health Gap Action Programme (mhGAP) is a programme initiated by World Health Organization (WHO), for epileptic patients (WHO, 2012). The aim of this programme is to reduce the treatment gap in diagnosis epileptic patients. In India, the Ministry of Health and Family Welfare has proposed a National Epilepsy Programme to reduce the discrimination and social stigma towards the epilepsy and ensured better care of the epileptic patients (Megiddo *et al.*, 2016). The social stigma towards the epilepsy is disclosures of personal details of the patients which encompasses feelings of isolation, shame and also fear to reveal the presence of epilepsy. The major challenges of these projects are lack of skilled Neurodiagnostic technologists to diagnose the epilepsy in earlier stages from EEG. Traditionally EEG recording is a widely used clinical procedure for the diagnosis and treatment of epilepsy. It can be used for monitoring and diagnosing the abnormalities of brain and neurological disorders. The EEG is also cheaper and has easy mobility to reach patients than MEG type diagnosis.

At present, visual screening method is used for detecting and classifying epileptiform discharges in EEG by Neurodiagnostic technologists. The accuracy and reliability of visual interpretation of the brain signal are limited. In the physical analysis, there are limitations for extracting certain features from EEG. Moreover, in the visual screening method, the human eye can only interpret and / or concentrate on perceptibly leading features. But in long period, observations of features in EEG are skipped or avoided due to difficulty to interpret and tackle. Also, for long time analysis, the physical interpretation of EEG wave become meaningless because of the dullness of Neuro-diagnostic technologist and the biased determination will affect the diagnosis of abnormalities in the brain. The decision making is depended on

person even though they are professional expertise or skilled Neuro-diagnostic technologists, sometimes, due to biased determination.

Therefore, the development of an accurate automatic epileptic detection is necessary. In addition, analysis and classification of different ictal stages in EEG is also important.

1.8 OBJECTIVE OF THE THESIS

The main objective of our work is to develop a methodology for distinguishing the ictal stages in the EEG. We concentrated on the following areas to narrow down this broad objective.

1. EEG recording and analysis is much developed in clinical, experimental setup of a real problem and/or pure computational study. The main objective of our work is to propose an effective method to improve the computer aided diagnosis system of ictal events in the EEG. This improves the development of both diagnosis and better treatment for patients with minimum cost. This will help to reduce the effort of Neurodiagnostic technologists for diagnosing the epilepsy pattern in EEG signal.
2. The EEG signal is highly non-stationary and has a nonlinear behaviour due to the effect of the underlying dynamics of brain activities. Most of the EEG signal processing techniques for analysis are considers the EEG as a wide sense stationary signal. The non-stationary and nonlinear signal analysis efficiently uses empirical mode decomposition method. The ictal is a change in the characterization of EEG signal due to elliptic seizure. Our objective is to propose ictal classification in an empirical mode decomposition domain. Then the analysis and classification of ictal EEG based on instantaneous amplitude function and instantaneous frequency function of IMFs.

3. During the ictal stages and interictal stages, the properties of the EEG are changed. However, it is difficult to distinguish between ictal and interictal actives with respect to healthy EEG signal in the temporal domain. Combination of empirical mode decomposition method (Huang transform) and Hilbert transform is an effective method to analyze and classify ictal EEG data. Our next objective is to develop the components of Hilbert- Huang transform in temporal and spectral domain for analysis and classification of different stages of ictal.
4. Model based EEG analysis is a new trend in biomedical signal classification. The nonlinear methods are found to be more effective for analysis of EEG signals because they could describe the complex nature of the signal in a more effective manner. Our next objective is to develop a system to observe the role of EMD components in the state space modeling for characterizing of ictal EEG signals.

1.9 HIGHLIGHTS OF THE THESIS

In items 1 to 4 below, we give the summary of proposed EEG analysis and classifications. In this research work, we developed a novel methodology for ictal classification using instantaneous amplitude-frequency contour of the IMF of an EEG. The different methodologies are effectively improving the computer diagnosis for ictal events in the EEG.

1. We developed a methodology to obtain the different EEG rhythm of healthy EEG and epileptic signals using wavelet packet transform. The features of selected packets, which are the different frequency band of EEG are analysed. The feature vectors of proposed sub-bands of healthy EEG and abnormal EEG signals are prepared from the energy, entropy mean energy and mean Teager energy parameters. The mean Teager energy shows the better performance of discrimination in epileptic activities in EEG. The values of features show that the characteristics of seizure activities are more in lower frequency bands

of EEG. The proposed method is also analysed in CHB-MIT scalp EEG database. The mean Teager energy parameter shows the significant result in Chb01, an EEG data set of CHB-MIT database.

2. Here we developed a novel method for ictal analysis and classification using features of instantaneous amplitude and instantaneous frequency functions. In this study the EEG signal is decomposed into intrinsic mode functions (IMFs), then amplitude envelope and frequency functions on a time-scale basis using the analytic function of Hilbert transform. The effect of ictal classification is done in individual IMF features, multiple features with individual IMF, and individual features with multiple IMFs. The instantaneous amplitudes and instantaneous frequencies of each IMF are computed using the analytic function. The energy features mean energy, mean Teager energy, and entropy-based features like entropy, approximate entropy were computed respectively from the instantaneous amplitudes of IMFs. The statistical features of the IMF frequency function are also tabulated. The main contribution is to analyse the features individually and in groups intelligently on both in statistical approaches and by using ANN and ANFIS classification methods. The IMF2 and IMF1 of energy and entropy-based features of instantaneous amplitude and standard deviation of instantaneous frequency have been obtained. The result shows a 100% total classification accuracy of ictal EEG classification.
3. In this work, we developed a novel ictal classification method that combines the spectral and temporal features of Hilbert-Huang transform. The spectral features of the instantaneous amplitude function are tabulated and compared using an autoregressive, AR (6) model and AR (10) model. The temporal features of both instantaneous frequency function (IF) and instantaneous amplitude function (IA) are

computed. The spectral analyses is tabulated from the AR power spectral density of IA components. The spectral features are spectral peak, spectral mean energy, spectral entropy, and spectral mean Teager energy, which are energy or entropy based features. The temporal features are coefficient of variation, skewness, Kurtosis, and interquartile range. The feature vector for ictal classification are tabulated in both spectral and temporal features of IA-IF and IA-IA respectively. Here four different Cases of ictal activities of EEG signals are classified. The potency of the feature vector in each class of data is statistically tested using one-way analysis of variance, and the classification results are verified using an artificial neural network classifier. The spectral features of IA-temporal features of IF are better in total classification accuracy than spectral - temporal features of IA in all the Cases. The spectral features of the AR(10) of IA and the temporal features of IA yielded 100% accuracy, 100% sensitivity, and 100% specificity in the ictal classification. The main observation is that instantaneous frequency function and instantaneous amplitude function of IMF2 have better ictal classification accuracy than IMF1, which indicates that the ictal information are accumulated in IMF2.

4. Here we developed nonlinear methods to analysis the ictal EEG classification using states-space model. The Kalman filter is used to estimate the state matrix of the IMF of the EEG signal. The features of the state value are used for analysing the classification of ictal EEG. The extracted features are Mean Energy, Mean Teager Energy, Approximate Entropy, Sample Entropy, Mean Autocorrelation, Interquartile Range, Mean Absolute Deviation, Kurtosis, Variance and Standard Deviation. Here results imply the features of IMF2 have discriminative information of ictal EEG than other IMFs, which help in better classification accuracy of the ictal classification. The artificial

neural network is used to classify ictal EEG and healthy EEG status. The study shows mean Teager energy have 100% accuracy in ictal classification. Apart from this, the combination of mean energy & mean Teager energy features shows sensitivity 100%, specificity 100% and accuracy 100% are achieved in classification of ictal EEG.

1.10 ORGANIZATION OF THE THESIS

The thesis is organized into seven chapters as follows:

Chapter 2 covers a detailed literature survey of the different EEG signal processing techniques in epileptic seizure detection. The critical analysis of the different methodologies is studied and finds a gap of the research, which ultimately leads to present work. Many techniques are explained for both feature extraction and classification of epileptic seizure detection. The detailed description of EEG time series data used in this thesis is also mentioned in this chapter.

Chapter 3 the EEG data are decomposed into the different frequency bands of the brain wave using Wavelet packet transform. Then the selected packets being mapped to each frequency band of EEG. This aids to analysis of the temporal behavior during a seizure attack. These feature vectors of each packet are used for ictal classification using adaptive neuro-fuzzy inference system (ANFIS) classification. WPT system is checked in T7-P7 and T8-P8 lobes of CHB-MIT Scalp EEG database.

Chapter 4 discusses a novel method in Instantaneous amplitude function and Instantaneous frequency function of the IMFs for effective ictal classification. In this the effect of ictal classification with multiple features of the individual IMFs of both amplitude and frequency contour are analyzed. In addition, the performance of the ictal classification of the individual features from multiple IMFs is analyzed. Then both the cases are classified using an artificial neural

network (ANN) and ANFIS. All the cases are statistically evaluated by the analysis of variance (ANOVA) test with feature ranking, in Instantaneous amplitude function and Instantaneous frequency function.

Chapter 5 discusses a method for the different stages of ictal EEG analysis by using autoregressive (AR) spectral and the temporal features of Hilbert-Huang transform. The feature vector is formulated from AR spectral features of the Instantaneous amplitude function and temporal features of Instantaneous frequency function of Hilbert-Huang transform. Different types of actual classification are mentioned in four cases and each case is classified by artificial neural network. Also, each Case is statistically evaluated by ANOVA test.

Chapter 6 proposes a state space modeling of first and second IMFs of EEG signal. The Kalman filter was used to obtain the state estimations. Here estimation of state vector will reflect the abrupt changes in EEG signals. Then multiple features are extracted from the state estimation matrix and are used for classification with the aid of ANN classifier. This eventually leads to an outstanding classification of the healthy EEG and ictal EEG class.

Chapter 7 Summarizes the conclusions drawn from each of research works. A few suggestions for future studies are also incorporated.

CHAPTER 2

LITERATURE REVIEW

The chapter deals with a review of the research work reported in the open literature in the areas of electroencephalogram (EEG) signal processing. In an EEG signal analysis the local information is an extremely important activity. Therefore the EEG signal processing method is the key to determine whether the physiological or pathological information on EEG can be accurately detected. Advanced signal processing techniques are required to efficiently analyse the brain waves. A precise characterization of an abnormal EEG pattern can lead to a clearer view of many diseases.

The biosignal is recorded with a proper data acquisition system, to convert the EEG signal into digital form. This is helpful to interface with the computer in order to analyse the events by suitable feature extraction. Then it is fed to a proper classification tool for pattern recognition, which helps in the diagnosis. The reordered EEG signal is always integrated with artifacts, which affects the analysis of EEG signal. The artifacts are undesirable signals which are mainly generated from environment noise, experimental error and physiological artifacts. The physiological artifacts are due to eye movement, muscle activity, electrode movement, sweating and even muscle movement due to breathing (Islam *et al.* 2016). Before processing the feature extraction, it has to be ensured that the recorded EEG signals are suppressed for all types of EEG artifacts. There are different techniques have been developed for removing unwanted artifacts from the EEG signal (Jiang *et al.* 2019). This literature study is not focused to such research work in order to eliminate the different artifacts. The artifacts shall change the characteristics of the EEG signal, which leads a wrong diagnoses of the events. This review primarily focuses on the EEG signals analysis and classification.

2.1 FEATURES EXTRACTION

There are many algorithms that are developed in feature extraction by the researchers for the epileptic detection. These methods are classified as time domain analysis, frequency domain analysis, joint time-frequency analysis, nonlinear methods and hybrid techniques (Alotaiby *et al.* 2014). The emerging works on these fields are discussed in detail as follows.

The time domain analysis is also known as a conventional method for EEG analysis. In conventional methods, the transient pattern of abnormal EEG was studied in term of spike waves and sharp waves (Jasper, 2012). Another study suggested a waveform analyzer proposed for a human EEG in term of first and second derivatives of the input waveform (Klein, 1976). The results of derivatives of EEG is as similar to the transient behaviour of the signal. These sharply contoured wave patterns carry the characterization of an epilepticform discharges (Dingle *et al.* 1993). In EEG, identify the multiphase transient discharges are subject to consider the inter and intra clinical evaluation of the status of the brain (Ktonas *et al.* 1981).

The principal component analyzer is to reduce the dimensionality of the data set. These sets are transformed into a new set of variable which are orthogonal to each other. The feature vectors of the eigen sets are used to differentiate the cause of the epileptic signal (Acharya *et al.* 2012) . An optimization technique is incorporated in the feature set to improve the accuracy of detection (Siuly and Li, 2015).

The linear prediction is the estimation of the present state and is based on the input and past outputs (Altunay *et al.* 2010). Here the energy of an estimated error output state of abnormal EEG signal is much higher than normal EEG signal. The linear prediction is more effective when it incorporates the fractional calculus error estimation. The energy of the model parameters will give the distinction between ictal and ictal free stages (Joshi *et al.* 2014). The least square

based linear modeling of EEG used to enhance the feature of a seizure signal (Zamir, 2016). The status of the ictal activity is projected to Poincaré plane, which reduces the dimensionality of the state of the system. This helps to give a new insight to predict the change in the transition of multiphase wave which causes the epileptic seizure (Sharif and Jafari, 2017).

The normalized value of Wilson amplitude was calculated and compared with a threshold value to classify signal as a normal or a non-convulsive seizure (Fatma *et al.* 2016). The Wilson amplitude is the sum of the difference of the present and past samples of event above the marginal value is treated as a non-convulsive seizure. The advantage of this method is that without the aid of any classifier, the method correctly identifies non-convulsive seizures by analyzing amplitude variations in time domain. The drawback of the time series analysis is that frequency information of signal is not present. It is well known that the activity of the brain is also dependent on the rhythms of the brain wave.

The power spectrum is characterized by the power of the signal as a function of the frequency. The power spectrum is classified into two non-parametric methods and a parametric method. In the non-parametric method, the spectrum estimation is not based on model assumption. Fourier Transform is used to analyse the energy-frequency assessment of an EEG signal (Dumermuth *et al.* 1970). The fast Fourier transform is used for reducing the computational complexity of events detection in EEG (Polat and Güneş, 2007). The power spectrum of the signal was calculated using fast Fourier transform (FFT) and then the spectrum was divided into 15 sub-bands, each of width 4Hz (Liang *et al.* 2010). Then entropy was also calculated for all these sub-bands are the main features for the detection. In non-parametric techniques for spectral estimation, Fourier transform of the sample autocorrelation function is computed. Though non-parametric methods are easy to compute, main drawback is spectral leakage due to windowing aspects.

The parametric power estimation technique is based upon the model based approach, which depends on the input signal, output signal and white noise. For power spectral features are extracting desired features, by using the model based estimation method (Übeyli *et al.*, 2010). Autoregressive (AR) coefficients were estimated using Burg method with an order of 10, since a lower order results in a smoothed estimation. The choosing of a large AR model order results in spurious peaks and instability. The EEG signals were collected before and during hypopnea, which is a type of sleep apnea syndrome. The mental stress and relaxation of a brain is also analyzed in parametric method (Saidatul *et al.* 2010). The EEG signal were collected from subjects keeping them relaxed after which they were subjected to a questionnaire and then they were allowed to relax. Signals feed through a notch filter to filter the line noise and then power spectrum was calculated using AR parameter estimation like Burg method and Yule Walker method.

The power spectrum of EEG signal was fed to an AR model of order 20 for calculating the AR coefficients. These coefficients were then fed for feature reduction, which then employed a principle component analysis and a genetic algorithm (Liang *et al.* 2010). This reduced feature set effectively diminished the computation time for classification. Parametric and non-parametric methods differentiate the evaluation of the EEG activity in young Children with controlled epilepsy (Van Vugt *et al.* 2007).

An efficient feature selection and linear discrimination of the EEG signals were developed (Rodríguez-Bermúdez *et al.* 2013). Initially, all the desired features like spectral features were extracted using FFT then Hjorth parameters like activity, mobility and complexity were calculated. The energy distribution of the signal was analyzed using the coefficients of AR model. The different parametric methods are used in spectral analysis. A random sequence is modeled using a time-series model and the model parameters are

estimated using the given data. Then spectrum is obtained by substituting the parameters in the model spectrum. To avoid the problem of spectral leakage in the parametric methods are widely employed for spectral estimation. However, if the spectrum is wrongly modeled the estimation can be misleading.

2.1.1 Time -Frequency Methods

A real time system for analysis of human EEG, the sharp and/ or slow wave (Gevins *et al.* 1976) of EEG will give both time domain transient as well as the spectral information. The time-frequency domain analysis is a much improved feature extraction method because it uses filtering transient pikes in biomedical data. The different version of the time-frequency analysis methods is windowed in Fourier transform, wavelet transforms (WT) and wavelet packet transforms (WPT).

In a windowed Fourier transform, analysis is achieved in both time and spectral resolution. The local spectral information is obtained in the time - frequency plane (TFP) by equally spaced windowing (Bigan and Woolfson, 2000). In singular value decomposition (SVD), u and v are the orthogonal matrix, which are unique for an event in EEG data. The new born EEG signal is mapped in TFP and apply the SVD algorithm for feature vector (Hassanpour and Mesbah, 2003).

An appropriate method is proposed in a time-frequency analysis to differentiate a normal EEG and seizure segments in EEG (Tzallas *et al.* 2009). Here the feature vectors are the energy distribution of power spectral density of each EEG segment. The TFP is the first moment and second moment of each sub-band of the EEG is extracted to classify the ictal stages (Musselman and Djurdjanovic, 2012). Another method is in the time frequency image pattern for analyzing the abnormal activities like seizures in a newborn baby (Boashash *et al.* 2015). Initially, the time domain features are found and it is later extended to

the time-frequency domain, which is succeeded by replacing one-dimensional time domain moments with two-dimensional time-frequency domain moments.

The analysis using WT and WPT decomposes the finite energy signal in successive stages each with different scaling factor. Thus, it gives the information in both time and frequency domains. But at higher frequencies discrimination of frequencies is sacrificed for localization of time (Mertins, 1999). This enhances the decomposition of signals into sub-bands and a simultaneous analysis of the various (wanted) spectral components. The wavelet transform is widely used in EEG analysis because of the multi-resolution capability (Zhang *et al.* 2003).

Different statistical parameters are tabulated from the detailed coefficient of the wavelet transform for the analysis of the seizure detection (Khan and Gotman, 2003). The accumulated energy of each level of the wavelet transform is computed as the feature set for the seizure detection (Gigola *et al.* 2004). The higher order of Daubechies wavelets, which are orthogonal wavelets used to retrieve the multi-resolution property of the EEG wave (Adeli *et al.* 2003). The fourth order Daubechies wavelets is most popular mother wavelet for the detection of 3Hz slow and spike epileptic form discharge of brain. Compare the classification accuracy and advantages of different wavelets, which are used for feature extraction in the seizure detection (Faust *et al.* 2015).

The energy index of multi level coefficients of both detail and approximation in wavelet transform analyses the temporal lobe seizure signal (Zandi *et al.* 2010). The healthy manner and level of alcoholic status is studied in the energy of wavelet packets in EEG signal (Faust *et al.* 2010). The classification result is statistically analyzed using *t*-test method.

The features of the TF plane image of seizure signal are used for total classification accuracy (Yusaf *et al.* 2016). Here the higher order statistical properties of the two dimensional discrete wavelet transforms (DWT) in TF image are extracted as the feature vectors. Permutation entropy value of the neighbouring sample is incorporated in a decomposed level of DWT as a feature vector in (Tawfik *et al.* 2016). The different statistical features are extracted from the selected coefficient of DWT (Sharmila and Geethajali, 2016), dual tree complex WT (Deivasigamani *et al.* 2016) and fuzzy approximate entropy (Kumar *et al.* 2014). is used for ictal classification. The wavelet transform is also used in long term EEG analysis (Liu *et al.* 2012). In this work, multi-channel wavelet decomposition is used for only three bands in an intracranial EEG and relative energy parameter is extracted.

The computational complexity of the seizure detection algorithm increases as a function of increasing the number of EEG channels for the processing (Sharmila and Geethajali, 2016). It is suggested that a method in the wavelet analysis is to optimize the minimum number of channels for the detection of seizure. Based on the optimal channel selection algorithms, it suggested 2-6 channels are enough for the seizure detection.

2.1.2 Nonlinear Methods

The EEG signal is mixture of nonlinear and non-stationary signal. The classical methods are not suit for extracting brain information. The nonlinear behaviour of these waves is an indication of seizure activities in the brain. The EEG signal is consists of spike wave, sharp wave and combination of sharp and spike wave are transient in nature. So, the nonlinear techniques are suitable for better analysis the EEG signal. The different nonlinear methods are Lyapunov Exponent, phase space plot, Hurst exponent, Fractal dimension, higher order spectra, state space analysis, etc.

A nonlinear method, which is Lyapunov exponent (LE), is trying to apply in EEG data to detect the nonlinearities present in EEG using surrogate data method (Das *et al.* 2002). The LEs and fractal dimension of the original and surrogate series were compared to check if the LEs can report the loss of nonlinearity and hence the loss of information from the dataset. But, since the change due to surrogating was small, they concluded that LEs did not represent the system complexity of EEG. Another work, (Übeyli, 2010) the coefficient of largest Lyapunov exponents is computed to set a feature vector, which is used to distinguish the status of EEG. In this method maxima, minima and lower order statistics of the largest Lyapunov exponents is extracted. Computation of LEs has served as the method of training the classifier.

A multi-channel EEG modeling was made in a correlation dimension and Lyapunov exponents' methods (Shayegh *et al.* 2014). The synthetic signals were generated from the model using intrinsic parameter sequences and coupling coefficients. The validation of these signals was done by a parameter identification procedure. Cross spectral difference and visual inspection were used to check the similarity of real and synthetic EEG signals. The main drawback of the method was computationally complex.

To compute the underlying nonlinear dynamical properties of EEG signals, a recurrence network based approach was presented (Subramaniam and Hyttinen, 2013). EEG signals in healthy, inter-ictal and ictal stages were used. The EEG time series was transformed into a phase space attractor and recurrence network. To characterize the underlying attractor, network measures such as clustering coefficient and path length on recurrence network were determined. The recurrence network based approach was capable of characterizing different classes of EEG signals depending on their attractor complexity. The epileptic seizure detection was also carried out using

Recurrence quantification analysis (RQA), which is a modern method to analysis nonlinear data (Sharanya *et al.* 2014). The RQA measures were obtained from a recurrence plot. Visualization of recurrence behaviour of phase space trajectories of dynamic systems could be performed in RQA. This method provided good results even for shorter and non-stationary data. No assumptions about the data set size or data distribution were required.

In the same year (Rangaprakash, 2014) analyzed the connectivity of multichannel EEG signals using recurrence based phase synchronization measure. The technique used to perform the study was inherently nonlinear. This was of great importance since the brain is indeed a nonlinear system. The nonlinear measure is called Correlation between probabilities of recurrence (CPR). To understand the interdependence between different brain regions, a connectivity analysis was performed. It was a post-processing technique applied in CPR matrix. Based on these, a brain connectivity graph and a brain, head map were prepared. These could aid in differentiating between EEG recordings under eyes open and eyes closed states as well as seizure and pre-seizure states. The nonlinear features like similarity index, phase synchronization, and nonlinear interdependence are obtained long term EEG for seizure prediction (Rabbi *et al.* 2013).

Hurst exponent is a complex nonlinear measure and used it in classifying epileptic EEG signal. It could also help in better understanding of the underlying chaos in brain signals (Sood and Bhooshan, 2014). The signal was initially split into small epochs and nonlinear features were extracted to enable classification. Due to fast computation capability, effectiveness in spotting repetitive patterns and satisfying stationary criterion, modular approach based on epochs were considered. The results emphasized the ability of Hurst exponent to explain seizure evolution. Low quantity data requirement and ability to explain the complexity of time series made this a superior method.

The different entropy measures are an important feature in EEG to discriminate the elliptic form of activity in the brain (Kannathal *et al.* 2005). The entropy related features of the events are the better dimensionality of the epileptic form discharge (Acharya *et al.* 2012). The entropies are an explicit gesture of uncertainty in the signal. Computation of different types of entropies may measure the level of chaos present in the signal. The various entropies were used to extract feature parameter for diagnosing epilepsy signals (Acharya *et al.* 2015).

EEG signals are considered as the fractal signals and based on this assumption various fractal properties are used in the analysis of EEG to detect the presence of spikes. The fractal dimension is the characterization of deduction in the dimension of a signal or an image in space filling capacity (Uthayakumar, 2013). In (Azami *et al.* 2012) introduced another method used for EEG analysis. In this method, a Savitzky-Golay filter is used for smoothening to accentuate spikes position. The spike detection was done in two phases. In the first phase, accentuate the spike position using Savitzky-Golay filter and then the fractal dimension is calculated. The fractal dimension is also used to calculate the dimension reduction of in alpha sub-band of EEG in ischemic attack with respect to the normal EEG signal (Zappasodi *et al.* 2014). The fractal dimension method is implemented to find the sleep disorders from the EEG data (Finotello *et al.* 2015).

The spectral behaviour of higher order statistics components are used for finding abnormalities in the functions of the heart (Martis *et al.* 2013). Here the coefficients of independent components of both higher order cumulants and bi-spectrum is used for analysis the abnormalities.

The capability to handle time varying parameters, missing data and the ability to incorporate changes makes the state space model quite attractive. A state space model is formulated to extract useful information from brain computer

interface in a fast and safe manner (Irie *et al.* 2010). The EEG signals with and without visual evoked potentials were considered for the study. The signal was then characterized by extracting features from it with the aid of Kalman filter. The results suggested that there were significant differences in the signal to noise ratio of the EEG signals with and without visual evoked potentials. The seizure occurrence is estimated with the aid of features extracted from characteristic variables associated with epileptic EEG data in Particle filtering method (Liu and Pang, 2008).

The cortical dynamics of multivariate autoregressive (MVAR) were given by the state equation and the physical relationship between the cortical signal and the measured EEG was given by the observation equation (Cheung *et al.* 2010). The dynamic estimate of Burst suppression ratio is expressed in terms of a state space model of computation (Chemali *et al.* 2011). The unobservable brain state whose evolution was to be tracked was expressed in terms of Gaussian state equation. Estimation of the model was done using an approximate expectation maximization algorithm.

In order to facilitate the epileptic seizure detection in a longer duration EEG monitoring system, with a state-space model with Cauchy observation noise (SSMC) is used. The SSMC used a nonlinear state-space model helped to identify the gradual changes brought by epileptic seizures (Wang *et al.* 2015). The main sub-band EEG signals are modeled in state space model using a variation of noise level. The model is useful for the monitoring brain activity during Anastasia patients (Wong *et al.* 2006).

As EEG is nonlinear and non-Gaussian signal, the estimation of EEG in nonlinear methods is more accurate than linear steady state methods. The effect of different nonlinear modeling methods compares in EEG sub-bands under epileptic seizure conditions (Martis *et al.* 2015).

2.1.3 Hybrid Techniques

The hybrid techniques in EEG signal processing and analysis are the combination of time domain methods, frequency domain methods, time-frequency methods or nonlinear methods. This will help to get better classification accuracy on a computer aided diagnosis of epilepsy detection. The comparison of some of the transformation methods used for the ictal detection is specified (Parvez, and Paul, 2014).

A multivariate autoregressive model inspired from state space formulation was developed (Cheung *et al.* 2010). to estimate cortical connectivity from noisy EEG recordings. The cortical dynamics of MVAR model were given by the state equation and the physical relationship between the cortical signal and the measured EEG was given by the observation equation. To trace the MVAR modeling, the coefficient of activity distribution components and the covariance matrix of electromagnetic noise are taken. The method worked well, even with relatively low signal to noise ratio, which is a characteristic of the EEG signal. There was a significant reduction in the number of unknown parameters to be estimated. In addition to these, the unknown spatial activity distribution could be incorporated within each region of interest. Analysis of Magneto Encephalogram (MEG) data using the same model was suggested as a future work.

A method is suggested for detecting artefact present in EEG signal is modeled using AR modeling (Lawhern *et al.* 2012). Since AR parameters are used for scaling the changes, these were employed for analysis. Thus variations like scalp and skull thickness will not affect AR parameters. Initially, EEG signal was collected from the subjects by making them perform eye movements, jaw movements and head movements. Then discrete Meyer wavelet transform was applied for decomposing the signal into sub-band frequency ranges.

The DWT is used for decomposing the EEG signal to get the frequency band closer to the EEG sub-band. To compute the coefficients of approximate entropy- $d1, d2, d3, a1$ and $a2$ of DWT coefficient are the feature vector for the classification. The lower value of approximate entropy of these coefficients will indicate possibility the seizure attacks (Ocak, 2009). The Intrinsic Mode Functions (IMF) of selected approximation and detail coefficients of DWT are extracted. Then Shannon entropy and Renyi entropy of DWT coefficients are computed for the effect of classification in ictal EEG (Das and Bhuiyan 2016). The different entropy based features, fractal dimension and statistical parameters of selected DWT coefficients are used for epilepsy detection (Upadhyay *et al.* 2016). Here 16 different wavelet functions are employed for decomposition of DWT in 4 sub-band of EEG.

Continuous Wavelet Transform of EEG signal is mapped to a 3D space of dilation translational and brightness of each sample (Acharya *et al.* 2013). Then the HOS feature of the image and texture feature of gray level co-occurrence of each window are figured out for classification of ictal stages. The bandwidth of approximation and detailed coefficient is flexibly adjusted during DWT decomposition (Sharma *et al.* 2017). This adjusted bandwidth is similar to the EEG sub-band. The Higuchi fractal dimension is tabulated for feature vector in the classification of ictal stages.

The Higher order spectra of selected packets of wavelet packet decomposition (WPD) are tabulated for an automatic detection (Acharya *et al.* 2011). The alcoholic index of brain is also studied in different nonlinear methods (Bairy *et al.* 2017). Initially the EEG signal is decomposed into six level of WPT, and then different packets of EEG signals are used for nonlinear modeling. The two dimensional singular value decomposition of time-frequency domain EEG is transformed into a S-domain and the features are computed (Xia *et al.* 2015). The two dimensional DWT features are calculated

in the time-frequency image of EEG signal for seizure detection (Yusaf *et al.* 2016).

2.1.4 Empirical Mode Decomposition Method

The EEG signal is nonlinear, non-stationary behavior in nature. Also the characteristics of EEG is depended on the status of gender, age and disease state. Also, it depends on the mental condition of the individual. Almost all the above mentioned EEG signal processing techniques implemented by the assumption that EEG signal is a wide sense stationary signal.

In the Fourier spectral analysis of a non-stationary signal, the presence of harmonic components causes energy spreading in the spectrum. This results in missing the interpretation of energy-frequency distribution of the signal. A novel method is developed (Huang *et al.* 1998), which is appropriate for processing of nonlinear and non-stationary time series signal. The new method is called as empirical mode decomposition (EMD) method. In the EMD method the signal is decomposed into different components called IMF.

The method of decomposition using EMD has found application in almost all the areas of brain wave signal processing. EMD has been applied in EEG signal pre-processing or enhancement as well as for feature extraction process in classification of normal and abnormal EEG signals, localization of sources, movement related task classification, motor imagery classification, etc. Recently, EMD method has been emerged with a major role in EEG signal processing, particularly in epilepsy detection. Losonczi *et al.* proposed analysis of EEG signal using instantaneous frequency and instantaneous phase of IMFs (Losonczi *et al.* 2012). Here analyses both synthesized signal and healthy EEG signal. The synthesized signal is generated by mixing of 5Hz and 10 Hz sinusoidal signal. The instantaneous frequency of IMF5 represents the lower events of a channel of EEG signal namely delta ocillation in the EEG. The EEG signal duration of the F8 EEG channel is 60s.

The local amplitude and local frequency information of IMFs in the EEG signal shows differences in the healthy EEG and ictal EEG signals (Oweis and Abdulhay, 2011). A more effective analysis was achieved by using bandwidth features of IMFs (Bajaj and Pachori, 2012). The lower frequency bandwidth parameters and higher frequency bandwidth parameters of four higher order IMFs of EEG signal is extracted. These parameters are represents the main features of the classification of seizure signal in the EEG segments of that work.

The chaotic features of IMFs were found effective in distinguishing the ictal, inter-ictal normal healthy EEG signals. The higher order moments that include variance, kurtosis, and skewness are extracted from the IMFs of the EEG signals, which is used as features to classify the EEG signals (Alam and Bhuiyan, 2013). The Coefficient of variation and fluctuation index of IMF1 to IMF5 are used for ictal classification (Li *et al.* 2013). The analytical signal of each IMFs of EEG signal is obtained and computed as the modified mean of each polar modulated signal (Bajaj and Pachori, 2013). This modified central tendency is the features for the classification of ictal signal and healthy EEG signal.

The DWT based analysis is in the Hilbert transform (HT) domain. A 5-level DWT decomposition perform to obtaine a sub-band of EEG signal (Li *et al.* 2017). Then to perform HT of each sub-band and setup the feature vector of each band by calculating different central tendency and energy of the analytical signal. The statistical features and spectral features of analytical function of IMFs are tabulated (Riaz *et al.* 2016). Here IMF1, IMF2 and IMF3 are being considered for procuring the status of the brain signal.

The Hilbert spectrum of each IMF will give superimposed view of energy-time- frequency distribution of the non-stationary signal. The spectral entropy of Hilbert–Huang spectrum of seizure signal shows wide

discriminating difference to healthy EEG (Fu *et al.* 2015) and to monitor patients undergoing anaesthesia (Li *et al.* 2008). The marginal spectrum of the EEG is studied in the anesthetic patients for knowing the depth of anaesthesia in the brain (Chen *et al.* 2016).

The first and second order statistics of IMFs components are used for classification of epileptic seizure signal from normal EEG signal. The first four IMFs have the complete information about epileptic form discharge on the brain (Djemili *et al.* 2016). So it doesn't compute the features from all the IMF components for the seizure classification.

The two dimensional and three dimensional phase space representation of first four IMFs component of EEG signal (Sharma and Pachori, 2015). A unique pattern is generated in phase space, which has an epic centre for a normal EEG signal. The seizure signal classification is performed in ensemble empirical mode decomposition and phase space representation (Jia *et al.* 2017). The time delay phase space method is used to execute in the higher order IMFs, then different statistical properties are segregated for feature vectors. The spectral parameters of ensemble empirical mode decomposition of EEG are used to automate the seizure detection (Hassan and Subasi, 2016). The spectral moments are widely scattered in EEG abnormality.

Variational mode decomposition (VMD) algorithm is similar to EMD. In VMD method, bandwidth of IMFs is varied from amplitude modulation to the frequency modulation oscillation. In each, IMFs is estimated using Burg's auto AR modeling. In this work, a system is modeled and the performance is compared in AR(6), AR(7), AR(8), AR(9) and AR(10) order respectively. The optimal classification accuracy was obtained in AR(10) order classification of inter-ictal and ictal signals (Zhang *et al.* 2017). In all EMD studies only the IMFs of EEG are used for analysis the seizure classification. The residual signal is not considered in the seizure detection (Losonczi *et al.* 2012; Bajaj and Pachori,

2012; Li *et al.* 2013; Sharma and Pachori, 2015; Djemili *et al.* 2016; Riaz *et al.* 2016).

2.2 CLASSIFICATIONS

A machine learning algorithm or a mathematical tool, which can map explanatory variables or features into desired outcome are called as classifier. The classification consists of predicting a certain outcome, based on a certain set of feature parameters. In order to predict the outcome, the algorithm process a training set containing a set of attributes and the respective outcome called prediction attributes. The algorithm tries to discover the relation between the attributes that would make it possible to predict the outcome.

A proposal for a new classifier is used with the existing datasets is beyond the scope of this thesis. This thesis does not focus the change of structure of the particular classifier for the EEG analysis. So standard classifiers have been used to verify the preceding steps and compare them with each other to achieve maximum efficiency and accurate results. There are a few classifiers, which give better classification performance for EEG analysis. The leading classifier used in EEG analysis are support vector machine (SVM), artificial neural network (ANN), adaptive neuro-fuzzy inference system (ANFIS), etc.

The SVM classification is an n-dimensional hyperplane, which optimally separates the data into two non-overlapping categories (Kumar, 2014). SVM is based on structural risk minimization principle, and could construct an optimal separating hyper plane in the feature space (Li *et al.* 2013). The SVM model used a sigmoid kernel functions to map the nonlinear feature set to higher dimensional space to obtain linear separable feature set (Fu *et al.* 2015). The least square support vector machine is which solve linear equation instead of quadratic programming having better result in EEG classification (Sharma and Pachori, 2015).

The artificial neural network is a connection of several neurons from the input level to the output level through hidden levels (Isler, 2016). ANN used in recent studies in biomedicine, especially in seizure classification, because of its good performance (Hassanien *et al.* 2014; Djemili *et al.* 2016). The different varieties of neural network are used, according to the taxonomy of neural network architecture (Basheer and Hajmeer 2000). However, various ANN algorithms like multilayer perceptron neural network (MLPNN), recurrent neural network (Subramaniyam and Hyttinen, 2013), probabilistic neural network (Übeyli, 2010) and neural network ensemble (Li *et al.* 2017) are used in seizure classification. The MLPNN, is one of the most efficient ANN model, which is widely used seizure classification (Djemili *et al.* 2016). The MLPNN comprises three layers. The first layer is the input layer that contains a number of neurons with the same size as that of the input feature vector. The second layer consists of the hidden layer that increases the classification ability of a given network, and the number of neurons in the hidden layer can be fixed without constraints. A small number of neurons can reduce the accuracy in classification rates, and a large number of neurons can exacerbate the complexity of a specific network. The third layer is the output layer composed of a number of neurons similar to that of the desired output class (Basheer and Hajmeer, 2000).

The ANN is optimally configured by applying train/learning algorithms. The weights and bias were updated using different learning algorithms namely, conjugate gradient back- propagation, gradient descent with momentum, adaptive learning rate back propagation, Levenberg-Marquardt, scaled conjugate gradient etc. (Raghu and Sriraam, 2017). The back propagation algorithm is most commonly used in ANN, rather than the simplest feed forward algorithms. The mean square error between calculated output and desired output of the network is back propagated to the previous layer to minimize error through adjusting the weight of each node. The

Levenberg–Marquardt algorithm converges faster, but it is memory-intensive (Patnaik and Manyam, 2008).

Neural network models require less formal statistical training compare to Logistic regression, which is a widely used statistical modelling technique. It means ANN is fast computation than Logistic regression (Tu, 1996). The advantages of ANN are work with incomplete knowledge, and it can use multiple different training algorithms. ANN is non-paramateric model while most of the statistical methods are parametric model that need higher background of statistic. ANN based classifiers achieves higher accuracy for epilepsy classification compared with SVM in the presence of the noisy dataset cases (Qazi *et al.* 2016). Drawback of ANN is hardware dependence and computation time is larger for higher network, like input neurons over 100. The another major disadvantage is that the most appropriate grouping of training, learning and transfer function for classifying the data sets with growing number of features and classified sets.

The adaptive neuro-fuzzy inference system is a mathematical model for machine learning that is inspired from the structure of both artificial neural networks and fuzzy inference system (Jang, 1993). Using a given input/output data set, it constructs a fuzzy inference system (FIS), whose membership function parameters are tuned using a back propagation algorithm or combination of back propagation gradient descent method and least squares approach (hybrid) algorithm. This allows fuzzy systems to learn from the data set to reach the desired destination. The basic structure of first order Sugeno-type fuzzy inference system is a model that maps input feature vectors to input membership functions, IF-THEN rules, a set of output characteristics, output membership functions, and to a single-valued decision associated output.

The Sugeno-type of fuzzy inference system has wider advantage of integrity of the output space and high optimized prediction (Blej and Azizi, 2016). The shape of the membership functions depends on parameters. Instead of just looking at the data to choose the membership function parameters, membership function parameters are automatically chosen. The network structure is similar to the ANN. The parameters associated with the membership functions changes through the learning process. The computation of these parameters is made easier by a gradient vector. When the gradient vector is obtained, any of several optimization routines can be applied in order to adjust the parameters to reduce some error measure. The error measure is defined by the sum of the squared difference between actual and desired outputs. The ANFIS classification provides the output as a linear regression time series rather than integer values, which represents classes and are compared with ANN classifier (Rabbi *et al.* 2013). The ANFIS classifier is effectively used for seizure detection (Yang *et al.* 2014; Deivasigamani *et al.* 2016).

The feature classification performance is statistically tested. The different statistically testing methods are student's t- test (Zappasodi *et al.* 2014), one way analysis of variance test (Acharya *et al.* 2011; Alam and Bhuiyan, 2013; Riaz *et al.* 2016; Jia *et al.* 2017), Wilcoxon rank sum test (Zhang *et al.* 2017), etc. The feature ranking is also tabulated for heighted and weighted features, among the future vector (Acharya 2015; Upadhyay *et al.* 2016; Acharya *et al.* 2013). The features with highest ranking aid to boost the performance of the classifiers.

2.3 DESCRIPTION OF THE DATABASE

The EEG data used ("EEG Time series data", 2015) for this work was provided by the Department of Epileptology, University of Bonn, Germany, which is a recognized epilepsy research Centre in Europe. The database is

widely used for several researchers around the world. There are approximately 1025 research works that were carried out from this data set. By using this data set, the researchers easily compare the performance of their work (Tzallas, *et al.* 2012); Acharya, 2013). The database comprises five classes of data, namely, groups A, B, C, D and E. Each set is a zip file of 100 .txt files (standard text document) containing American standard code for information interchange (ASCII) files of EEG time series data. So each group has 100 single-channel records with a duration of 23.6 s. Groups A and B are taken in awoken with the relaxed state with the patient's eyes open and closed, respectively. The groups A and B are considered as the normal state of the brain wave. They are recorded using surface electrodes placed by the standard 10–20 electrode placement scheme. Group C consists of seizure-free intervals (i.e., interictal) from the epileptogenic zone, and group D corresponds to the hippocampal formation of the opposite hemisphere. The hippocampal formation is located near to temporal lobe of the brain. The Group E contains pure ictal EEG. A sampling frequency of 173.61 Hz is used for the data acquisition of the EEG signal and each channel length is around 4097 samples. The each segments in the EEG data base is cut out by visual inspection for removal of artifacts affected segments from the continuous multichannel EEG recordings (Andrzejak *et al.* 2001). Thus, the secondary database of EEG is suppressed all types of artifacts. The spectral bandwidth of the aquisition system is 0.5 Hz to 85 Hz.

The seizure classification work using this EEG data with time–frequency based methods (Sharmila and Geethanjali,2016; Kumar *et al.* 2014; Parvez, M. Z., and Paul, 2014; Ocak, 2009; Acharya *et al.* 2013). Also, different nonlinear methods are implemented for EEG classification using the same database (Acharya *et al.* 2013; Redelico *et al.* 2017). Recently the seizure classification research work using empirical decomposition this EEG database (Oweis and Abdulhay, 2011; Alam and Bhuiyan, 2013; Riaz *et al.* 2016; Djemili *et al.* 2016;

Jia *et al.* 2017; Martis *et al.* 2012). To ensure the cross validation in this work we spilt the original data set into random samples for training set data and testing set data.

Another popular EEG database was from CHB-MIT Scalp EEG database, which is prepared and hosted by Children's Hospital Boston (CHB) and the Massachusetts Institute of Technology (MIT) (“CHB-MIT Scalp EEG database”, 2014). The signals are in the .edf (European data format) file format, which is a standard file format used for the storage and exchange of medical time series in European Union nations. The EEG resource is open to public for to test the algorithms of Biomedical researchers (Goldberger *et al.* 2000). In most cases, files are with a duration of 60 minutes and are in 10-20 international electrode placements system. All the files are sampled at 256 samples per second with 16 bit resolution and each file includes signals from 23 different channels. This database is suppressed all the artifacts. In each set of files having a summary text with information of file name, file start time, file end time, number of seizures in file, seizure start time and seizure end time. From this meta data information, it can split file into seizure affected files and seizure free (healthy) files.

2.4 INFERENCES

EEG signal can be used as an efficient tool to understand the complex dynamics of the brain, to discriminate various mental states and to aid in disease diagnosis. The signals are non-Gaussian, nonlinear, random and subject dependent and hence special type methods are required for of analysis.

The different methods have been proposed in literature for analysis of EEG signals. They can be broadly classified as time domain methods, frequency domain methods, time-frequency methods and nonlinear methods. However the studies have shown that hybrid techniques are more efficient in quantifying the EEG signal. Recently, an empirical mode decomposition method has emerged with a major role in EEG signal processing. It does not require any assumption

about linearity and stationarity of the data. The literature reviews mainly focus on different application in empirical mode decomposition methods and Hilbert-Huang transform method in EEG signal processing. HHT method is the decomposition of the IMF component into instantaneous amplitude function and instantaneous frequency function. The characterization of these twin components of IMFs create a new arena in the EEG signal processing. There are different classifiers are discussed which help to segregate different stages of ictal detection.

CHAPTER 3

ANALYSIS OF EPILEPTIC SEIZURE USING WAVELET PACKET TRANSFORM

In this chapter, EEG data are decomposed into different frequency sub-band using wavelet packet transform (WPT). Here we have used 4-level WPT decomposition in order to obtain packets. The packets in each level are linear combinations of wavelet basis functions. The frequency band of selected packets are similar to frequency rhythms of EEG, which are delta, theta, alpha, beta and gamma sub-bands. The different energy-entropy features of each frequency rhythms are tabulated for analysis the effect of epileptic seizure in EEG. Finally, the constructed feature vector is used to input ANFIS for better classification of the healthy region and epileptic seizure in EEG signals. The proposed system also analyses the effects of EEG sub-bands of seizure at temporal lobes, T7-P7 and T8-P8.

3.1 INTRODUCTION

The continuous wavelet transform (CWT) provides a time–frequency representation of arbitrary signals with finite energy. The CWT of a signal is the integral multiple of translation and dilation of window function called wavelets. The CWT provides multi-resolution representation of a continuous signal (Grossmann *et al.* 1990) and is defined as

$$S_t(a, b) = \frac{1}{\sqrt{|a|}} \int_{-\infty}^{+\infty} s(t) \psi\left(\frac{t-b}{a}\right) dt \quad (3.1)$$

Where a is the scaling parameter, b is the shifting parameter, S_t is a temporal signal and $\psi(t)$ is the wavelet function. By changing, the value of the scaling parameter and shifting parameter, a precise time resolution and precise frequency resolution are obtained respectively.

For increasing the computation efficiency of CWT, the scaling parameter and shifting parameters are replaced by the power of two, in form 2^j . In such analysis the transformation is known as discrete wavelet transforms (DWT). The DWT can be defined as (Ocak, 2009).

$$S_n(j, k) = \frac{1}{\sqrt{|2^j|}} \int_{-\infty}^{+\infty} s(t) \psi\left(\frac{t-k \cdot 2^j}{2^j}\right) dt \quad (3.2)$$

Here scaling parameters and shifting parameters of CWT are replaced by 2^j and $k \cdot 2^j$ respectively. This helps an easy computation of both wavelet analysis and synthesis of the signal. For computing DWT, an efficient method is implemented with the combination of quadrature mirror filters which is made up of low pass filter, $h(k)$ and high pass filter, $g(k)$ (Mallat, 1989).

However, this transform does not allow a flexible choice of the regions into which the time–frequency plane is divided (Adamczak, 2010). This flexibility is in the sense that both approximation coefficient and detailed coefficient are decomposed into its sub-band given by the wavelet packet transform. The WPT is a generalization of the wavelet transform (WT).

3.2 WAVELET PACKET TRANSFORM

The wavelet packet transform is a useful extension of wavelets. The flexibility of the wavelet packet transform will help to analysis many applications in Communications and Biomedical Engineering. The WPT is the continuation of the wavelet transform that provided complete set of all level decomposition. The decomposition of each level results in packets of the original signal. The WPT will provide resolution in both lower frequency and higher frequency (Gao and Yan, 2010).

The wavelet packet transform is defined as

$$W_{j,k}^n(t) = 2^{\frac{j}{2}} W^n(2^j t - k) \quad (3.3)$$

Where j is the scaling parameter, k is the shifting parameter and n is the modulation parameter of WPT. The first two wavelet packet function in terms of scaling function, $\phi(t)$ and shifting function, $\varphi(t)$ can be written as

$$W_{0,0}^0(t) = \phi(t) \text{ and } W_{0,0}^1(t) = \varphi(t) \quad (3.4)$$

For higher indexing number $n= 2, 3, 4\dots$ it can be replaced as the function of recursive relation

$$W_{0,0}^{2n}(t) = \sqrt{2} \sum_k h(k) W_{1,k}^n(2t - k) \quad (3.5)$$

$$W_{0,0}^{2n+1}(t) = \sqrt{2} \sum_k g(k) W_{1,k}^n(2t - k) \quad (3.6)$$

where $g(k)$ and $h(k)$ are quadrature mirror filters with scaling and shifting functions.

The wavelet packet coefficients of different levels are calculated by the inner product of wavelet function and temporal signal.

$$w_{j,k}^n = \langle s(t), W_{j,k}^n \rangle = \int s(t) W_{j,k}^n(t) dt \quad (3.7)$$

The WPT and WT are often implemented using a tree-structured filter bank. The tree structure of wavelet packet transform is shown in the Figure 3.1. In the WT only the output of the low-pass filter progresses to the next stage, while the output of the high-pass filter only gives the detailed coefficients of the signal. On the other hand, the WPT is a set of $W_{0,0}^{2n}(t)$ and $W_{0,0}^{2n+1}(t)$ functions, which can construct any type of tree-structure in the filter bank.

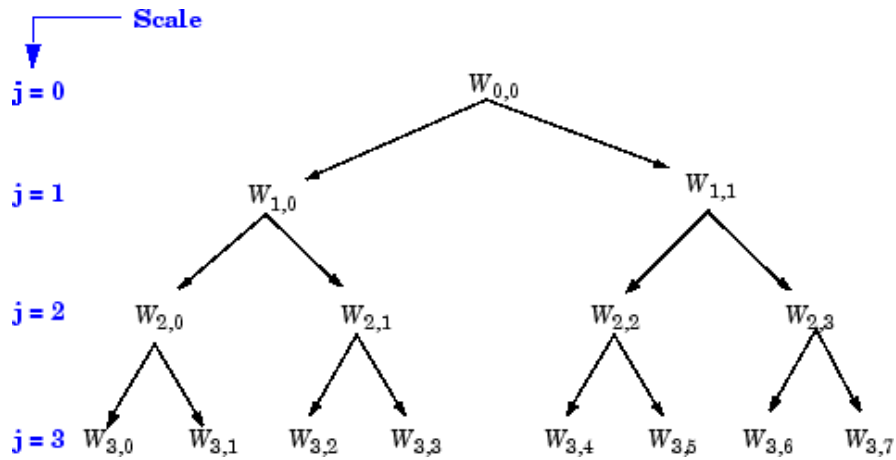


Fig. 3.1 Tree structure of Wavelet packet Transform

The wavelet packet transform can be viewed as a generalization of the classical wavelet transform, which provides a multi-resolution and time-frequency analysis for non-stationary EEG data. The potential of wavelet packets is enriched with menu of orthonormal bases, from which best of them can be chosen. The WPT can be fully decomposed into a tree structure. The quadrature mirror filters with scaling and shifting functions are repeatedly applied to produce complete sub-band tree decomposition of the desired depth. The WPT not only decomposes the approximation coefficients of the signal but also the detailed coefficients. Therefore, it also holds the important information located in higher frequency components, which are used in certain applications (Xiong, *et al.* 1998).

3.3 METHODOLOGY

Most of the biosignal analysis are either in time domain, frequency domain or time-frequency analysis followed by a linear or nonlinear classifier. However, in case of the epileptic seizure detection, the EEG signal features are extracted in time-frequency domain and pick out a suitable classification method, which provides good success rate in seizure detection (Kıymık *et al.* 2005). The Figure 3.2 shows signal flow diagram of the WPT based epileptic analysis system.

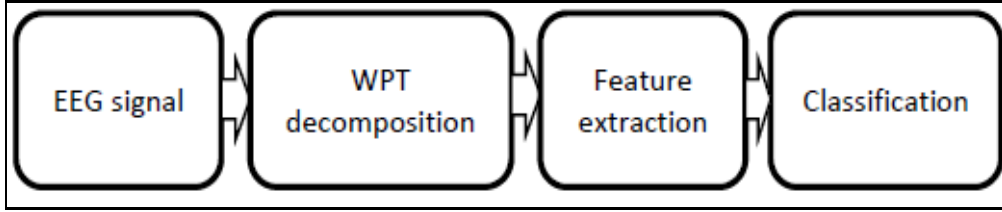


Fig. 3.2 Signal flow diagram of the epileptic detection system.

In this chapter, we have proposed a wavelet packet transform, which decomposes the EEG signal into four levels. Therefore, the original signal is decomposed into different sub-bands, known as packets. Each wavelet packet has a frequency band according to the level of selection. The ranges of frequency of some of the packets are correlated to frequency rhythm of EEG, like delta, theta, alpha, beta and gamma. The different features of each selected packets are extracted according to two types of EEG signal. The classification of normal and abnormal EEG is performed using the ANFIS, a hybrid system of artificial neural network and fuzzy inference system. We used fourth order Daubechies wavelet (db4), which is most suitable for the EEG application (Faust *et al.* 2015). After the four levels of wavelet packet decomposition, the selected packets are assigned as the frequency rhythm of EEG. The packet W(4, 0) is assigned as delta band (0-4 Hz), W(4, 1) as theta band (4-8 Hz), W(4, 2) as alpha band (8-12 Hz), combination of W(4, 3) and W(2, 1) as beta band (12-32 Hz) and W(1, 1) as gamma band (32-64 Hz).

3.4 FEATURE EXTRACTION

In this section, we deal with feature parameters of EEG signal, which are energy, mean energy, mean Teager energy and entropy.

(i) Energy:

Energy of a signal indicates the strength, over a period of time. The larger energy level will indicate the presence of spike and slow wave, which is the after effect of a seizure. The energy, is defined as

$$E_j = \sum_{k=1}^{N_j} |w_{j,k}^n|^2 \quad (3.8)$$

where $j = 1, 2 \dots M$ and $k = 0, 1 \dots 2^M - 1$

and $w_{j,k}^n$ is the k^{th} coefficient of the wavelet packet transform.

M is the total number of nodes corresponding to the frequency sub-band,

N_j is the number of wavelet packet coefficients at j^{th} nodes.

The epileptic EEG contains maximum energy compared to normal EEG signal (Artameeyanant *et al.* 2012).

(ii) Entropy:

The entropy is the measure of uncertainty in the EEG segments. The low level of uncertainty is indicating the normal EEG, while high levels show the abnormal EEG. So the measure of unpredictability in the signal is represented mathematically as (Coifman and Wickerhauser, 1992).

$$En_j = - \sum_{k=1}^{N_j} |w_{j,k}^n|^2 \log |w_{j,k}^n|^2 \quad (3.9)$$

where $j = 1, 2 \dots M$ and $k = 0, 1 \dots 2^M - 1$

The entropy is the information contained in the signal and it is the measure of the disorder of the system (Krstacic, 2002).

(iii) Mean Energy:

Mean energy is highly sensitive parameters that contributes to the increase in signal energy associated with seizure and is given as

$$ME_j = \frac{1}{N_j} \sum_{k=1}^{N_j} |w_{j,k}^n|^2 \quad (3.10)$$

where $j = 1, 2 \dots M$ and $k = 0, 1 \dots 2^M - 1$

(iv) Mean Teager Energy:

Mean Teager energy (MTE) is a nonlinear energy operator, which is obtained from three adjacent samples. The MTE is the energy estimated for a short-term duration of a signal (Teager, 1980). MTE is theoretically derived and demonstrated (Kaiser, 1990). MTE is efficient for analysis intermittent

and intermixed signal, which cause the abnormal activities of brain (Kamath, 2011). The MTE can be defined as:

$$MTE_j = \frac{1}{N_j} \sum_{k=1}^{N_j} |w_{j,k}^n|^2 - |w_{j,k-1}^n w_{j,k+1}^n|^2 \quad (3.11)$$

where $j = 1, 2 \dots M$ and $k = 0, 1 \dots 2^M - 1$

The MTE is the reflection of instantaneous energy difference in neighbouring samples. The mean Teager energy gives significant difference between epileptic EEG and healthy EEG signals (Gopan, 2013).

3.5 CLASSIFICATION

Here, we used an adaptive neuro fuzzy inference system, which is a popular classification model (Yildiz *et al.* 2009). ANFIS is the extension of ANN model and Sugeno type fuzzy inference system (FIS) model (Jang, 1993). The Sugeno type ANFIS consists of five different layers. The first and fourth layers of ANFIS, having adaptive nodes and other layers are fixed nodes. The hidden layer nodes perform the duty of membership functions and rules. The FIS analogues to IF – THEN rule based learning capability of a fuzzy set for a nonlinear system. The membership function attributes of FIS are modified using hybrid algorithm or back propagation algorithm (Güler and Übeyli, 2005). This facilitates the learning of FIS from the data and automatically modifies the membership function parameters. The parameters of input membership function are selected and desired output membership function type is to be either linear or constant. The network type structure is similar to neural network, which map the input layer to input membership function. The weight of the parameter in the membership function is changed as per learning process. A gradient vector expedites the adjustment of these parameters. The gradient vector provides how the FIS modeling the input/output data for a given set of feature parameters.

The *anfis* function in MATLAB R2014b is without tuning or self-turning FIS, which is generates a single-output Sugeno type FIS and tunes the system parameters using the training data. Here FIS is automatically generating using grid partitioning. The training algorithm uses as a combination of the least-squares and back propagation gradient descent methods (hybrid) The *anfisedit* GUI (Graphical user interface), the raw FIS structure generation based on grid partitioning or subtractive clustering. The training algorithm uses is a combination of the least-squares and back propagation gradient descent methods (hybrid) or back propagation gradient descent method. Select appropriate input membership function and output membership function is linear or constant. The epoch and error tolerance is also optional (Jang, 1993).

3.6 RESULTS AND DISCUSSION

The EEG data used in this study was obtained from the Department of Epileptology, University of Bonn (“EEG Time series data,” 2015). The data set comprises 5 sets of 100 single channel data of 23.3 s duration and sampled at 173 samples per second. A total of 4096 samples were present in each segment of the dataset. Figure 3.3 shows the EEG signal corresponding to Set A and Set E of the Bonn EEG database. The healthy EEG signal has less amplitude variations when compared to the epileptic EEG signals. The frequency band of EEG signal is fixed as 0.5 to 64 Hz. The frequency greater than 64 Hz is considered to be as noise and hence it is eliminated. The supply noise of 60 Hz is eliminated using notch filter.

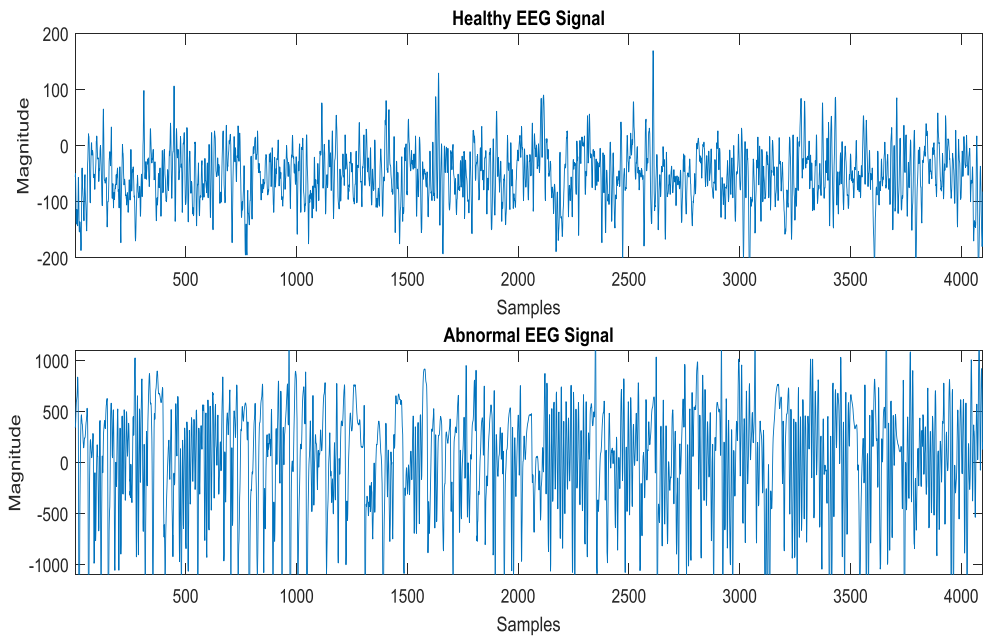


Fig. 3.3 Healthy EEG and abnormal EEG Signal in the EEG database.

The signal is first decomposed into four levels of WPT. The selected decomposed packets are the sub-bands of EEG rhythm. It appears that db4 is the most suitable wavelet for seizure detection. The sub-bands frequency (0.5-4 Hz), (4-8 Hz), (8-12 Hz) and above 32 Hz are available in $W(4, 0)$, $W(4, 1)$, $W(4, 2)$, and $W(1, 1)$ packets respectively. The sub-bands frequency (12-32 Hz) is obtained by combining the packets $W(4, 3)$ and $W(2, 1)$. The MATLAB R2014b tool in Intel R Core (TM) 2 Duo CPU with 4GB RAM, system is used for all computations. The Figures 3.4 and Figures 3.6 shows the different feature performance of normal EEG signal in delta band and theta band respectively. The Figures 3.5 and 3.7 shows the different features performance of abnormal EEG signal in delta band and theta band respectively.

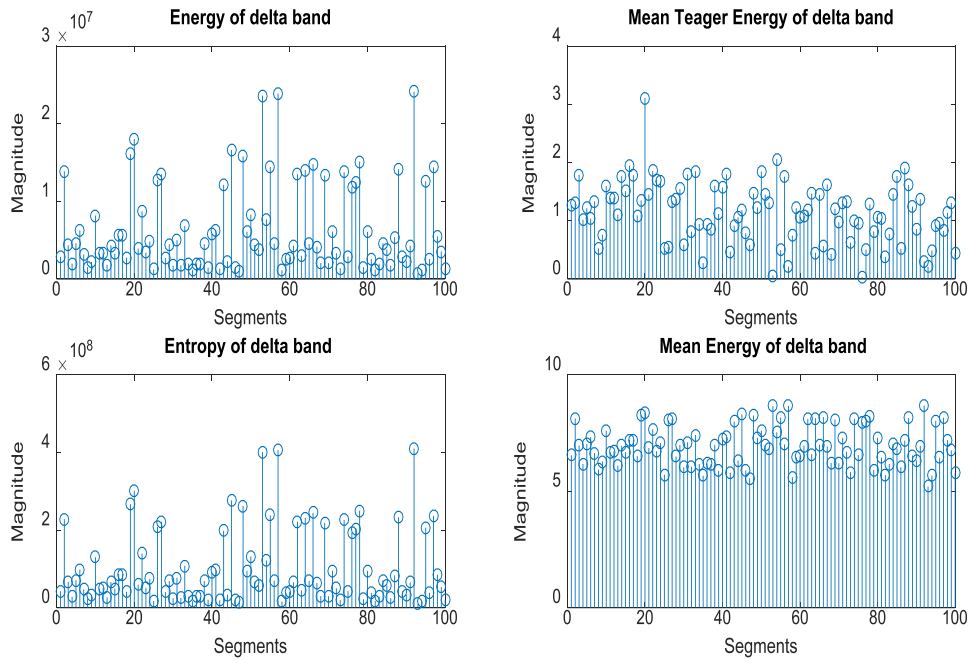


Fig. 3.4 Feature extraction of delta band in the healthy EEG signal

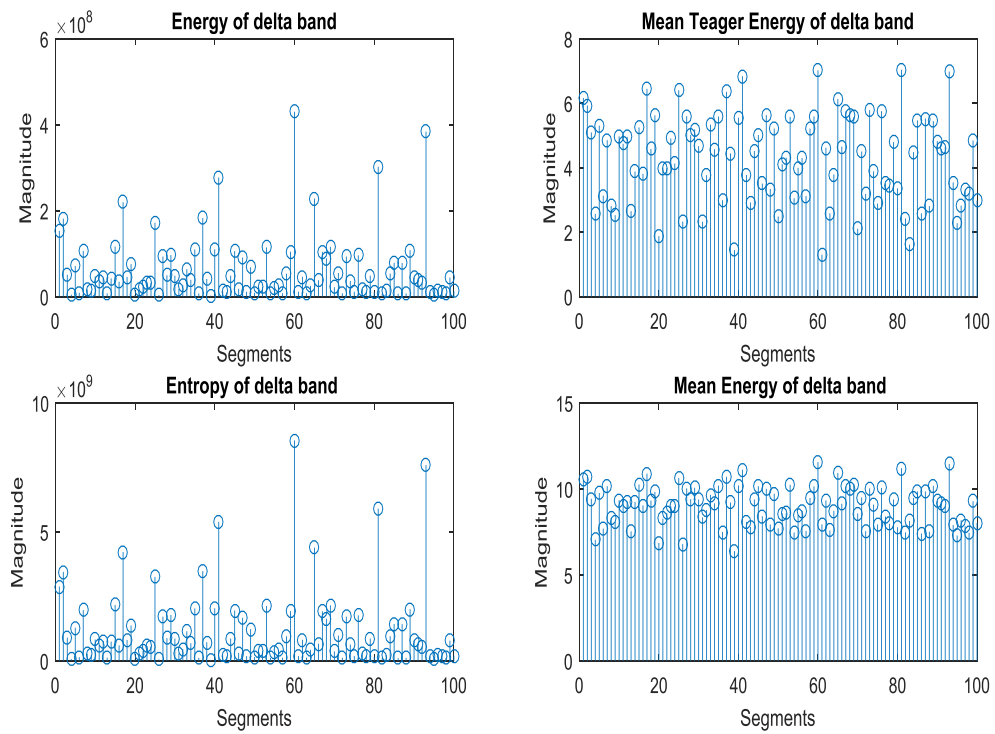


Fig. 3.5 Feature extraction of delta band in the abnormal EEG signal

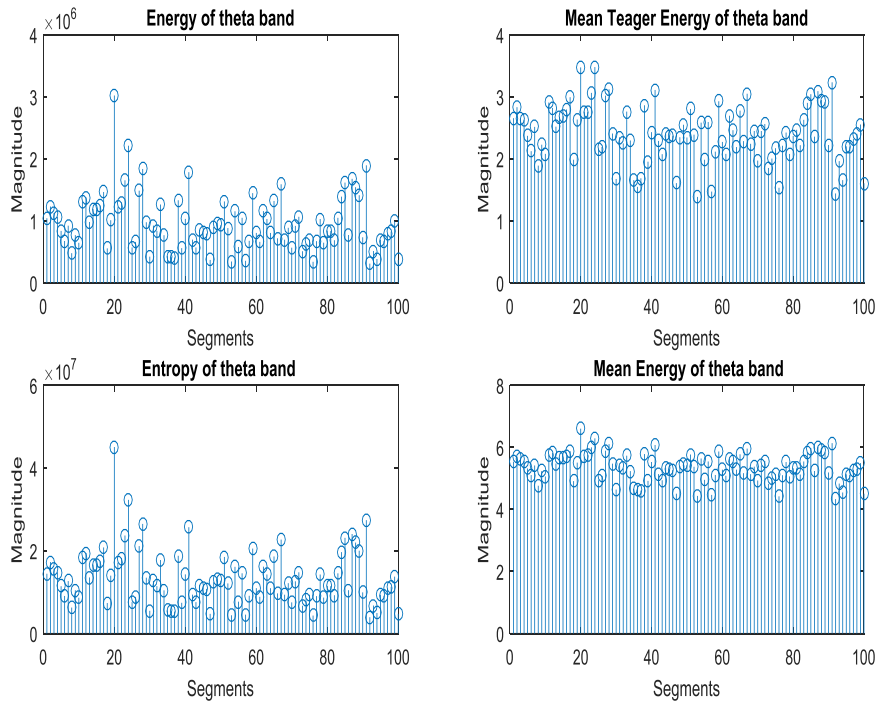


Fig. 3.6 Feature extraction of theta band in the healthy EEG signal

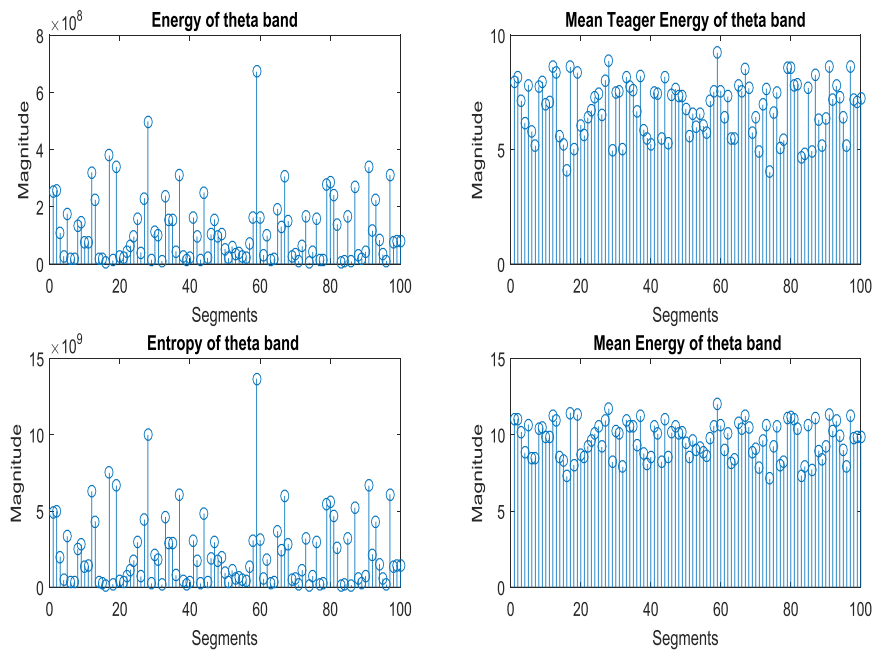


Fig. 3.7 Feature extraction of theta band in the abnormal EEG signal

The feature vectors of proposed sub-bands of healthy EEG and abnormal EEG signals are prepared from the energy, entropy mean energy and mean Teager energy parameters. The parameters extracted from the healthy EEG shows high values than the parameters extracted from it seizure EEG segments. Among the parameters, mean energy and mean Teager energy shows highest values in both the healthy EEG and abnormal EEG signals.

In the case of seizure EEG, the delta band has the highest mean energy than other sub-bands. The next highest value of mean energy is theta sub-band. This indicates that in the abnormal state (epilepsy) the brain produce a high level of energy compare to healthy condition. The feature vectors are given as an input to the Sugeno-type of FIS. Using ANFIS the given input/output data constructs by FIS, whose membership function parameters are tuned using a hybrid optimum algorithm. The input membership function is trimf, which is a triangular form built-in function and output membership function is a linear type. This allows fuzzy systems to learn from the input/output data and model an expert system. Table 3.1 shows average error of FIS training for 500 epochs in different frequency sub-bands of EEG in different feature parameters. Here we used 140 samples for training data, 30 samples for testing data and remaining samples for checking data. We used 7-fold cross validation to verify the performance of the classifier.

Table 3.1: Training error for 500 epoch of EEG sub-bands

Frequency sub-band of EEG					
Features	delta	theta	alpha	beta	gamma
E	0.15416	0.14812	0.27587	0.43215	0.47749
ME	0.16907	0.18527	0.28945	0.47112	0.48058
MTE	3.059 e-07	1.15 e-02	0.38754	0.43137	0.43969
En	0.17257	0.1952	0.28754	0.47529	0.4795

(E-energy, MTE- mean Teager energy, ME-mean energy, En- entropy)

Initially data is loaded for training, testing and checking then FIS is generated by choosing the membership function. Then it starts to train the FIS and finally test the FIS net. The Table 3.1 reveals that the lowest average error in FIS training is in delta and the theta sub-band of EEG. It is understood that characteristics of an epileptic discharge happens in the delta sub-band, but the effect of seizure is also reflected in the theta sub-band. The Figure 3.8 shows the training error of mean Teager energy on the delta band in ANFIS Editor GUI.

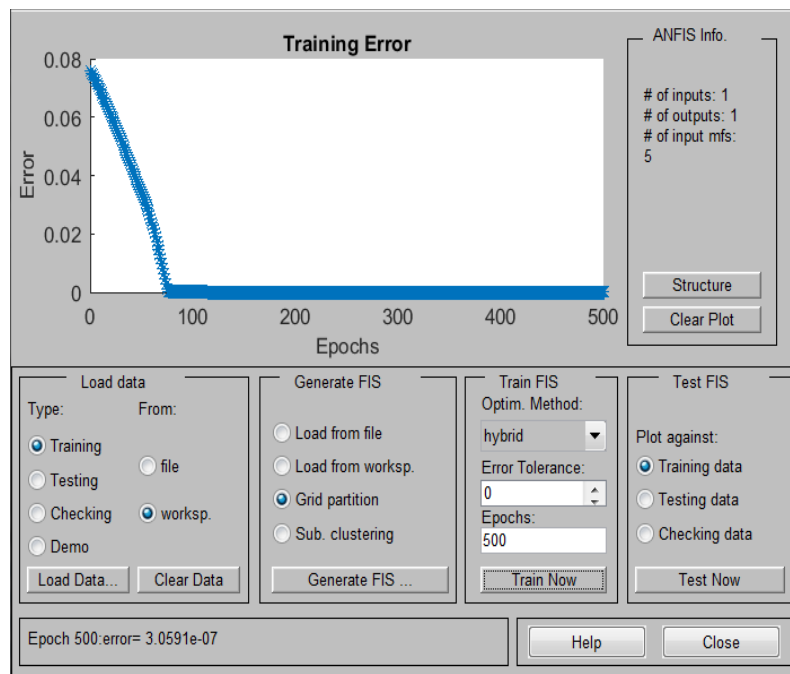


Fig. 3.8 Training error of mean Teager energy on the delta band in ANFIS Editor GUI.

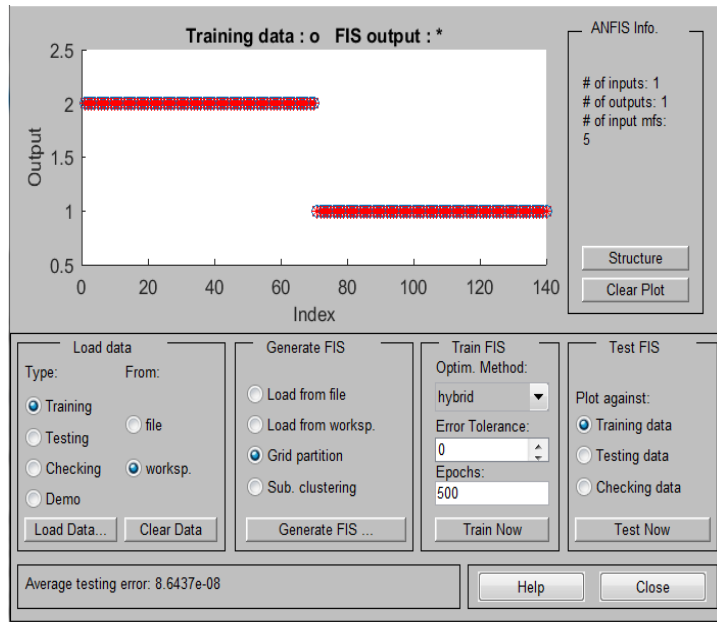


Fig. 3.9 Training data and average testing error of mean Teager energy on the delta band.

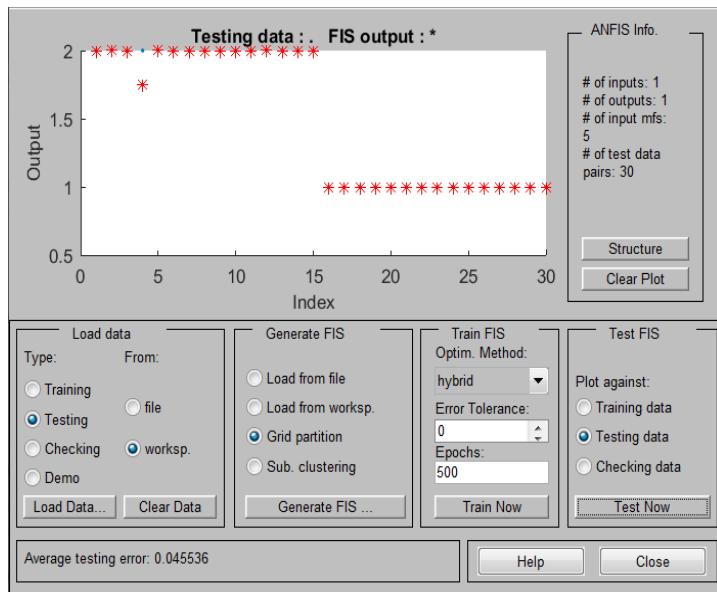


Fig. 3.10 Testing data and FIS output of mean Teager energy on the delta band.

Figure 3.8 shows the mean Teager energy has a training error of 3.059 10-07 in the delta sub-band of EEG. The training error of the mean Teager energy in all EEG sub-bands have much low values compared to other parameters. Figure 3.9 shows training data and average testing error of mean Teager energy on the delta band. The checking data and FIS output of mean Teager energy on the delta band is shown in Figure 3.10. The blue stars are assigned as the desired results, obtained from the EEG metadata and the red stars are the observation of the ANFIS classifier. The Figure 3.10 shows the mean Teager energy on the delta band and it has a total accuracy of 98.33%. The average computation time required for feature extraction of the proposed sub-band is 8.11 s. The average computation time required for classification time of all features in the delta band is 25.02 s (with tuning) and 12.56 s (without tuning). The results show that mean Teager energy is a more suitable parameter for further classification of EEG signals. The total accuracy is same to both ANFIS with tuning and without tuning.

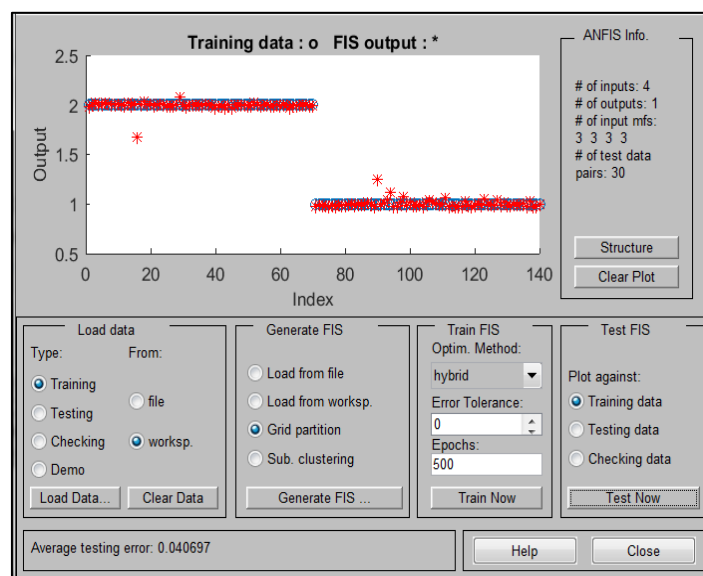


Fig. 3.11 Training data and average testing error of all features in the delta band

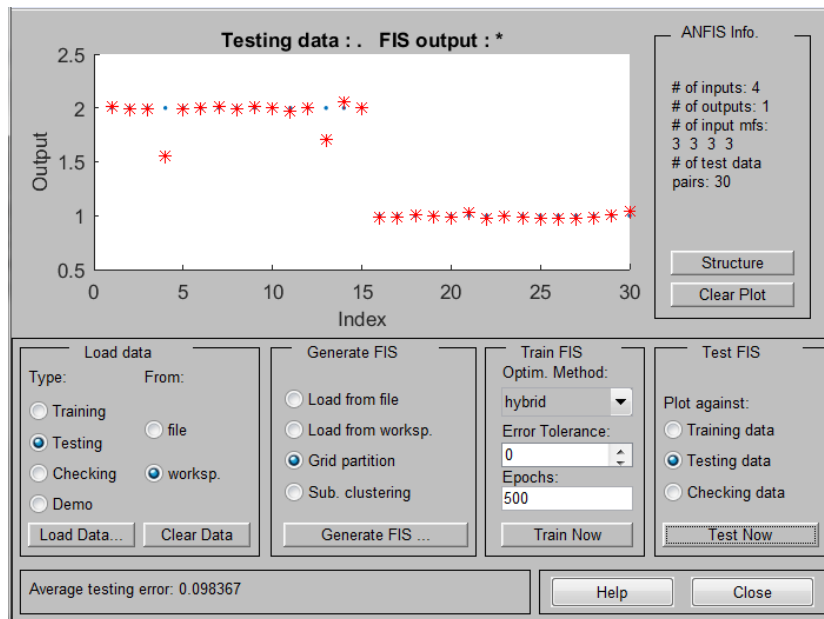


Fig. 3.12 Testing data and FIS output for all features in the delta band.

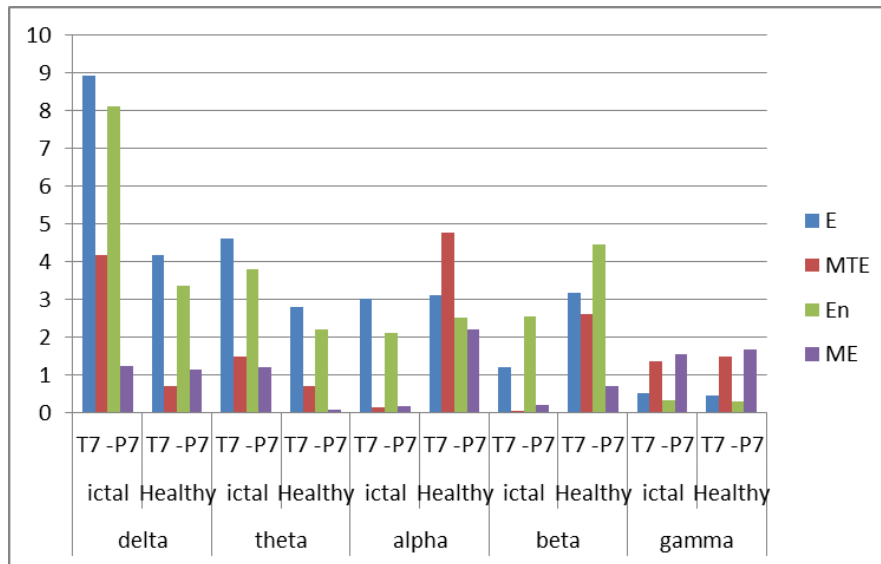
Then all the features of delta band are used as the feature vector for the classifier. Here ANFIS Editor GUI having 4 inputs and one output and hence overall 280 samples for training and 120 samples are employed for testing the classifier. Here, got a training error of 0.04069 for 500 epochs. Figure 3.11 shows the average testing error is 0.0406. Figure 3.12 shows that three samples are misclassified and the testing error is of 0.098. The total classification accuracy for the delta band is obtained as 97.5%. The feature vector of other frequency bands having less classification accuracy than delta band. The average computation time required for classification of the features vectors in the delta band is 13.37 s (with tuning) and 12.92 s (without tuning). Table 3.2 shows the comparison of other methods in wavelet features for the EEG classification.

Table 3.2 Comparison with other methods in wavelet features for EEG classification.

Authors	Methods	Classifier	Classification accuracy (%)
Adeli <i>et al.</i> 2003	Daubechies and harmonic wavelets	Nil	-
Tzallas <i>et al.</i> 2009	Time–frequency distributions	ANN	89
Ocak <i>et al.</i> 2009	ApEn on DWT coefficients	Surrogate data analysis	96
Cao <i>et al.</i> 2010	Wavelet Packet Energy Spectrum	Nil	-
Acharya <i>et al.</i> 2012	Entropies	Fuzzy	98.1
Artameeyanant <i>et al.</i> 2012	WPD and ApEn	BPNN	89.7
Musselman and Djurdjanovic, 2012	Time–frequency distributions features	SVM	99.3
Kumar <i>et al.</i> 2014	Fuzzy ApEn of DWT	ANN, SVM	100
Yang <i>et al.</i> 2014	Permutation entropy and sample entropy	ANFIS	89
Proposed method	EEG sub-band using WPT with MTE	ANFIS	98.33

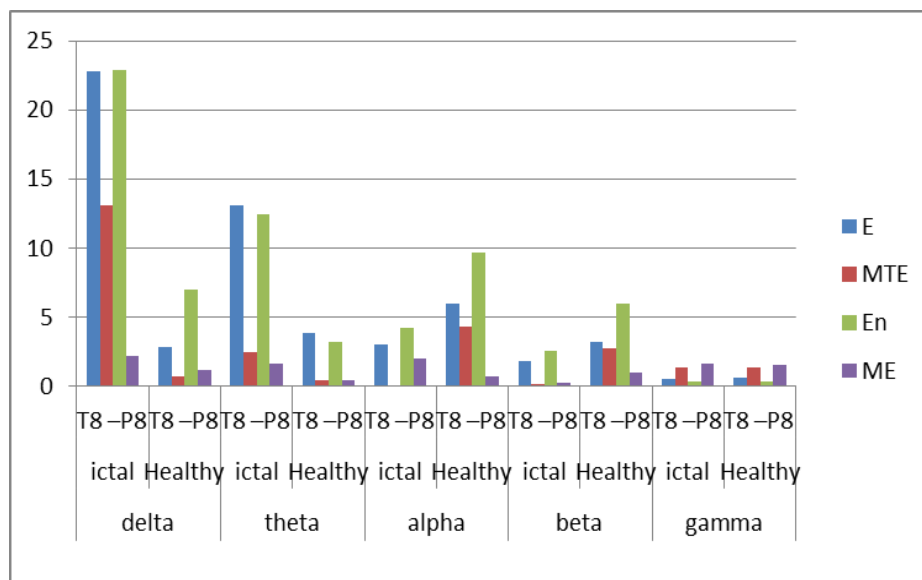
Then the proposed WPT system is applied to another popular EEG database for analysis of the EEG signal. Here the EEG signals at the Temporal- Parietal lobes of T7-P7 and T8-P8 scalp EEG is separated from the CHB-MIT Scalp EEG database (“CHB-MIT Scalp EEG database”, 2014). An unprovoked focal seizure is originated from the temporal lobe of the brain, and is known as temporal lobe epilepsy (TLE). The channel T7-P7 is for EEG recording from the left hemisphere of brain and channel T8-P8 is for recording from the right hemisphere of brain. The duration of each data set varies from 9 hrs. to 48 hrs. The signals are sampled at 256 Hz. The data set Chb01, consists of seven different epileptic seizure occurrences within 45 hrs. Each seizure has an average length of 57 seconds. Each set is sub-divided into 10 seconds

duration with 2560 samples. Initially the EEG data undergoes 64 Hz low pass filter before it decomposes to the different frequency rhythm of delta, theta, alpha, beta and gamma bands using WPT.



(E-energy, MTE- mean Teager energy, ME-mean energy, En- entropy)

Fig. 3.13 Different feature parameters of healthy and abnormal EEG in different EEG sub-bands of channel T7-P7



(E-energy, MTE- mean Teager energy, ME-mean energy, En- entropy)

Fig. 3.14 Different feature parameters of healthy and abnormal EEG in different EEG sub-bands of channel T8-P8

Each sub-band of the two channels is subjected to calculate the entropy, energy, mean energy and mean Teager energy of the EEG signal. This analysis is only focuses on the effect of differential signals at Temporal- Parietal lobes of T7-P7 and T8-P8. Figure 3.13 and Figure 3.14 shows coefficients of different statistical parameters of abnormal (ictal) and healthy EEG in different frequency bands of T7-P7 and T8-P8 channels respectively. It is observed that in Figure 3.13 and Figure 3.14, a sizeable variation exists in the feature parameters of delta band during abnormal EEG (ictal) and a small notable variation is found in theta band. There is no significant change in the high frequency band. During the healthy brain condition, the feature parameters of the alpha band are high. The reason for this is in normal brain the alpha sub-band frequency are active and dominant compare to the other EEG sub-band. The mean Teager energy feature in abnormal state has higher discrepancy between normal EEG in alpha band with respect to other energy-entropy parameters. This indicates that the mean Teager energy feature is the dominated parameter for correlation coefficient between abnormal and normal EEG classification compared to other energy-entropy parameters in the proposed method. It is observed that the values of feature parameters in channel T8-P8 is higher than the parameters of channel T7-P7. The mean Teager energy coefficients show significant variation compared to other feature parameters. The Figures 3.8 and 3.9 shows that the data set Chb01 as a case of TLE, which is a focal seizure originated from the right hemisphere. Table 6.4 shows the comparison of other non-linear algorithms in the EEG classification using the EEG data set.

3.7 INFERENCES

In this chapter, the EEG signal is analysed using wavelet packet transform for feature extraction and '*anfiseditor*' tool of MATLAB R2014b is used for the classification analysis. The wavelet packet transform decomposes the EEG signal into four levels to obtain the frequency rhythm of delta, theta, alpha, beta and gamma bands. Then features of the sub-band coefficients are analysed by different feature parameters like entropy, energy, mean Teager

energy and mean energy. It is observed that at normal condition the brain produce high energy in the alpha sub-band. However at seizure state, the brain energy level in both the delta sub-band and theta sub-band are increased. It is observed that out of four parameters, mean Teager energy coefficient of features have the minimum training error. The total classification accuracy for the mean Teager energy in delta band is 98.33%. The total classification accuracy for the delta band is obtained as 97.5%. The average computation time required for classification of ANFIS without tuning is faster than ANFIS with tuning in this case. It shows that the mean Teager energy is taken as a suitable feature parameter for the classification of healthy EEG and seizure EEG signals.

The proposed system also analyses the effects of EEG sub-band during seizure at temporal lobes of T7-P7 and T8-P8 in another popular EEG database. It is observed that high variations of the proposed energy-entropy parameters, both in the delta sub-band and theta sub-band occurs during seizure EEG. Among the parameters the mean Teager energy shows the significant result in the EEG data set, Chb01.

The limitation of the work is that during the wavelet packet transform decompositions the selected packets do not exactly map to the sub-band of the EEG rhythm. The packets in the tree of the wavelet packet transform, $W(4, 0)$, $W(4, 1)$, $W(4, 2)$ and $W(1, 1)$ are equivalent to EEG sub-bands frequency (0.5-4 Hz), (4-8 Hz), (8-12 Hz) and above 32 Hz respectively. The combined of packets $W(4, 3)$ and $W(2, 1)$ is equivalent to (12-32 Hz). This happens only when $W(0, 0)$ is assigned as 0-64 Hz EEG signal. But some of the assigned sub-band in the WPT band is not exactly same as the EEG frequency. The alpha sub-band is (8-13 Hz), but here we take alpha as (8-12) Hz in $W(4, 2)$. In addition, beta band is (13-30 Hz), but here we took beta as (12-32 Hz). Which is the combination of $W(4, 3)$ and $W(2, 1)$. The gamma band is greater

than 30 Hz, but we compute gamma as (32-64 Hz). There is an overlap in these frequency bands for EEG, which also depends on cut-off frequency of low pass filter selected for the EEG data.

CHAPTER 4

ICTAL EEG ANALYSIS USING HILBERT-HUANG TRANSFORM

EEG is an important tool in clinical diagnosis and research on human brain activity. Recently, empirical mode decomposition (EMD) method is used to analyze the EEG data in a more simple and meaningful approach than other methods. The EEG signal decomposes into intrinsic mode functions (IMF) using EMD. The instantaneous amplitude or envelope and instantaneous frequency information is extracted from each of the IMF components using analytic function. These parameters are used for ictal EEG analysis by computing feature vectors from these twin components. The energy - entropy parameters are extracted from the amplitude contour and statistical parameters are extracted of the instantaneous frequency contour of each the IMF.

In our study, the above discriminative features are extracted using a popular database to classify healthy and ictal EEG signals in three different cases. The different conditions are individual IMF features, multiple features with individual IMF, and individual features with multiple IMFs. Discriminating capability of the three cases were tested using artificial neural network (ANN) and adaptive neuro fuzzy inference system (ANFIS) classification. In addition, we used the analysis of variance (ANOVA) method to analyze the statistical performance of the feature vectors in the above cases.

4.1 INTRODUCTION

The characteristics of the EEG signal exhibit a non-linear and non-stationary behavior. In addition, the characteristic of EEG depends upon the gender, age, disease state or mental condition of the individual. Most of the EEG studies assume that EEG is a wide sense stationary signal and are

analysed either in time-domain and/or frequency-domain, which are mentioned in the literature review. However, analysis of the EEG requires special techniques, which effectively handles the non-stationary behaviour of the signal.

In 1998, Norden E. Huang, proposed a new method known as EMD method, which is suitable for analysis of nonlinear and non-stationary time series signal (Huang *et al.* 1998). In the EMD method any arbitrary time varying signal is decomposed into a finite number of component and residue. Each component is known as intrinsic mode functions (IMF) of the original signal. The IMFs of an arbitrary signal are orthogonal to each other. According to EMD method, during decomposition process the components are said to be an IMF, if it satisfies the following criteria.

- a) In the entire data set, the total number of maxima and minima equal to zero crossings or the difference should not exceed one
- b) The average of the envelopes of local maxima and minima at any instant should be null.

In the EMD method, any data can be decomposed into different independent modes of oscillations. The frequency of the IMF components is descending from higher frequency of the original signal to lower frequency. Finally, in the EMD method the complex signal is converted into IMF components. The instantaneous frequencies of each IMF are a function of intra wave and inter wave modulation in the EEG signal. The inter wave modulation can be analysed using the Fourier transform. The intra wave modulation is because of the nonlinear behavior of the EEG signal (Huang *et al.* 1998).

The EMD decomposition is adaptive because it does not have a fixed basis. The basis of the method is derived from the data. The EMD is based on local information of time series data, which is suitable for the analyses of non-stationary and nonlinear signals.

4.2 THE SIFTING PROCESS: EXTRACTING IMFs

The algorithm for the extraction of IMFs from a raw data is given as below (Huang *et al.* 1998). The sifting process helps to suppress transient wave and keep off the skewness behaviour of the original signal.

For a time series $x(t)$, different steps in the sifting process are:

(i) Interconnecting all the local maxima and local minima of $x(t)$ by cubic spline interpolation to get the envelop $x_{upper}(t)$ and $x_{lower}(t)$ respectively.

(ii) Compute the mean of $x_{upper}(t)$ and $x_{lower}(t)$ envelops, say $m_k(t)$

(iii) Find , $x(t) - m_k(t) = h_k(t)$ (4.4)

Check whether the $h_k(t)$ satisfies the conditions of being an IMF,

If not step (i)-(iii) is repeated, then increment $k = k + 1$ and equate $x(t) = h_k(t)$,

Let initially $k = 0$

else, we get the first component as

$$c_k(t) = h_k(t) \tag{4.5}$$

The $c_k(t)$, where $k = 1$ is a first IMF component

(iv) After getting the first component,

$$x(t) - c_k(t) = r_1(t) \tag{4.6}$$

Where $r_1(t)$ is known as residual signal.

(v) If $r_1(t)$ is monotonic function or a constant, then stop the computation process.

else

Repeat the step (i) to (v)

Finally obtain $r_k(t)$ which satisfies the condition for IMFs.

Figure 4.1 shows the trace of the lower envelopes and the upper envelopes of the data set. To plot that, first we need to identify all the local maxima, and then connect them with a cubic spline line to get the upper envelope. Repeat the procedure for the local minima to produce the lower envelope. Then mean of upper envelope and lower envelope are to be developed. The mean waveform is shown in Figure 4.2. Then check the condition of being an IMF as mentioned in the step (iii). If not repeat the step (i) to (iii). Figure 4.3 shows the first IMF component of the signal. Similarly, obtain all the IMFs of the signal.

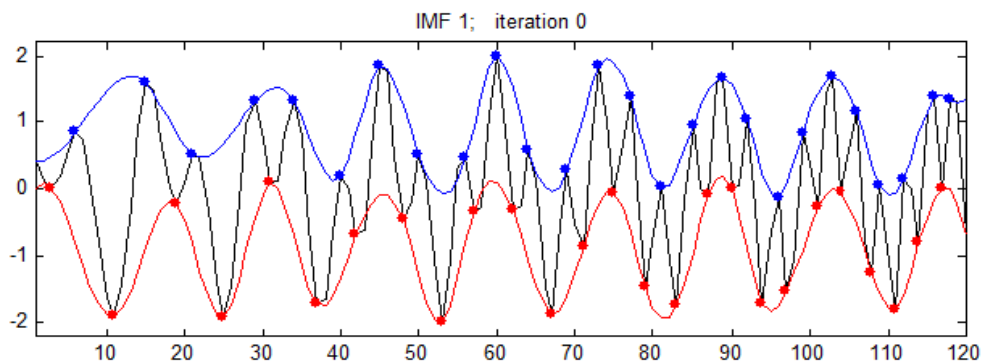


Fig. 4.1 Envelop $x_{upper}(t)$ and $x_{lower}(t)$

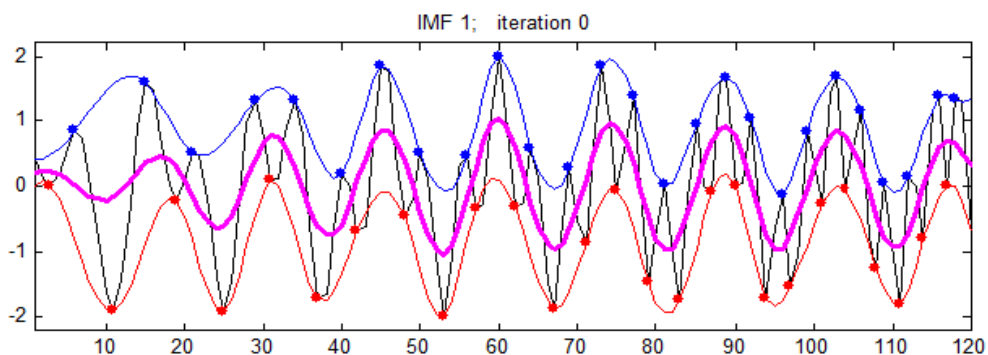


Fig. 4.2 Compute the mean of $x_{upper}(t)$ and $x_{lower}(t)$

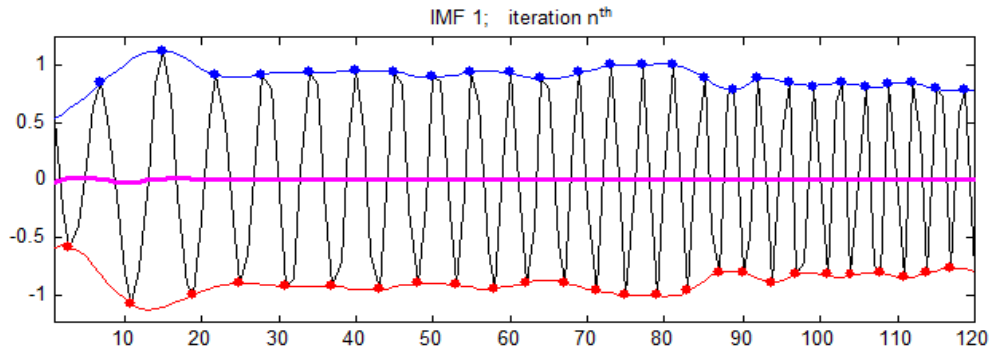


Fig. 4.3 Extract the first IMF

Finally, the arbitrary signal can be expressed as a summation of the residual component and all the IMF components. The decomposed IMF components can be written as

$$x(t) = \sum_{i=1}^k c_i(t) + r_k(t) \quad (4.7)$$

The original signal can be reconstructed by the summation k of all IMFs and the residual of signal. So an arbitrary signal can be expressed as a linear combination of all the IMFs and the residual signal. Each IMF oscillation may be a combination of amplitude modulation and frequency modulation. The number of IMFs depends upon the band of frequency in the EEG segments.

4.2.1 Hilbert-Huang Transform

The Hilbert-Huang transform (HHT) technique is developed to investigate the non-linear and non-stationary behavior of water waves (Huang *et al.* 1998). HHT is a combination of the empirical mode decomposition method and the Hilbert transform (HT) analysis. The Hilbert transform (Bedrosian, 1962), of an arbitrary signal, is defined as the convolution of $\frac{1}{\pi t}$ with $x(t)$. The main advantage of HHT is that it is a powerful tool to convert a

real function of the IMFs into analytic function, which is suitable for analyzing non-linear and non-stationary time series data.

The HT of $x(t)$ is defined as

$$\hat{v}(t) = x(t) * \frac{1}{\pi t} \quad (4.8)$$

The convolution of $x(t)$ and $\frac{1}{\pi t}$ is written as

$$\hat{v}(t) = \frac{1}{\pi} PV \int_{-\infty}^{+\infty} \frac{x(\tau)}{t-\tau} d\tau \quad (4.9)$$

Where PV is the Cauchy Principal Value of the integral

As per equation (4.9), $\hat{v}(t)$ is a single sided signal. A major advantage of Hilbert transform is that real valued continuous signal is extended to an analytical function.

If a signal $z(t)$ is said to be an analytical function of an arbitrary signal $x(t)$, then it can be expressed in terms of real part as $x(t)$ and imaginary part as $\hat{v}(t)$. The $\hat{v}(t)$ is the Hilbert transform of $x(t)$.

$$z(t) = x(t) + i\hat{v}(t) = a(t)e^{-i\theta(t)} \quad (4.10)$$

Where $a(t) = \sqrt{x^2(t) + \hat{v}^2(t)}$ is the instantaneous amplitude of $x(t)$ and the instantaneous phase of $x(t)$ is

$$\theta(t) = \arctan \left[\frac{\hat{v}(t)}{x(t)} \right] \quad (4.11)$$

The instantaneous frequency (IF) of $x(t)$ is defined as the derivative of instantaneous phase given by

$$\omega(t) = \frac{d\theta(t)}{dt} \quad (4.12)$$

The equations (4.10) and (4.12), which are expressed in time-frequency distribution of instantaneous amplitude is defined as the Hilbert Spectrum, $H(\omega, t)$. The marginal spectrum, $h(\omega)$ of $x(t)$ is defined as

$$h(\omega) = \int_0^T H(\omega, t) dt \quad (4.13)$$

The Hilbert spectra will give a wide view of the energy–time distribution of each frequency in an arbitrary signal. The Hilbert spectrum appears better than Wavelet spectrum. The spectrum shows the frequency variations of each IMF.

The instantaneous frequency of the IMFs eliminated the spurious harmonic components in the signal, which contribute the nonlinear effect in the EEG signal. The analysis of instantaneous frequency of the EEG signal is much important, which will reflect the sudden change due to the ictal activities (Picinbono, 1997). In this chapter, statistical nature of the instantaneous frequency and energy-entropy features of instantaneous amplitude are the feature parameters of the different stages of ictal classification.

4.3 METHODOLOGY

The proposed method is shown in Figure 4.4. The objective is to classify seizure attack in EEG segments using features of instantaneous amplitude (IA) and instantaneous frequency (IF). Energy-based features, such as the mean energy (ME), mean Teager energy (TE), and entropy-based features like entropy (En), approximate entropy (ApEn) are calculated as amplitude variation of the EEG. The frequency variation is studied using statistical features of interquartile range (IQR), mean absolute deviation (MAD), and standard deviation (STD) of the frequency function.

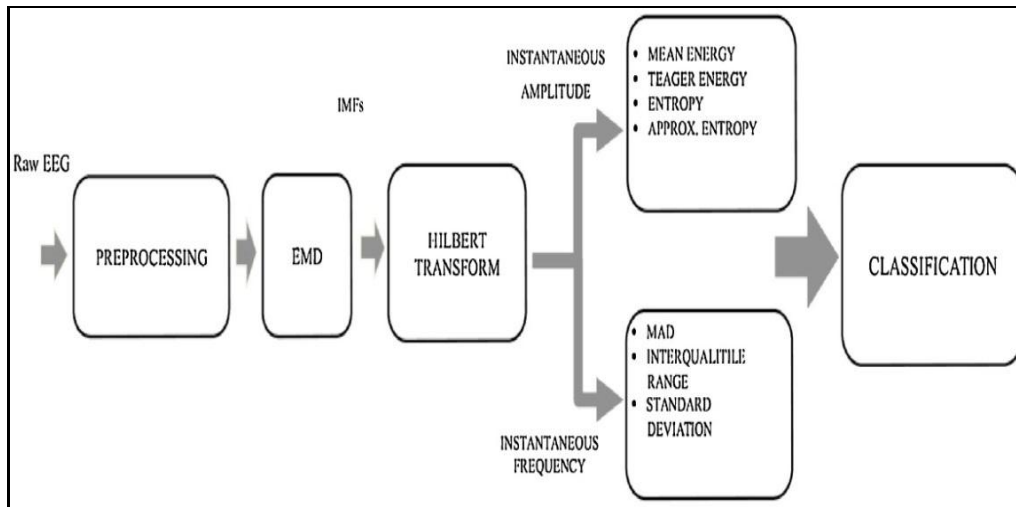


Fig. 4.4 Proposed Methodology

In this study, ANN and ANFIS classifiers are used to examine how features are effectively extracted using discriminating EEG segments with seizure attacks from healthy EEG. In this study, classifications are grouped into three cases depending on the feature vector used. After the classification process, the different classes of the feature vectors are validated using ANOVA, a well-established statistical test.

4.4 FEATURE EXTRACTION

After the HHT computation, the amplitude envelope and frequency functions of the first five IMFs are used for further computations of feature extraction (Oweis and Abdulhay, 2011). According to the Hilbert amplitude spectrum, energy and entropy parameters are essential for extracting feature vectors of IA in HHT (Acharya *et al.* 2012). Statistical parameters, such as interquartile range, mean absolute deviation, and standard deviation, are the parameters for constructing the feature vector of IF in HHT (Gopan *et al.* 2012). The features opted for this work are discussed in Table 4.1, where $x(n)$ is the input EEG sequence of length L.

Table 4.1: Basic equation of energy, entropy and statistical parameters

Sl.no	Feature Parameter	Equation	Remarks
1	Mean energy (ME)	$ME = \log\left(\frac{1}{L} \sum_{n=1}^L x(n) ^2\right)$	
2	Mean Teager-Kaiser Energy (TE)	$MTE = \log\left(\frac{1}{L} \sum_{n=1}^L (x(n)^2 - x(n+1)x(n-1))\right)$	
3	Entropy (En)	$En = - \sum_k p_k \log p_k$	p_k is the probability of the datum being in bin k.
4	Approximate Entropy (ApEn)	$ApEn(N, m, r) = \Phi^m(r) - \Phi^{m+1}(r)$ $\Phi^m(r) = (N - (m - 1))^{-1} \sum_{i=1}^{N-m-1} \ln C_{m,i}(r)$	$C_{m,i}(r)$ is correlation integral, r, N, m integer
5	Interquartile Range (IQR)	$IQR = Q_3 - Q_1$	Q_3 is the third quartile and Q_1 is the first quartile
6	Mean Absolute Deviation (MAD)	$MAD = \frac{1}{L} \sum_{i=1}^L (x(i) - \bar{x})$	\bar{x} is the mean value of $x(i)$
7	Standard Deviation (STD)	$STD = \sqrt{\frac{1}{L} \sum_{i=1}^L (x(i) - \bar{x})^2}$	

4.5 CLASSIFICATION

Here ANN and ANFIS classifiers are being used to classify different cases, which are mentioned as follows and the performance of each classifier is compared. ANN used here is three layer feed forward multilayer perceptron neural network (MLPNN). The number of hidden layer chooses as 15. The number of neuron in the input layer is depends on the different cases used in the study. The output layer is a bilinear classifier. The ANN acquires knowledge from the training set of feature vector using the learning algorithm. The popular back-propagation learning algorithm is used in ANN. The back-propagation is a scaled conjugate gradient-based algorithm, which has many different types. Through back-propagation, ANN attempts to correlate inputs and the desired output. To achieve the desired output, the weights of the interlink nodes are adjusted in each epoch using the training process (Vogl et al. 1988; Møller, 1993). The different cases of feature vector are given as an input to ANFIS. The ANFIS Editor, which a toolbox function in MATLAB R2016b, constructs a fuzzy inference system (FIS) using input/output data set and membership function parameters are tuned using back-propagation algorithm (Güler and Übeyli, 2005). The ANFIS with tuning and without tuning for FIS structure generation (Jang, 1993) are explained in section 3.5. To facilitate ictal classification, we formulated different cases based on the feature vector. The three different cases are

Case 1: Use of a single feature of individual IMF

Case 2: Use of multiple features of individual IMF

Case 3: Use of single feature of multiple IMFs

4.5.1 Performance Evaluation

The effectiveness of the proposed feature parameters is evaluated using total classification accuracy, sensitivity, and specificity. Based on the classification and metadata in the database, the True Positive (TP), True

Negative (TN), False Positive (FP), and False Negative (FN) events in the performance measures are computed as follows (Brodu *et al.* 2012; Sharma and Pachori, 2015; Riaz *et al.* 2016). The true positives are the data, which are correctly identified as ictal EEG, or healthy EEG. False positives are the data, which are incorrectly identified as ictal EEG, or healthy EEG. True negatives are the data which are correctly rejected. False negatives are the data, which are incorrectly rejected. The sensitivity is the ratio of the number of true positive values to the number of actual positive cases. The specificity is the ratio of the number of true negative values of the number of actual negative cases. The total classification accuracy is the ratio of the number of correctly detected values to total number of cases for the machine learning process. The performance measures are defined as.

$$\text{Total Classification Accuracy} = \frac{TP+TN}{TP+TN+FP+FN} * 100\% \quad (4.14)$$

$$\text{Sensitivity} = \frac{TP}{TP+FN} * 100\% \quad (4.15)$$

$$\text{Specificity} = \frac{TN}{TN+FP} * 100\% \quad (4.16)$$

4.6 RESULTS AND DISCUSSION

This study proposes the use of ictal classification, which is based on the amplitude and frequency contours of IMFs. It is comprised of the raw EEG data of each group acquired using a low-pass filter with cutoff frequency of 60 Hz, so as to avoid noise components in the higher frequencies. Section 4.1, gives a clear-cut description about computation of IMF by applying the EMD algorithms.

In the EEG database, discussed in Section 2.2, we considered 100 EEG segments in the proposed work. Each set of the segments has a length of 4096 samples. Each segment was further divided into blocks with a length of 256. Each segment has 16 blocks, and each EEG set has 1600 data blocks. Figure 4.5 shows the sample waveform of different IMFs of the healthy EEG from

group A. Figure 4.6 shows the sample waveform of different IMFs of the ictal EEG from group E respectively. In this study, EEG signals are decomposed into only five sets of IMFs. Abscissa represents the number of samples considered and the ordinate represents the signal amplitude in microvolts. Figure 4.5 and Figure 4.6 show that the first IMF components are having higher cycles than the upcoming IMFs components. It is clearly seen from the Figures that there is remarkable difference between the two set of IMF components.

Orosco *et al.* conducted several initial tests and concluded that the lower frequency components in the IMFs do not contribute to seizure detection. So these IMFs are discarded in the EEG analysis including the residual signal, which is a monotonic slope, or a function with only one extrema (Orosco *et al.* 2011). The residual signal is have non-zero values during the sifting process of EMD, which does not obey criteria for an IMF. In EMD decomposition of an EEG segment of 1 s length in its IMF, the higher IMFs is discarded because the amplitude of these IMFs are 20 times minor than IMF1 (Diez *et al.* 2009). In this study, the residual signal is not considered for ictal classification (Sharma and Pachori, 2015; Djemili *et al.* 2016; Riaz *et al.* 2016). The main features of the ictal EEG are closely related to the initial IMFs (Li *et al.* 2013).

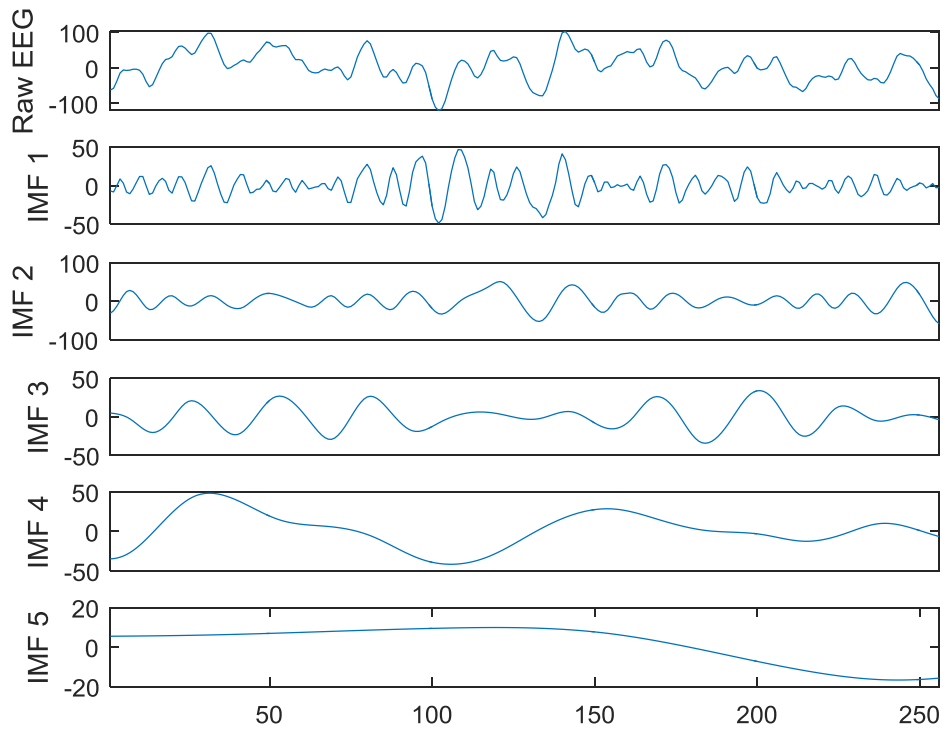


Fig. 4.5 IMFs of healthy EEG

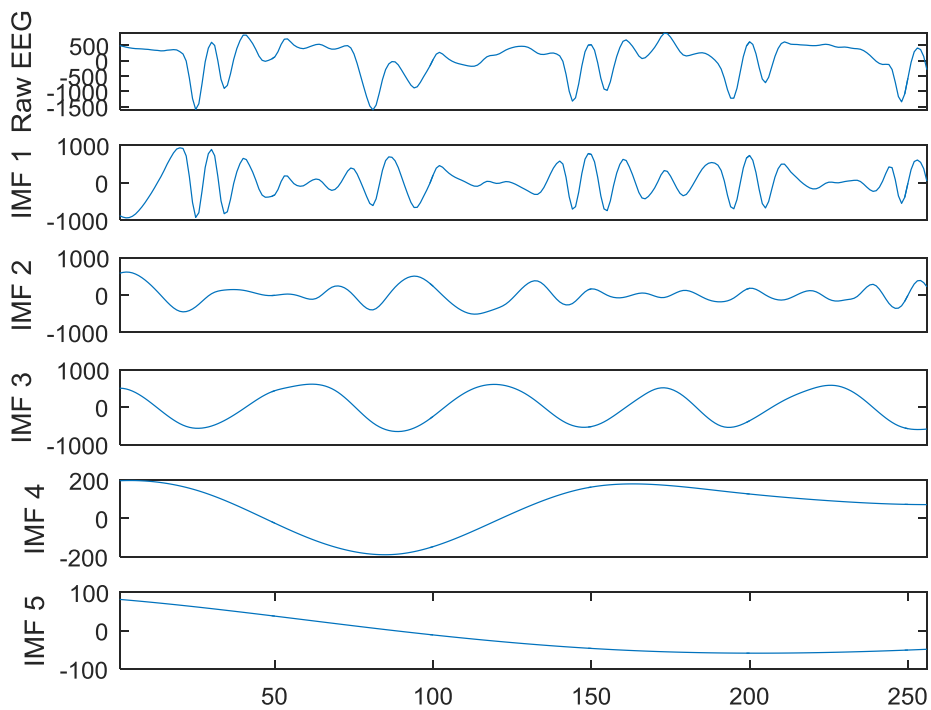


Fig. 4.6 IMFs of ictal EEG

The instantaneous amplitudes and instantaneous frequencies of each IMF are computed using the analytic function. The energy features mean energy, mean Teager energy, and entropy-based features like entropy, approximate entropy were computed respectively from the instantaneous amplitudes of IMFs. The statistical features of the IMF frequency function are also tabulated. Two classifications, namely, ANN and ANFIS, are considered in this study as mentioned in Section 4.5.

In this study, we considered all the available EEG segments in the database, so there is no need of population sampling. The features obtained from the first four IMFs are considered in the study. Thus, each IMF is treated using Hilbert transform. Then IA and IF functions are obtained. The energy and entropy feature parameters are tabulated in each IA function, and statistical features are tabulated in IF function. The healthy class comprises the features of groups A and ictal class from group E of the EEG data. Out of the total feature set, 70% was used for training and 15% was for validation. The rest of the data were used for testing purposes to ensure 7-fold validation. The MATLAB R2016a tool in Intel R Core (TM) 2 Duo CPU with 4GB RAM, system is used for all computations. The computation time required for extracting IA and IF components from the EEG is 10.4 s per each category of the data set.

Figure 4.7 (a) shows the distribution of energy of HHT on a time–frequency scale for healthy EEG. Figure 4.7(b) shows the distribution of energy of HHT on a time–frequency scale for ictal EEG. The Hilbert amplitude spectrum in Figure 4.7 indicates that a shift in energy spread toward lower frequencies and increase in the magnitude of energy can be observed when seizure occurs. Based on this finding, we examined the energy and entropy based features extracted from instantaneous amplitude function for ictal classification. The variation of the instantaneous frequency is also statistically extracted. The features are then analyzed for the characterization of EEG signal.

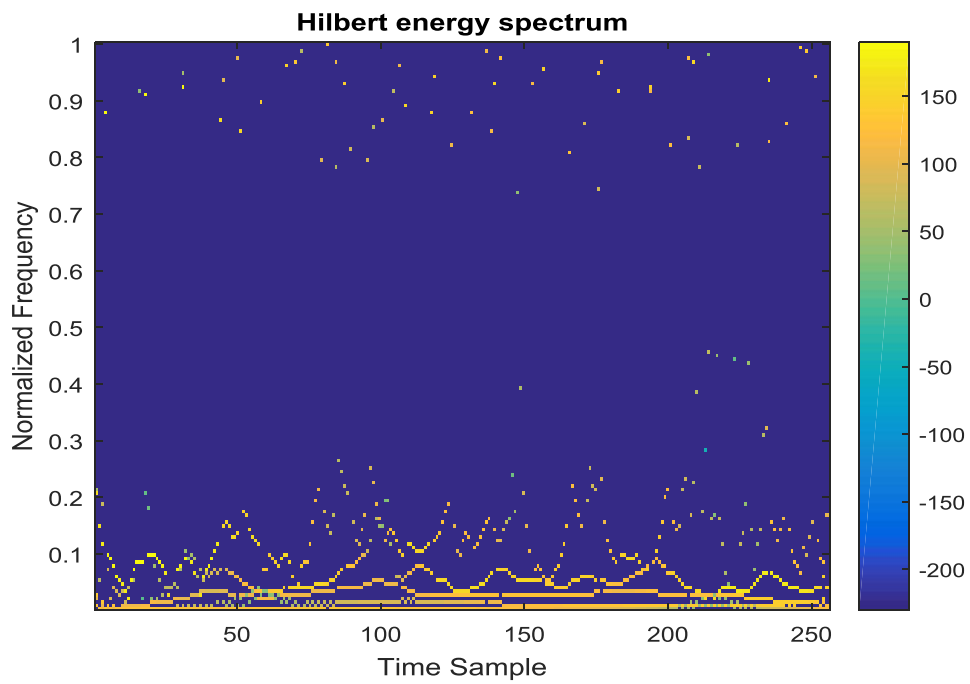


Fig. 4.7 (a) Hilbert–amplitude spectrum for healthy EEG and ictal EEG

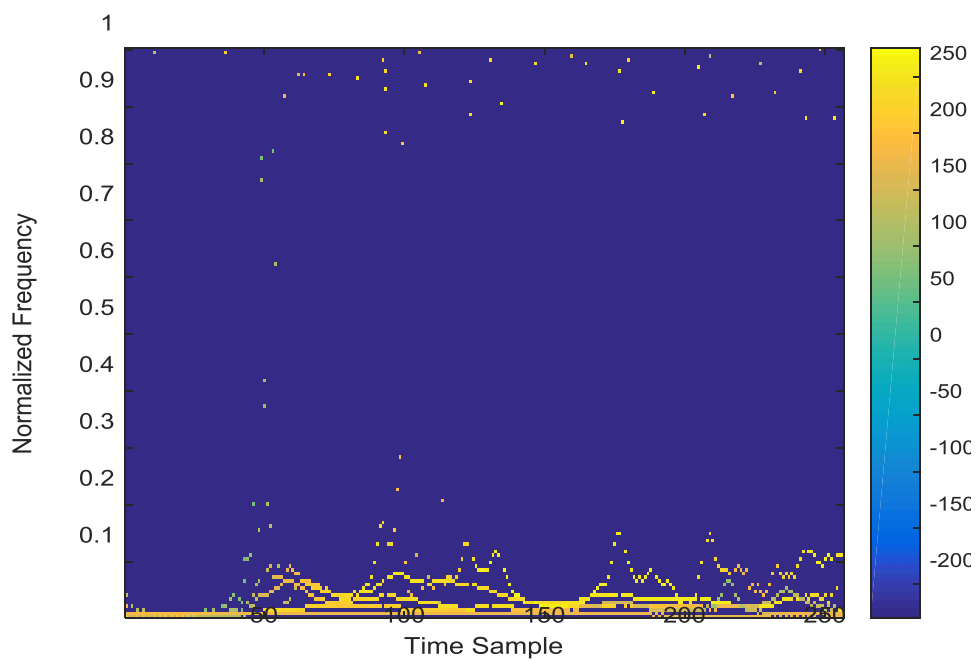


Fig. 4.7 (b) Hilbert–amplitude spectrum for ictal EEG

Three cases were considered in this study. In Case 1, every single feature was used independently for each IMF in a separate manner. In Case 2, multiple features of IA and IF are considered as the feature vector of each individual IMF. In Case 3, single feature was used from multiple IMFs of IA and IF. Thus, energy features ME and TE and entropy features En and ApEn in Case 1 were computed from the instantaneous amplitudes of the first five IMFs. Each EEG sets is computed. Instantaneous frequency features are then tabulated from the first five IMFs of each EEG set. Thus, twenty different parameters were found in IA. Fifteen parameters are taken in IF. Every feature was obtained independently from each IMF. Figures 4.8(a), 4.8(b), 4.8(c), 4.8(d), 4.9(a), 4.9(b), and 4.9(c) show the average values and standard deviation within different data set of features under study. The mean values of the feature sets indicate that they vary significantly in the two groups for all the features computed. It also have small values of standard deviation. In Case 2, IMF1, IMF2, IMF3, IMF4 are the vectors of combined features of individual IMF. In Case 3, ME_IA, TE_IF, En_IA, and ApEn_IF are feature parameters of instantaneous amplitude function of ME, TE, En, ApEn respectively, and IR_IF, MAD_IF, and STD_IF are feature parameters of instantaneous frequency function of IR, MAD, and STD respectively. The average computation time for feature extraction of the instantaneous amplitude of IMFs is 53.38 s per each IMF in each category of the data set. The average computation time for feature extraction of the instantaneous frequency of IMFs is 9.44 s per each IMF in each category of the data set.

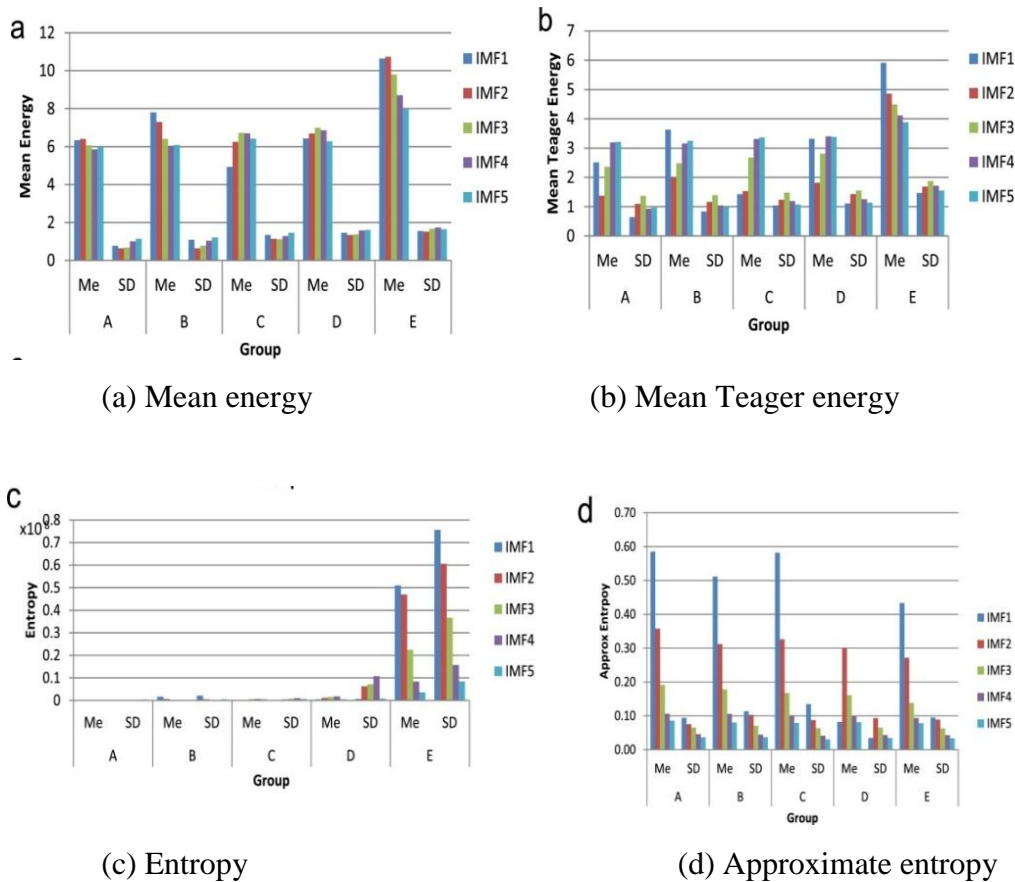


Fig. 4.8 Mean and standard deviation of feature from amplitude function

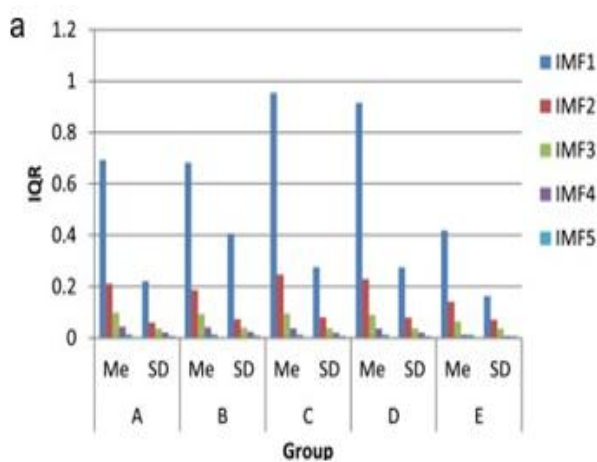


Fig. 4.9 (a) Mean and standard deviation of interquartile range feature from frequency function

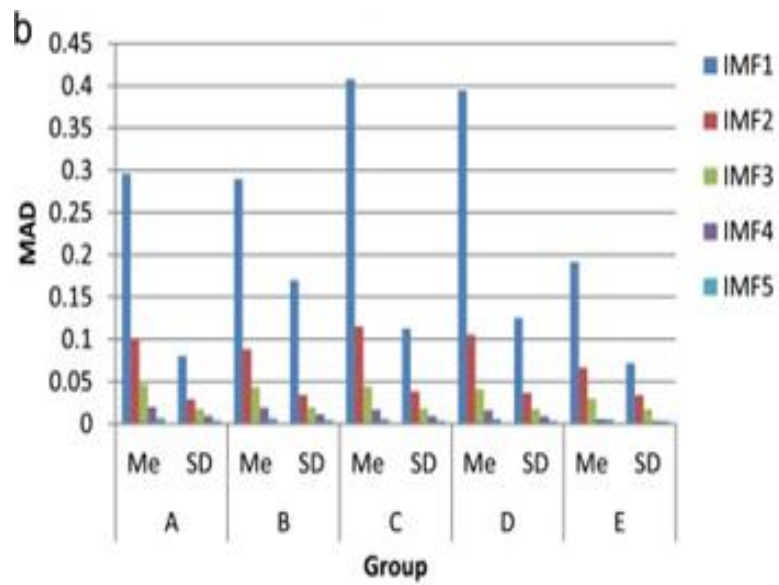


Fig. 4.9 (b) Mean and standard deviation of mean absolute deviation feature from frequency function

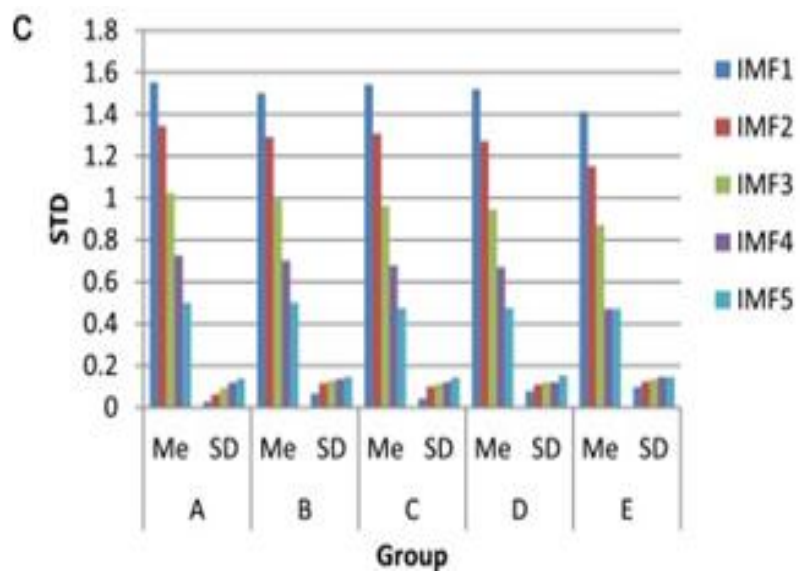


Fig. 4.9 (c) Mean and standard deviation of standard deviation feature from frequency function

Table 4.2 Statistical analysis of different individual IMF features

Features	N	mean	std	std Error	F	sig	F-Rank
Statistical analysis of features from IA							
ME_IA1	4800	8.260553	2.142585	0.030926	7732.511	0.000	3
TE_IA1	4800	4.018363	1.75992	0.025402	6613.37	0.000	4
En_IA1	4800	1.76E+08	4.96E+08	7164612	1399.418	0.000	10
ApEn_IA1	4800	5.10E-01	1.19E-01	0.001713	1276.942	0.000	11
ME_IA2	4797	8.142716	2.124049	0.030668	13752.17	0.000	1
TE_IA2	4797	2.738934	2.027118	0.029268	5788.537	0.000	5
En_IA2	4797	1.59E+08	4.13E+08	5961133	1889.718	0.000	8
ApEn_IA2	4797	3.14E-01	9.62E-02	0.001389	506.122	0.000	15
ME_IA3	4797	7.425251	2.026768	0.029263	10341.95	0.000	2
TE_IA3	4797	3.110604	1.842065	0.026596	1863.837	0.000	9
En_IA3	4797	76298988.1	2.36E+08	3413544	1175.222	0.000	12
ApEn_IA3	4797	0.169141	6.99E-02	0.00101	530.892	0.000	14
ME_IA4	4782	6.869021	1.843094	0.026653	2395.779	0.000	6
TE_IA4	4782	3.489095	1.350156	0.019525	290.926	0.000	18
En_IA4	4782	29326356.9	98658681	1426693	660.023	0.000	13
ApEn_IA4	4782	0.101958	0.044755	0.000647	78.647	0.000	19
ME_IA5	4515	6.672518	1.630384	0.024264	2058.366	0.000	7
TE_IA5	4515	3.44823	1.237119	0.018411	300.371	0.000	17
En_IA5	4515	13764413.5	51307150	763570.3	459.486	0.000	16
ApEn_IA5	4515	0.081539	0.035785	0.000533	18.454	0.000	20
Statistical analysis of features from IF							
IQR_IF1	4746	0.598322	0.31085	0.004512	948.541	0.000	7
MAD_IF1	4746	0.259068	0.125909	0.001828	790.863	0.000	8
STD_IF1	4746	1.49E+00	9.10E-02	0.001322	2630.822	0.000	2
IQR_IF2	4746	1.80E-01	7.38E-02	0.001072	738.668	0.000	12
MAD_IF2	4746	0.085488	0.035515	0.000516	780.769	0.000	9
STD_IF2	4746	1.262892	0.131955	0.001915	2563.289	0.000	3
IQR_IF3	4774	8.51E-02	4.02E-02	0.000582	757.657	0.000	11
MAD_IF3	4774	4.01E-02	1.94E-02	0.000281	764.93	0.000	10
STD_IF3	4774	0.96223	0.13625	0.001972	1338.985	0.000	6
IQR_IF4	4558	0.032605	0.023641	0.00035	2375.008	0.000	4
MAD_IF4	4558	0.01492	1.10E-02	0.000163	2307.345	0.000	5
STD_IF4	4558	0.634434	1.76E-01	0.002606	3278.079	0.000	1
IQR_IF5	4650	0.013991	0.00916	0.000134	25.101	0.000	15
MAD_IF5	4650	0.006385	0.004332	6.35E-05	29.426	0.000	13
STD_IF5	4650	0.490645	0.143553	0.002105	28.287	0.000	14

Table 4.3 Statistical analysis of multiple features with individual IMFs

Feature vector	N	mean	std	std Error	F	sig	F-Rank
IMF1	33411	25309121.1	1.98E+08	1083310	1010.392	0.000	2
IMF2	33426	22878935.7	1.66E+08	908400.8	1252.083	0.000	1
IMF3	33510	1.09E+07	9.34E+07	509949.9	896.4	0.000	3
IMF4	32801	4.28E+06	3.91E+07	215684	709.808	0.000	4

Table 4.4: Statistical analysis of Individual features from multiple IMFs

Feature vector	N	mean	std	std Error	F	sig	F-Rank
Statistical analysis of features from IA							
ME_IA	19176	7.675107	2.114221	0.015268	27464.17	0.000	1
TE_IA	19176	3.339238	1.824955	0.013179	9882.568	0.000	2
En_IA	19176	1.10E+08	3.53E+08	2546220	4224.966	0.000	3
EnAp_IA	19176	2.74E-01	1.79E-01	0.001293	480.771	0.000	4
Statistical analysis of features from IF							
IQR_IF	18797	0.22583	0.275569	0.00201	524.011	0.000	2
MAD_IF	18823	0.100637	0.116338	0.000848	482.598	0.000	3
STD_IF	18770	1.09E+00	3.48E-01	0.002538	931.357	0.000	1

We have computed the feature ranking of both instantaneous amplitude (IA) features and instantaneous frequency (IF) features. The feature ranking (F-Rank) was also applied in all three cases as single feature of individual IMF, multiple features of individual IMF, and single feature of multiple IMFs respectively.

The ANOVA test is a popular statistical test for finding significant differences between two or more groups. Here ANOVA was done in all the three cases to study about the discriminatory level of the features in the data

set. Table 4.2 shows the statistical analysis of different individual IMF features are calculated. The features of the IMF5 having low F-value in the ANOVA table. This indicates that the residual signal is the offset of EMD and these dc values contained no information about ictal EEG. Table 4.3 shows the ANOVA test of multiple features with individual IMFs. Table 4.4 shows the ANOVA result of individual features from multiple IMFs. The statically analysis is carried out by using SPSS, a popular statistics software for business and research activity.

Table 4.2 shows the significant difference among groups under study where all the p-value is less than 0.001. The results of ANOVA test are performed at the 95% confidence level in all cases. A feature rank is obtained from the descending F-value of the ANOVA table of both IA parameters and IF parameters. In Table 4.3 ANOVA results of multiple features with individual IMFs. The table shows that a significant value (p- value) is less than 0.001 is obtained in every case. As per the F-ranking, IMF2 dominates among the IMFs and it is followed by IMF1, IMF3 and IMF4 respectively. Significant difference between the two groups and exact zero value, are obtained in all the IMFs. The Table 4.4 shows the result of individual features from multiple IMFs. In feature ranking, ME_IA, TE_IA, and STD_IF are dominating in each category. The features from amplitude contour exhibits significant difference between the two groups and p-value is equal to 0.000 in all vectors. These results strongly suggest the suitability of the representative features of data for classification.

The ANN and ANFIS classifiers are employed to study how the extracted features can be effectively used in discriminating EEG segments with seizure attacks from healthy ones. Here the three cases of classification are performed, which was explained earlier. The performance of the classifiers is determined by the computation of sensitivity, specificity, and total

classification of accuracy as mentioned in Equations 4.14, 4.15 and 4.16, respectively. Tables 4.5, 4.6 and 4.7 revealed that the achievement of performance of the ictal classification in term of accuracy, sensitivity, and specificity.

Table 4.5 : Accuracy (%) for Case1: Single features for individual IMFs

	CL-1	CL-2	CL-3	CL-4	CL-5
Features from IA					
ME	100.00	100.00	84.60	95.00	100.00
TE	100.00	92.00	62.00	88.00	83.00
En	99.00	100.00	83.60	95.00	100.00
ApEn	75.00	70.00	83.00	60.00	61.00
Features from IF					
IQR	80.85	95.74	77.73	89.14	92.17
MAD	76.6	94.89	79.62	88.69	95
STD	92.55	100	84.03	92.08	72.61

Table 4.6 : Sensitivity (%) for Case1: Single features for individual IMFs

	CL-1	CL-2	CL-3	CL-4	CL-5
Features from IA					
ME	100.00	100.00	97.20	90.00	100.00
TE	100.00	88.00	91.00	90.00	80.00
En	100.00	100.00	98.00	90.00	100.00
ApEn	64.00	72.00	90.00	74.00	50.00
Features from IF					
IR	79.57	94.89	100.00	84.62	88.70
MAD	78.30	94.04	100.00	85.52	93.48
STD	100.00	100.00	94.54	84.16	97.83

Table 4.7: Specificity (%) for Case1: Single features for individual IMFs

	CL-1	CL-2	CL-3	CL-4	CL-5
Features from IA					
ME	100	100	72	100	100
TE	100	96	33	86	86
En	98	100	69	100	100
ApEn	86	68	76	46	72
Features from IF					
IR	82.13	96.60	55.46	93.67	95.65
MAD	74.89	95.74	59.24	91.86	96.52
STD	85.11	100.00	73.53	100.00	47.39

In Case 1, every feature was used independently for each IMF in a separate manner to check how each feature behaves independently. The average computation time for the ANN classifier of single features for individual IMFs is 13.14 s. In the Tables 4.5, 4.6, and 4.7 shows that the energy-based features had better performance than the entropy-based features. Frequency-based features also perform well in the classification. Among the IMFs, first and second IMFs have high classification accuracy. Table 4.8 shows the results of two classifiers with multiple features of individual IMFs.

Table 4.8: Classification for Case 2: Multiple features with individual IMFs

	ANN			ANFIS		
	Accuracy (%)	Sensitivity (%)	Specificity (%)	Accuracy (%)	Sensitivity (%)	Specificity (%)
IMF_CL-1	98.80	100.00	97.61	100.00	100.00	100.00
IMF_CL-2	99.52	100.00	99.04	100.00	100.00	100.00
IMF_CL-3	98.09	96.19	100.00	97.00	95.00	98.00
IMF_CL-4	98.00	96.19	100.00	89.00	78.00	100.00

In Case 2, multiple features with individual IMFs are considered as feature vectors to the classifiers. Four classes with representative features from amplitude and frequency contour were used, namely, IMF_CL-1, IMF_CL-2, IMF_CL-3, and IMF_CL-4. The last component of IMF-5 is not considered

here because it is almost monotonous in nature. All the cases compare the classification performance of both ANN and ANFIS classifiers. The average computation time for the ANN classifier of multiple features with individual IMFs is 9.67 s and for the ANFIS classifier is 855 s (with tuning) and 750 s (without tuning). Table 4.8 shows that the performance of ANFIS in IMF_CL1 and IMF_CL2 was better than that of ANN. However, performance of ANN is not much difference in the four classes of IMFs.

Table 4.9: Classification for Case 3: Individual features from multiple IMFs

	ANN			ANFIS		
	Accuracy (%)	Sensitivity (%)	Specificity (%)	Accuracy (%)	Sensitivity (%)	Specificity (%)
ME_IA	100.00	100.00	100.00	92.00	94.00	90.00
TE_IA	99.29	99.00	100.00	100.00	100.00	100.00
En_IA	100.00	100.00	100.00	61.00	100.00	22.00
ApEn_IA	88.33	93.81	82.86	81.00	76.00	86.00
IQR_IF	95.00	93.33	96.67	65.00	100.00	30.00
MAD_IF	95.71	94.76	96.67	48.00	56.00	40.00
STD_IF	100.00	100.00	100.00	74.00	84.00	64.00

In Case 3, all the four IMFs were used to form the feature vector with only one feature for classification. A four-dimensional vector was obtained with one feature, which was used as the input to the classifier. Thus, we have seven classifiers with seven separate features in both IA and IF contours. Table 4.9 gives the result of individual features from multiple IMFs. The average computation time for the ANN classifier of individual features from multiple IMFs is 10.21 s. and for the ANFIS classifier is 50.72 s (with tuning) and 12.62 s (without tuning). Entropy-based features have better classification accuracy than that in Case 1 where they were used individually.

The features in the CL-2, is same as the second IMF components have good sensitivity and specificity in the classification. Among the features considered, the mean energy and entropy of the amplitude contour of IMF2

has 100% accuracy with 100% specificity. The standard deviation of the frequency contour has 100% accuracy, sensitivity, and specificity. The mean Teager energy shows good performance of IMF1 with 100% accuracy, but the performance is lower for other IMFs. Even though MAD and IQR do not have good performance as standard deviation, accuracy above 94% was maintained for IMF2. Table 4.10 presents a comparison of this ictal classification with other time-frequency based method.

Table 4.10 Comparison with other ictal classification algorithms in the literature

Authors	Methods	Classification Accuracy (%)
Oweis and Abdulhay, 2011	EMD weighted frequency	94
Martis <i>et al.</i> 2012	AR spectrum features of EMD with regression tree	95.33
Liu <i>et al.</i> 2012	features of EMD and SVM	98
Bajaj and Pachori, 2012	EMD bandwidth LSSVM	99.5 - 100
Alam and Bhuiyan, 2013	Higher order statistics of IMFs and ANN	80-100
Bajaj and Pachori, 2013	Area measure of analytic IMFs of EEG signals	93.7
Kumar <i>et al.</i> 2014	Fuzzy ApEn of DWT & ANN,SVM	100
Fu <i>et al.</i> 2015	HHT of EEG TF images and SVM	99.12
Riaz <i>et al.</i> 2016	Temporal and Spectral EMD and SVM	96
Djemili <i>et al.</i> 2016	EMD and MLPNN	97.7
Proposed method	Energy of IA and SD of IF from HHT	100

4.7 INFERENCES

Empirical mode decomposition is an efficient tool in the analysis of non-stationary signals. The IMFs obtained from Hilbert transform provide an excellent time–frequency representation of signal energy. In this chapter, after computing Hilbert–Huang transform, the different features of instantaneous amplitude and instantaneous frequencies of HHT are calculated for the feature vectors of the classifiers. Here, two types of classifiers, namely, artificial

neural network and adaptive neuro-fuzzy inference system models, are used to evaluate the performance of the system. Features such as mean energy, mean Teager energy, entropy, and approximate entropy are calculated from the amplitude contour of each IMFs and other features such as interquartile range, absolute deviation, and standard deviation are computed from instantaneous frequencies. In this study, classification was grouped into three cases depending on the feature vector used a single feature of individual IMF, multiple features of individual IMF and single feature of multiple IMFs. Before classifying, the different classes of features are validated using ANOVA, a well-established statistical test. The result shows that significant differences (value of $p < 0.001$) are obtained in every individual IMF of ictal EEG and healthy EEG. By employing ANN, we see that all these features can perform well in the identification of seizure segments of EEG data. In particular, IMF 2 has shown good performance with 100% accuracy of energy/entropy of amplitude distribution and the standard deviation of frequency distribution. In this work, a higher degree of performance was obtained with a single feature that represents the information about the time series EEG data. The process had less complicated computation than other time-frequency analysis techniques.

The limitation of the work is the ictal classification is done only between healthy and seizure class EEG data. The work is focus on ictal classification based on three cases and each cases are statistically verified the discrimination level of the features of all four IMFs. Also two types of classifiers are used to evaluate the performance of the system. In this scenario the work is more complicated, while considering the interictal EEG signals. So here interictal EEG signal is not being considered for the classification between ictal EEG or healthy EEG. If consider interictal EEG- ictal EEG classification, we have to repeat same the procedure.

CHAPTER 5

CLASSIFICATION OF ICTAL USING MODELING BASED SPECTRAL AND TEMPORAL COMPONENTS OF HILBERT-HUANG TRANSFORM

This chapter deals with the different types of ictal classification using Auto Regressive (AR) spectral features and temporal features of HILBERT-HUANG transform (HHT) twin components. The spectral features of instantaneous amplitude (IA) function are obtained based on the power spectral density of AR modeling. The temporal features of instantaneous frequency function (IF) and instantaneous amplitude function are computed as well. The discriminating power of each vector is evaluated through one-way analysis of variance (ANOVA), and classification results are verified using an artificial neural network (ANN) classifier, which is a well-known classifier with low computation complexity. Here four different cases of interictal, ictal, and normal activities of EEG signals are classified and the classification performance indices are compared.

5.1 INTRODUCTION

EEG is a complex signal, which reflects the status of the brain, is difficult to be modeled (Garrett *et al.* 2013). Spectral estimation is a method to know the strength of the frequency components in the EEG. The spectral analysis of an arbitrary signal is generally classified into non-parametric method or classical method and parametric method. In non-parametric method, Fourier transform of autocorrelation of the signal is taken for a power spectral estimation. The signal is first masked by a window function and then power spectral density of the windowed signal is computed. The drawback of this method is the spectral leakage due to windowing (Subha *et al.* 2010). In

parametric or model based spectrum estimation method, the spectral leakage is eliminated and gets a better spectral resolution of the signal. It requires less number of samples for spectral estimation as compared to that in FFT spectrum (Subasi *et al.* 2005). Here, the signal is supposed to be a random process and the input signal is white noise. The signal is modeled in three ways- Moving Average process, Auto Regressive process and Auto Regressive Moving Average process. More efficient and accurate method to model EEG signal is AR modeling (Khamis *et al.* 2009).

5.1.1 Hilbert–Huang Transform

Hilbert–Huang transform (HHT) involves two stages of EEG signal analysis:

- (a) Obtaining the IMF components of the original signal through EMD method.
- (b) Finding the Hilbert transform of each IMF of the signal.

HHT is explained in Section 4.2.1. The twin components of HHT, instantaneous amplitude (IA) and instantaneous frequency (IF), provide local information about energy and frequency of EEG signal respectively. The IA and IF are the major components that help to identify the presence of ictal information in EEG signal (Fu *et al.* 2015; Biju *et al.* 2017).

5.1.2 AR Model Spectra

Spectral analysis is an elementary tool used to determine whether a particular frequency component is present in a primary signal. As discussed earlier, spectral estimation is classified into parametric and non-parametric method. To avoid the effects of spectral leakage in the non-parametric method, researchers obtain superior results in EEG signals by using parametric spectrum estimation methods, such as AR modeling. The AR modeling, also termed as all pole system design models, is used for the power spectrum estimation. If the majority of input signals are unrecognizable by a system, and

the output signals are known, then AR model is preferably used to define the system (Jansen *et al.* 1981; Khan and Gotman, 2003). Most of the input to the brain is unknown and the only available signal is the scalp EEG signal (Zhang *et al.* 2017). Therefore, the AR modeling is more suitable for EEG power spectrum estimation. An AR Burg's method is a power spectral estimation technique which minimizes the forward and backward prediction errors and at the same time it constrains the AR parameters to satisfy Levinson–Durbin recursion for an AR coefficient calculation (Khamis *et al.* 2009).

The proposed work makes use of the AR Burg's algorithm to estimate the power spectrum of the IA of each of the IMF channel. It is observed that the AR power spectrum estimation closely matches the original signal since closely packed sinusoid signals are being resolved with a low noise level. The accuracy of the Burg's method is inversely proportional to the order of the model. For EEG signal, the 10th order AR model yields higher classification accuracy and hence shows better performance in seizure detection (Zhang *et al.* 2017).

In parametric AR modeling, the signal is modeled as the sum of the linear combinations of the previous inputs $x(k - i)$ multiplied by the corresponding weights $A(i)$ and ε_k , the white noise in the signal (Anderson *et al.* 1998). Let $x(k)$ be the incoming signal to be modeled where $0 \leq x(k) \leq N - 1$, where N is the length of the sequence.

The signal is thus represented as follows:

$$\hat{x}(k) = -A(1)x(k - 1) - A(2)x(k - 2) \dots - A(p)x(k - p) + \varepsilon_k \quad (5.1)$$

Where p is the number of past samples considered for modeling.

The estimated signal, $\hat{x}(k)$ is expressed as

$$\hat{x}(k) = -\sum_{i=1}^p A(i)x(k - i) + \varepsilon_k \quad (5.2)$$

Prediction error, $e(k)$, is the difference between the original signal and the estimated signal and is given by:

$$e(k) = x(k) - \hat{x}(k) \quad (5.3)$$

Now, the power spectral density (PSD), $p_{xx}(f)$ is determined by using the estimated AR coefficients:

$$p_{xx}(f) = \frac{\hat{e}_p}{|1 + \sum_{k=1}^p \hat{a}_p(k)e^{-j2\pi fk}|^2} \quad (5.4)$$

Where $\hat{a}_p(k)$ is the estimated AR parameter obtained from the Levinson–Durbin algorithm and \hat{e}_p is the total least-square error given by the following (Subha *et al.* 2010):

$$\hat{e}_p = \hat{e}_{f,p} + \hat{e}_{b,p} \quad (5.5)$$

Where $\hat{e}_{f,p}$ is the forward prediction error, which is defined as

$$\hat{e}_{f,p} = x(n) + \sum_{i=1}^p \hat{a}_{p,l}^* x(n-i) \quad (5.6)$$

and $\hat{e}_{b,p}$ is the backward prediction error defined as

$$\hat{e}_{b,p} = x(n-p) + \sum_{i=1}^p \hat{a}_{b,p} x(n-p+i) \quad (5.7)$$

Where $n = p + 1 \dots N$.

5.2 METHODOLOGY

Figure 5.1 shows the proposed method for ictal classification based on spectral and temporal features of amplitude–frequency contour of HHT. The entire diagnostic process can be divided into three stages: Hilbert–Huang transform, AR modeling and feature extraction and classification technique. In this work, the different types of ictal signals are classified. The spectral and temporal features of the local informatics components of HHT, IA and IF are then tabulated.

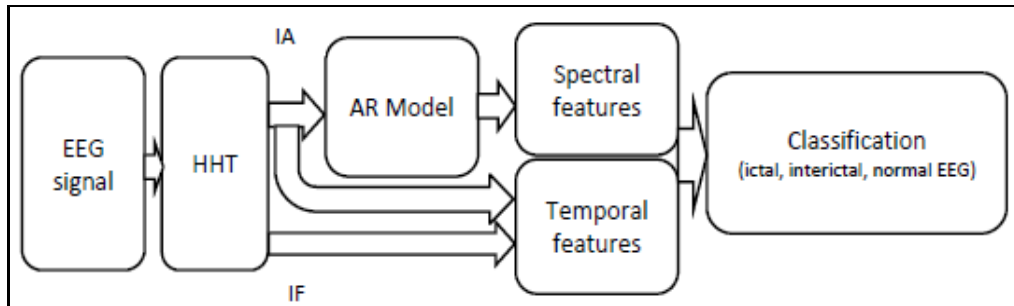


Fig. 5.1 Illustrations of the proposed method for ictal classification based on spectral and temporal features of amplitude–frequency contour of HHT

Here, two different set of parameters; AR model parameters of IA with IF and AR model parameters of IA with IA, are compared for ictal classification. Firstly, the spectral components of IA and the temporal components of IF are computed. Then the spectral components of IA and the temporal components of IA are computed, to form the feature vector for classification. Four different features are extracted in each, from spectral domain and temporal domain. The spectral analyses is tabulated from the AR power spectral density of IA components. The higher-order statistics (HOS), interquartile range, and coefficient of variation, which are the different descriptive statistics of temporal features, are computed. Thus, the feature vectors are obtained and then classified using ANN classifier.

5.3 FEATURE EXTRACTION

In this study, four types of spectral parameters and four types of temporal features are collected for the feature vector. The spectral parameters are tabulated from the power spectral density using the Burg's AR model. Here the power spectral density represents the distribution of power as a function of the frequency. The spectral features are spectral peak (S_P), spectral mean energy (S_{ME}), spectral entropy (S_{En}), and spectral mean Teager energy (S_{TE}), which are energy or entropy based features (Martis *et al.* 2012). The peak of the spectrum of each set of samples is known as spectral peak. The spectral entropy is calculated from the amplitude in the power spectral density of the different classes of ictal EEG. The spectral entropy reflects the irregularity pattern in the PSD of EEG. The spectral mean energy is the normalized energy of power spectral density. The difference of energy of neighbouring sample in the power spectral density is extracted as spectral mean Teager energy.

The temporal features are tabulated from the IMF1 and IMF2 of the twin components. The features are coefficient of variation (C_V), skewness (S_k), Kurtosis (K_U), and interquartile range (IQR) (Riaz *et al.* 2016; Alam and Bhuiyan, 2013). The coefficient of variation is a function between the standard deviation and the mean of the samples. The coefficient of variation measures the variability of instantaneous amplitude and instantaneous frequency of different ictal EEG. It is used to compare the difference in the sample distribution in the different set of samples. The skewness is the measure of an asymmetric behaviour of the probability distribution of samples. The null value of skewness indicates the perfection of symmetry on both sides of the mean. The skewness tabulated is the third moment of data. The Kurtosis is a measure of the relative peakedness of the probability distribution of samples. The Kurtosis is obtained from the fourth moment of the data. The interquartile range is the measure of spread of the sample. In IRQ the spread of samples on both sides of the median is considered. Table 5.1 shows the spectral features and temporal features used and the corresponding relevant mathematical expressions for its computation. Hence, the combination of spectral and temporal features of HHT twin components, IA and IF forms the final feature vector to the classifier with eighth order.

Table 5.1 Spectral features and temporal features in this study

Spectral features used in this work.		
SL NO	Feature name	Mathematical formulation
1	<i>Spectral Peak</i>	$S_p = \max(P_{xx}(f))$
2	<i>Spectral mean energy</i>	$S_{ME} = \log \frac{1}{N} \sum_{f=0}^N P_{xx}(f)$
3	<i>Spectral Entropy</i>	$S_{En} = - \sum_k p_k(P_{xx}(f)) \log p_k(P_{xx}(f))$
4	<i>Spectral Mean Teager Energy</i>	$S_{TE} = \log \frac{1}{N} \left(\sum_{f=0}^N (P_{xx}^2(f) - P_{xx}(f-1)P_{xx}(f+1)) \right)$

Temporal features used in this work.		
5	<i>Coefficient of variation</i>	$C_v = \frac{\frac{1}{N} \sum_{i=1}^N (x(i) - \bar{x})^2}{\bar{x}^2} = \frac{\sigma}{\bar{x}}$
6	<i>Skewness</i>	$S_k = \frac{1}{N} \sum_{i=1}^N \frac{(x(i) - \bar{x})^3}{\sigma^3}$
7	<i>Kurtosis</i>	$K_U = \frac{1}{N} \sum_{i=1}^N \frac{(x(i) - \bar{x})^4}{\sigma^4}$
8	<i>Interquartile range</i>	$IQR = Q_3 - Q_1$ Q1 and Q3 are the 1 st and 2 nd quartile respectively

5.4 CLASSIFIER

ANN is a connection of several units or nodes called artificial neurons from the input level to the output level through hidden levels (Isler, 2016). The proposed method employs a multilayer perceptron neural network (MLPNN), which is the most efficient type ANN model, to recognize the different ictal EEG patterns (Hassanien *et al.* 2014). MLPNN comprises of three layers. The first layer is the input layer that contains a number of neurons with the same size as that of the input feature vector. The second layer consists of the hidden layer that increases the classification ability of a given network, and the number of neurons in the hidden layer can be fixed without constraints. A small number of neurons can reduce the classification accuracy, and a large number of neurons can exacerbate the complexity of a specific network. The third layer is the output layer composed of a number of neurons similar to that of the desired output class (Basheer and Hajmeer, 2000). The performance index in automatic detection of diagnostic methods is tabulated from ANN (Van *et al.* 2009). The total classification accuracy, sensitivity, and specificity are the performance index of detection, which are discussed in Section 4.4.1.

ANN involves the following phases: training, validation, and testing. In the first two phases, a neural network, namely MLPNN, should be initially trained to adjust its weighing factor in accordance with the required output and should be subsequently validated to access network generalization. In the testing

phase, the network should be provided with a set of data to measure network performance in terms of sensitivity, specificity, and accuracy.

The categorical data is deriving from observations made of qualitative data. Here feature vectors of spectral-temporal data are qualitative data. In categorical data or grouped data the sample size can be determined by Cochran's sample size formula (Barlett *et. al* 2001)

$$n = \frac{Z^2 p(q)}{e^2} \quad (5.8)$$

Where n is sample size, Z is Z - value of 95% confidence level, $p(q)$ is estimate of variance and e is the margin of error.

Here in this work, four different cases of EEG signals, normal, ictal and interictal EEG signals are taken. Four classification problems are being considered as follows:

- Case 1: Classification of normal and ictal EEG signal;
- Case 2: Classification of normal and interictal EEG signal;
- Case 3: Classification of interictal and ictal EEG signal;
- Case 4: Classification of combined normal signal and interictal signal with ictal EEG signal.

In each case, the HHT twin components of first and second IMFs, that is the IA and IF of each IMF, are compared. For each case considered, the spectral vector of IA and temporal vector of IF or temporal vector of IA are tabulated. The frequency resolution of the spectrum is considered by two different AR modeling in 6th order and 10th order respectively (Zhang *et al.* 2017).

5.5 RESULTS AND DISCUSSION

The EEG database used in this novel ictal classification is discussed in Section 2.2. The normal signals are in groups A and B, ictal signals are in group E

only and interictal signals are in groups C and D. The EEG signal contains 100 segments, and the duration of each segment is 23 s in each category of the database. A sampling frequency of each EEG segments is 173.61 Hz. Hence, each EEG segment comprises 4,096 samples. These segments are further subdivided into blocks with a sample size of 256. The total size of the population is 1600 in each category. Here only 250 segments are taken as the random sample with 95% confidence level. In this study assume margin of error as ± 0.05 . As per Cochran's sample size formula for grouped data the n , sample size is calculated as 384. So for each feature approximately 500 samples are taken for classification.

An EEG signal initially undergoes empirical mode decomposition to obtain different IMFs of each segment. In the EMD method, it is revealed the local information of the frequency content in a signal. The frequency bands of the IMF components are to pass from a higher frequency of the original signal to lower frequency and the DC components are accumulated in the residue. The residue is not considered for analysis, so effectively DC components are eliminated. As per inference from our second work, the first IMFs and second IMFs are only considered in this study because the ictal information is accumulated into these components (Biju et al. 2017). These findings are also mentioned in the recent study on EEG (Mahapatra and Horio, 2018). Thus the proposed method makes use of the features calculated from the first and second IMFs. Then Hilbert transform is applied to each IMF to obtain the corresponding IA and IF components. The computation time required for extracting IA and IF components from the EEG is 10.4 s per each category of the data set.

Figure 5.2 shows the first and second IF components, IF1 and IF2, of normal, interictal and ictal EEG respectively. The IMF1 has higher frequency components than IMF2. So the IF1 components are highly packed than IF2 components in the Figures 5.2(a), 5.2(b) and 5.2(c). Therefore, IF1 has much difference than IF2 values in Figure 5.2.

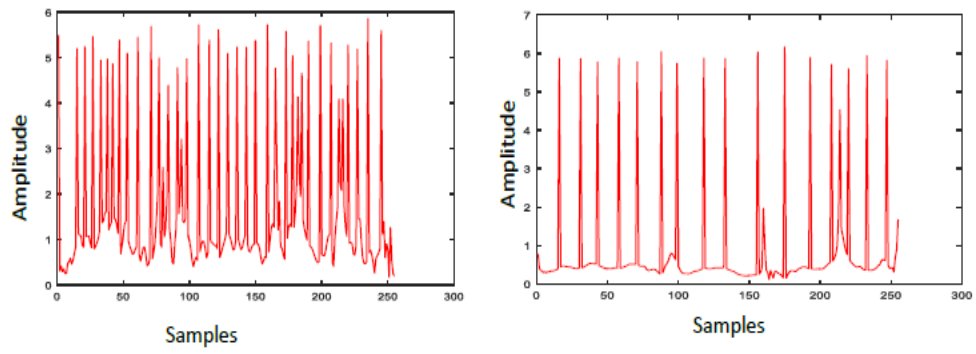


Fig. 5.2 (a) Plots of IF1 and IF2 of normal EEG

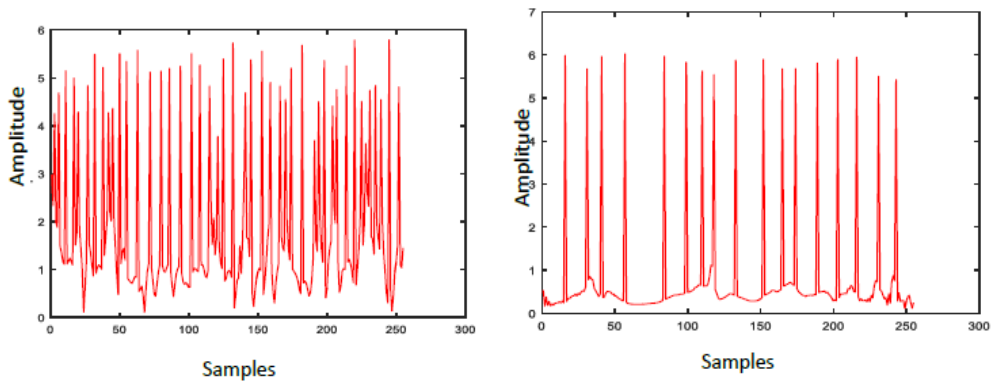


Fig. 5.2 (b) Plots of IF1 and IF2 of interictal EEG

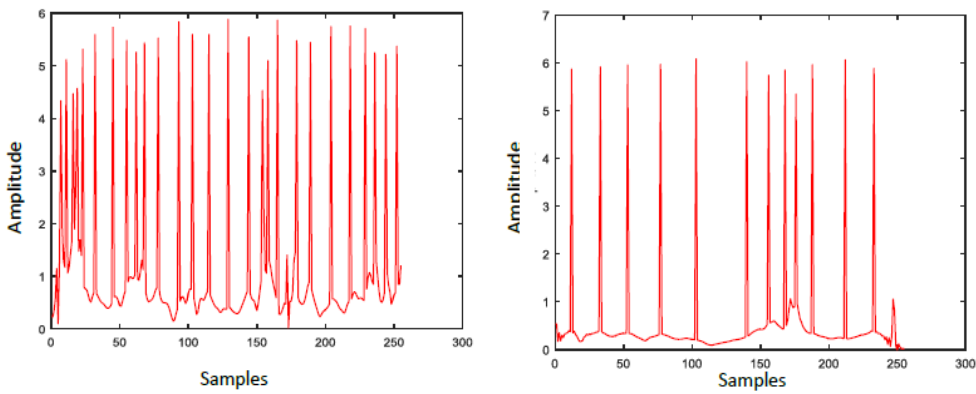


Fig. 5.2 (c) Plots of IF1 and IF2 of ictal EEG

To enhance ictal classification, we obtain the spectral characterizations of IA and temporal features of IA or IF. This defines the feature vector to the classifier. The work compares better classes of feature vector among IMFs and orders of AR models. The spectra of IA1 and IA2 are modeled by Burg's method with an order of the AR (6) and AR (10), respectively. The IA1 and PSD of IA1 in normal EEG signal is shown in Figure 5.3 (a), while those in the interictal EEG signal is illustrated in Figure 5.3 (b). The IA1 and PSD of IA1 in ictal EEG signal are shown in Figure 5.3 (c). The PSD plotted in Figure 5.3 are modeled in Burg's method with an order of the AR (10). The IA2 and PSD of IA2 in normal EEG signal is shown in Figure 5.4 (a), while those in the interictal EEG signal is demonstrated in Figure 5.4 (b). The IA2 and PSD of IA2 in the ictal EEG signal shown in Figure 5.4 (c). The PSD plotted in Figure 5.3 are modeled using the AR (10) Burg's method. Similarly, the PSD of AR(6) Burg's method of model is also used for constructing with the IA1 and IA2 of normal, interictal and ictal EEG signals, respectively for comparison.

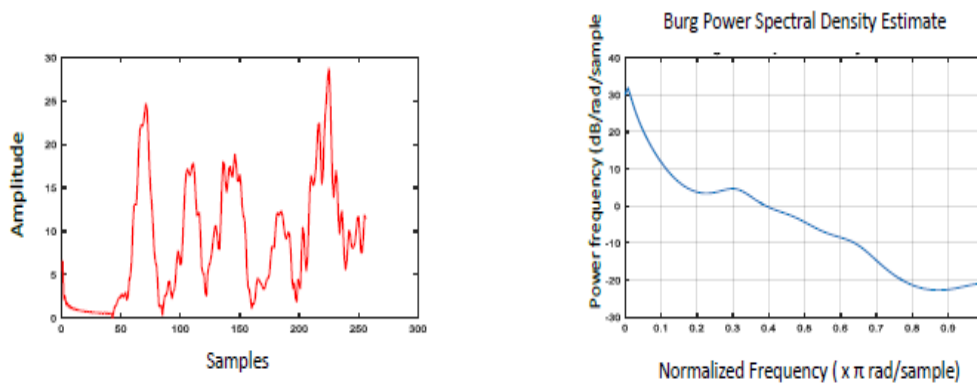


Fig. 5.3 (a) Plots of IA1 and PSD signals of IA1 in normal EEG

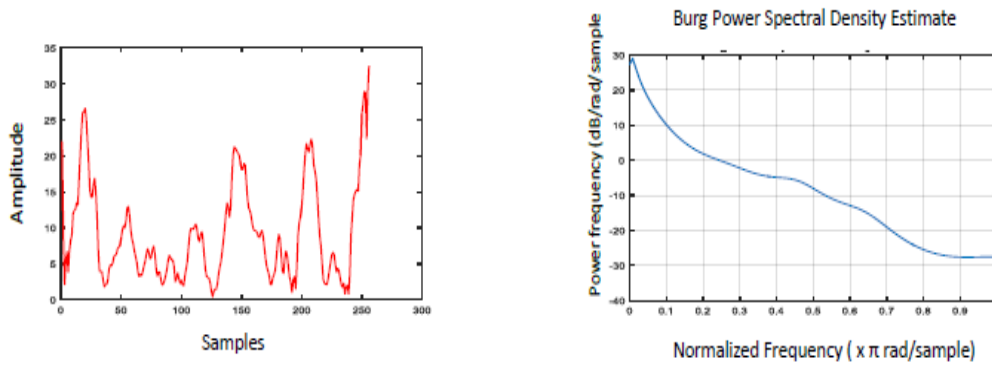


Fig. 5.3 (b) Plots of IA1 and PSD signals of IA1 in interictal EEG

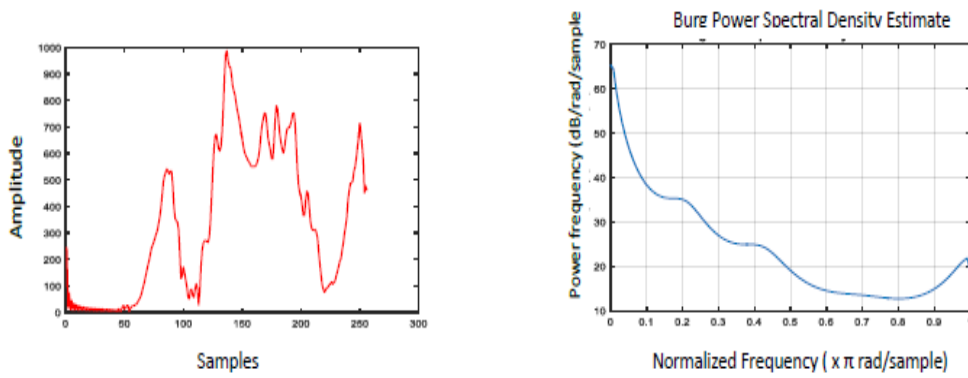


Fig. 5.3 (c) Plots of IA1 and PSD signals of IA1 in ictal EEG

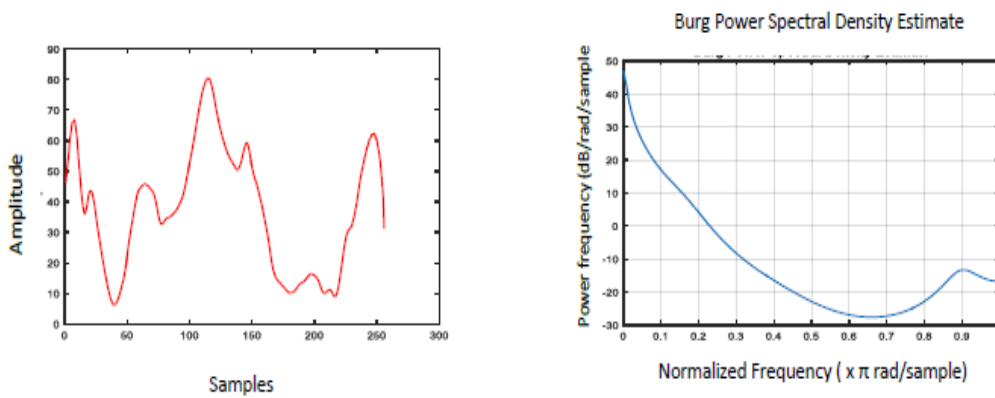


Fig. 5.4 (a) Plots of IA2 and PSD signals of IA2 in normal EEG

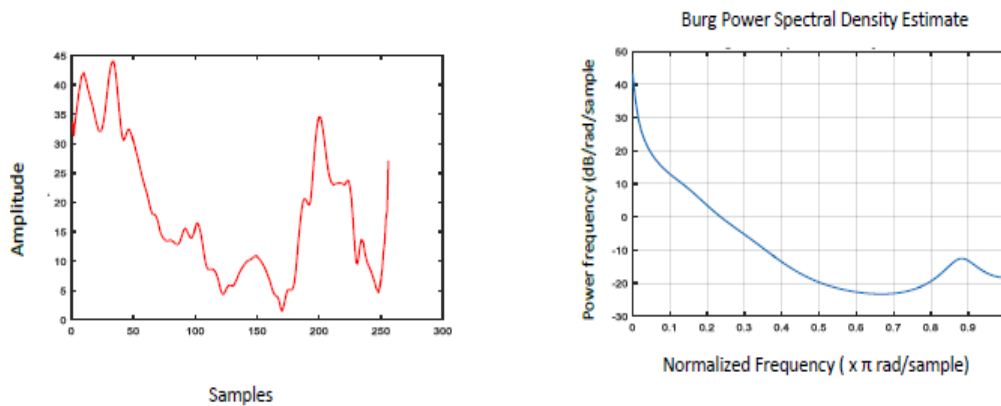


Fig. 5.4 (b) Plots of IA2 and PSD signals of IA2 in interictal EEG

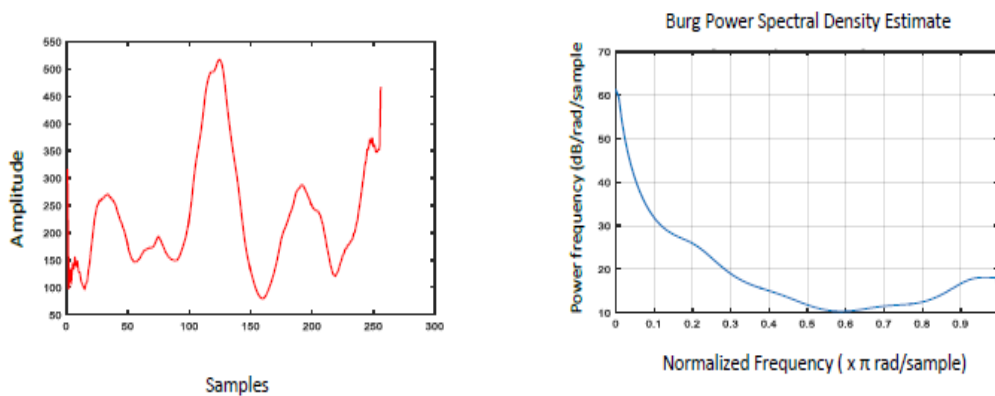


Fig. 5.4 (c) Plots of IA2 and PSD signals of IA2 in ictal EEG

In Figure 5.3, amplitude scale of IA1 in ictal EEG is higher than amplitude of IA1 in normal and interictal EEG. However, amplitude of IA1 in the normal and interictal EEG are closely being associated with each other. In Figure 5.4, also the amplitude of IA2 in ictal EEG is higher than the amplitude of IA2 in normal and interictal EEG. In Figure 5.3, Burg power spectral density of IA1 in ictal EEG is higher than of IA1 in normal and interictal EEG. Comparing the Figures 5.3 and 5.4 in the case of Burg power spectral density of ictal EEG, IA2 is dominated than IA1 signal.

The spectra of IA1 and IA2 are modeled in AR Burg's method with an order of the AR (6) and AR (10), respectively. The spectral features of IA S_P , S_{ME} , S_{En} , and S_{TE} are computed from the Burg power spectral density estimation. The temporal features considered are C_V , S_K , K_U , and IQR from

IA1, IA2, IF1, and IF2 respectively. In this study spectral mean and spectral Teager energy are used for the difference and differential energy of the spectra respectively. The HOS parameter in the temporal features S_K and K_U are used to ensure the recurrence of IF components in ictal stages.

Figure 5.5 shows the mean of mean values and standard deviation of spectral features of normal, ictal and interictal EEG signal. The Figure 5.5(a), 5.5(b), 5.5(c) and 5.5(d) shows the IA1_AR(10), IA1_AR(6), IA2_AR(10) and IA2_AR(6) plot of spectral peak, spectral mean energy, spectral Teager energy and spectral entropy of feature for the classification respectively. The mean and standard deviation of ictal EEG and normal EEG shows significant difference. The average computation time required for feature extraction of the spectral features of IA in each IMF is 55.06 s per each IMF in each category of the data set.

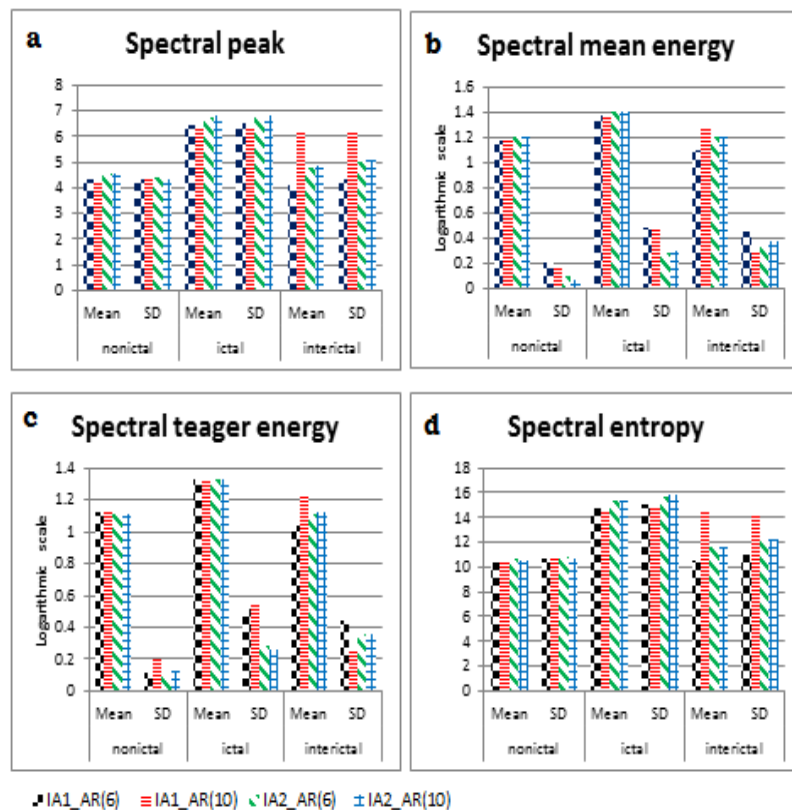


Fig. 5.5 Mean and standard deviation of (a) spectral peak (b) spectral mean energy (c) spectral Teager energy (d) spectral entropy.

Figure 5.6 shows the mean of mean values and standard deviation of temporal features of the different ictal EEG signals. The Figures 5.6(a), 5.6(b), 5.6(c) and 5.6(d) shows the IA1, IA2, IF1 and IF2 plots of coefficient of variation, skewness, Kurtosis and interquartile range of feature for the classification. Here, the ictal EEG has notable differences with healthy EEG and interictal EEG signal for classification. The mean values of the feature sets indicate that they vary significantly between normal, interictal and ictal EEG for all the features computed. The average computation time required for feature extraction of the temporal features of IA in each IMF is 9.76 s per each IMF in each category of the data set and for IF in each IMF is 10.09 s per each IMF in each category of the data set.

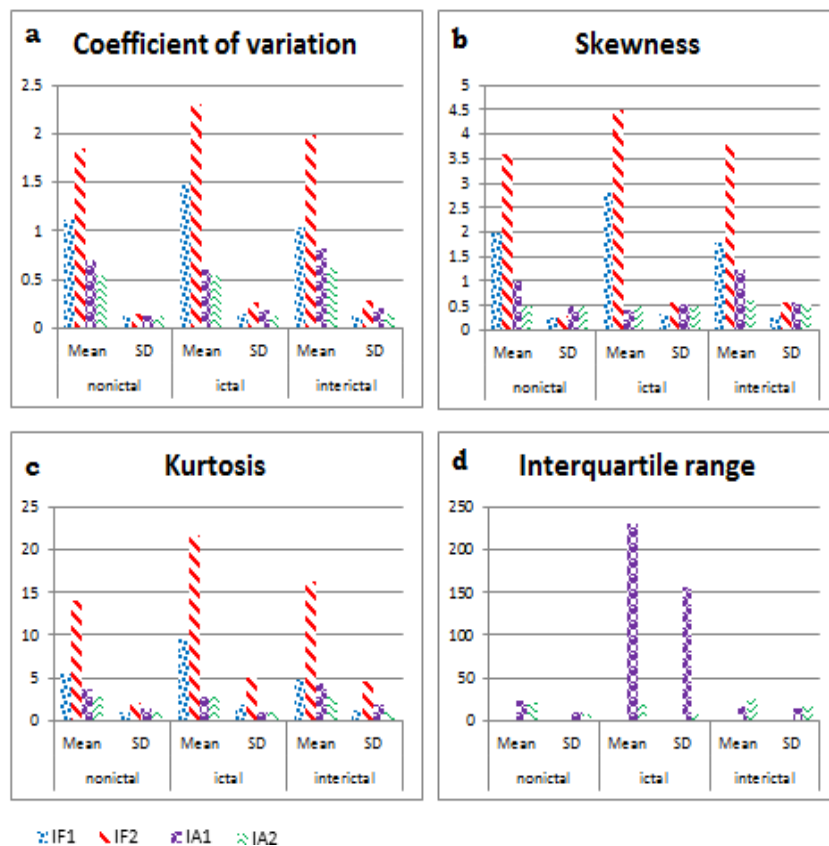


Fig.5.6 Mean and standard deviation of (a) coefficient of variation (b) skewness (c) Kurtosis (d) interquartile range.

In this chapter, four different cases of ictal classification are computed and compared with each other. Case 1, normal and ictal EEG signal; Case 2, normal and interictal EEG signal; Case 3, inter-ictal and ictal EEG signal; and Case 4, combined normal signal and interictal signal with ictal of HHT1 and HHT2 components.

In all the classifications, the hypothesis testing will help to check the significance level of each case. Each parameter in the feature vector is statistically validated. The discriminating power of Case 1, Case 2, Case 3, and Case 4 are examined through one- way ANOVA using different parameters of the feature vectors. 32 parameters are considered in each case. The discrimination is determined at 95% confidence level. Therefore, in all cases, the significance value (p-value) was set as 0.05. The F-value and p-value of Case 1, Case 2 and Case 3 of the ictal stages are tabulated and shown in Tables 5.2-5.4. The feature ranking of each parameter can be calculated according to the F-value.

Table 5.2 Statistical analysis of one- way ANOVA
in Case 1: normal-ictal EEG class

Features	n	mean	std	Std Error	F	sig
SP_IA1_AR(6)	500	1.26498E+06	2.38069E+06	1.68340E+05	75.191	0.000
SP_IA1_AR(10)	500	1.05021E+06	1.77534E+06	1.25536E+05	101.799	0.000
SP_IA2_AR(6)	500	2.71972E+06	4.62386E+06	3.26956E+05	101.323	0.000
SP_IA2_AR(10)	500	2.90825E+06	5.22583E+06	3.69522E+05	86.671	0.000
SME_IA1_AR(6)	500	19.02225	4.94693	3.49801E-01	621.751	0.000
SME_IA1_AR(10)	500	19.01192	4.840067	3.42244E-01	678.940	0.000
SME_IA2_AR(6)	500	20.62538	5.017526	3.54793E-01	1720.936	0.000
SME_IA2_AR(10)	500	20.56578	5.111017	3.61403E-01	1754.848	0.000
STE_IA1_AR(6)	500	17.10084	4.65619	3.29242E-01	518.152	0.000
STE_IA1_AR(10)	500	17.22209	4.920614	3.47940E-01	435.121	0.000

Features	n	mean	std	Std Error	F	sig
STE_IA2_AR(6)	500	16.94918	4.489431	3.17451E-01	1327.632	0.000
STE_IA2_AR(10)	500	16.97732	4.579471	3.23818E-01	1453.233	0.000
SEn_IA1_AR(6)	500	2.93171E+14	7.97603E+14	5.63990E+13	31.103	0.000
SEn_IA1_AR(10)	500	2.08284E+14	4.84754E+14	3.42773E+13	45.095	0.000
SEn_IA2_AR(6)	500	9.62229E+14	3.78904E+15	2.67926E+14	13.721	0.000
SEn_IA2_AR(10)	500	1.20504E+15	4.96131E+15	3.50817E+14	12.479	0.001
Cv_IF1	500	1.30201E+00	2.39436E-01	1.69307E-02	420.770	0.000
Cv_IF2	500	2.06844E+00	3.12306E-01	2.20834E-02	203.374	0.000
Cv_IA1	500	0.653481	0.157579	1.11426E-02	21.157	0.000
Cv_IA2	500	0.512927	0.150887	1.06693E-02	5.617	0.019
Sk_IF1	500	2.40094E+00	5.05281E-01	3.57288E-02	456.858	0.000
Sk_IF2	500	4.01796E+00	6.35032E-01	4.49035E-02	184.862	0.000
Sk_IA1	500	0.700926	0.577909	4.08643E-02	64.175	0.000
Sk_IA2	500	0.324129	0.539604	3.81557E-02	14.044	0.000
Ku_IF1	500	7.44877E+00	2.49714E+00	1.76574E-01	378.985	0.000
Ku_IF2	500	1.77825E+01	5.38825E+00	3.81007E-01	172.447	0.000
Ku_IA1	500	3.220242	1.2470560	8.81802E-02	24.432	0.000
Ku_IA2	500	2.9752	2.24968	1.59076E-01	4.078	0.045
IQR_IF1	500	0.504971	0.187083	1.32288E-02	202.418	0.000
IQR_IF2	500	0.160750	0.069954	4.94648E-03	29.049	0.000
IQR_IA1	500	126.844731	151.0957811	1.06841E+01	174.607	0.000
IQR_IA2	500	101.872000	114.7008447	8.11057E+00	196.166	0.000

Table 5.3 Statistical analysis of one- way ANOVA in
Case 2: normal-interictal EEG class

Features	n	mean	std	Std Error	F	sig
SP_IA1_AR(6)	500	1.56925E+04	2.14463E+04	1.51648E+03	5.243	0.023
SP_IA1_AR(10)	500	1.50683E+04	2.10497E+04	1.48844E+03	4.720	0.031
SP_IA2_AR(6)	500	4.88484E+04	7.03354E+04	4.97346E+03	6.623	0.011
SP_IA2_AR(10)	500	4.96657E+04	8.20803E+04	5.80395E+03	9.715	0.002
SME_IA1_AR(6)	500	1.35135E+01	2.60205E+00	1.83993E-01	55.130	0.000
SME_IA1_AR(10)	500	13.53439	2.538478	1.79498E-01	61.075	0.000
SME_IA2_AR(6)	500	15.96693	1.809751	1.27969E-01	.402	0.527
SME_IA2_AR(10)	500	15.89305	1.857753	1.31363E-01	1.490	0.224
STE_IA1_AR(6)	500	1.19690E+01	2.46275E+00	1.74143E-01	59.542	0.000
STE_IA1_AR(10)	500	12.02165	2.541101	1.79683E-01	49.262	0.000
STE_IA2_AR(6)	500	12.78418	1.815592	1.28382E-01	.009	0.923
STE_IA2_AR(10)	500	12.91954	1.869992	1.32228E-01	2.992	0.085
SEn_IA1_AR(6)	500	2.54862E+10	8.05648E+10	5.69679E+09	.167	0.683
SEn_IA1_AR(10)	500	2.48657E+10	8.62063E+10	6.09570E+09	.270	0.604
SEn_IA2_AR(6)	500	1.98186E+11	9.94188E+11	7.02997E+10	4.870	0.028
SEn_IA2_AR(10)	500	2.48964E+11	1.38301E+12	9.77939E+10	4.940	0.027
Cv_IF1	500	1.30201E+00	2.39436E-01	1.69307E-02	420.770	0.000
Cv_IF2	500	1.90705E+00	2.34368E-01	1.65724E-02	21.697	0.000
Cv_IA1	500	0.657712	0.142968	1.01093E-02	21.474	0.000
Cv_IA2	500	0.576206	0.139391	9.85645E-03	15.000	0.000
Sk_IF1	500	2.40094E+00	5.05281E-01	3.57288E-02	456.858	0.000
Sk_IF2	500	3.68257E+00	4.75492E-01	3.36223E-02	16.071	0.000
Sk_IA1	500	0.790226	0.535187	3.78434E-02	30.814	0.000
Sk_IA2	500	0.624728	0.493943	3.49271E-02	9.499	0.002
Ku_IF1	500	7.44877E+00	2.49714E+00	1.76574E-01	378.985	0.000
Ku_IF2	500	1.50715E+01	3.76489E+00	2.66218E-01	19.472	0.000
Ku_IA1	500	3.197499	1.2650579	8.94531E-02	26.703	0.000
Ku_IA2	500	2.8504	0.948390	0.067061	3.157	0.077
IQR_IF1	500	5.04971E-01	0.187083	0.013229	202.418	0.000
IQR_IF2	500	2.07781E-01	6.59880E-02	4.66606E-03	15.345	0.000
IQR_IA1	500	19.545288	12.4619979	8.81196E-01	24.511	0.000
IQR_IA2	500	16.653601	8.0135283	5.66642E-01	12.846	0.000

Table 5.4 Statistical analysis of one- way ANOVA in Case 3 : interictal-ictal EEG class

Features	n	mean	std	Std Error	F	sig
SP_IA1_AR(6)	500	2.71972E+06	4.62386E+06	3.26956E+05	101.323	0.000
SP_IA1_AR(10)	500	1.50683E+04	2.10497E+04	1.48844E+03	100.342	0.000
SP_IA2_AR(6)	500	2.92596E+06	5.21664E+06	3.68872E+05	85.580	0.000
SP_IA2_AR(10)	500	2.92596E+06	5.21664E+06	3.68872E+05	85.580	0.000
SME_IA1_AR(6)	500	17.20493	4.557472	3.22262E-01	776.041	0.000
SME_IA1_AR(10)	500	17.20493	4.557472	3.22262E-01	776.041	0.000
SME_IA2_AR(6)	500	20.72591	5.167870	3.65424E-01	912.259	0.000
SME_IA2_AR(10)	500	20.72591	5.167870	3.65424E-01	912.259	0.000
STE_IA1_AR(6)	500	12.02165	2.541101	1.79683E-01	781.477	0.000
STE_IA1_AR(10)	500	1.69492E+01	4.48943E+00	3.17451E-01	1520.936	0.000
STE_IA2_AR(6)	500	13.53439	2.538478	1.79498E-01	1005.929	0.000
STE_IA2_AR(10)	500	2.06254E+01	5.01753E+00	3.54793E-01	1720.936	0.000
SEn_IA1_AR(6)	500	9.62229E+14	3.78904E+15	2.67926E+14	13.721	0.000
SEn_IA1_AR(10)	500	2.48657E+10	8.62063E+10	6.09570E+09	13.717	0.000
SEn_IA2_AR(6)	500	1.20525E+15	4.96125E+15	3.50814E+14	12.474	0.001
SEn_IA2_AR(10)	500	1.20525E+15	4.96125E+15	3.50814E+14	12.474	0.001
Cv_IF1	500	1.26909E+00	2.70142E-01	1.91019E-02	529.301	0.000
Cv_IF2	500	2.13802E+00	3.14462E-01	2.22358E-02	66.746	0.000
Cv_IA1	500	0.714964	0.222053	1.57015E-02	65.324	0.000
Cv_IA2	500	0.549825	0.176807	1.25022E-02	29.256	0.000
Sk_IF1	500	2.30015E+00	6.00966E-01	4.24947E-02	618.775	0.000
Sk_IF2	500	4.14002E+00	6.53416E-01	4.62035E-02	66.869	0.000
Sk_IA1	500	0.824036	0.682514	4.82610E-02	111.232	0.000
Sk_IA2	500	0.389845	0.575448	4.06903E-02	28.777	0.000
Ku_IF1	500	7.13848E+00	2.77217E+00	1.96022E-01	483.350	0.000
Ku_IF2	500	1.88620E+01	5.53043E+00	3.91061E-01	60.379	0.000
Ku_IA1	500	3.543422	1.6983331	1.20090E-01	45.982	0.000
Ku_IA2	500	3.0253	2.28026	1.61239E-01	2.737	0.100
IQR_IF1	500	6.20274E-01	3.01447E-01	2.13155E-02	421.052	0.000
IQR_IF2	500	1.80095E-01	8.42338E-02	5.95623E-03	81.332	0.000
IQR_IA1	500	122.718965	154.0893085	1.08958E+01	188.216	0.000
IQR_IA2	500	104.377086	113.4370393	8.02121E+00	181.115	0.000

In Case 1, SME_IA2_AR(10), SME_IA2_AR(6) STE_IA2_AR(10) and STE_IA2_AR(6) have the higher feature values which are compared with other spectral features. In the temporal features, Sk_IF1, Cv_IF1 and Ku_IF1 are the dominating parameters. In Case 2, SME_IA1_AR(10), SME_IA1_AR(6), STE_IA1_AR(10) and STE_IA1_AR(6) having the highest values that to compared with other parameters in spectral features, but here each values is similar F-value index. The parameters Sk_IF1, Cv_IF1 and Ku_IF1 are the highest valued in temporal features. In the Case 3, STE_IA2_AR(10) and STE_IA1_AR(6) have the highest feature values in the spectral feature group. The parameters Sk_IF1, Cv_IF1 and Ku_IF1 have highest weights in the temporal features.

According to the p-value in the Table 5.2, the significance level of each parameter in Case 1 and Case 3 is less than 0.001, except in Case 2. This shows that all the parameters in the Case 1 and Case 3 have strong significant differences. Interictal signal is the signal between the two adjacent ictal stages. If interictal period in the EEG signal is larger, then interictal signal may be similar to normal EEG signal. In Case 3, significant level of some of the parameters is greater than the expected value, 0.05. This indicates that normal EEG and interictal EEG signals are correlated if the durations of the interictal period in an EEG signal is extremely high.

In this study, an ANN classifier is used for different ictal classification stages. All of the obtained features are collected to constitute an input feature vector, which is fed as an input to the three-layer feed-forward neural network classifier. The number of hidden layer neurons is set to 15; the network contains sigmoid hidden neurons and softmax output neurons. The output layer is binary classification of the four different cases. The network is then trained with a scaled conjugate gradient back-propagation (trainscg) algorithm. Approximately 70% of the samples are used for training. During the training,

the network weights are adapted based upon error in each node. Approximately 15% of the samples are employed for validation to determine the generalization of the network and consequently terminate the training when generalization stops improving. The remaining 15% of the samples are effectively used for testing to measure network performance during and after training. The training samples, checking samples and testing samples are interchanged to verify the cross validation of the classifier result. The classification is performed in the first set of HHT components, HHT1 and second set of HHT components, HHT2 respectively. The spectral vector of IA and the temporal vector of IF or temporal vectors of IA are classified using ANN classifier. Here 4000 samples are taken for each case, out of that 70% samples are used for training. The details of samples considered for classification in each feature vector of spectral domain and temporal domain are shown in the Table 5.2, Table 5.3 and Table 5.4 respectively. The effect of spectral resolution in modeling is also tested in AR(6) and AR(10). The MATLAB R2016a tool in Intel R Core (TM) 2 Duo CPU with 4GB RAM, system is used for all computations

The performance and classification efficiency are computed in terms of total classification accuracy, sensitivity, and specificity. The four Cases are tested with spectral feature of IA and temporal features of IF or temporal features of IA as feature vector. Table 5.5 shows the classification efficiency of different classes for spectral features of IA and temporal features of IF. The average computation time for the ANN classifier of spectral features of IA and temporal features of IF is 8.21 s. The Table 5.6 shows the classification efficiency of different classes of spectral features of IA and temporal features of IA. The average computation time for the ANN classifier of spectral features of IA and temporal features of IA is 8.26 s.

Table 5.5 Performance measures of Spectral features of IA and temporal features of IF

Spectral features of IA 1 and temporal features of IF1						
AR order	AR(6)			AR(10)		
	Acc	Sen	Spe	Acc	Sen	Spe
Case 1	93.33	100.00	86.67	93.33	100.00	86.67
Case 2	96.67	100.00	93.33	100.00	100.00	100.00
Case 3	93.33	100.00	86.67	96.67	100.00	93.33
Case 4	93.33	96.67	86.67	93.33	96.67	86.67
Spectral features of IA 2 and temporal features of IF2						
	Acc	Sen	Spe	Acc	Sen	Spe
Case 1	100.00	100.00	100.00	100.00	100.00	100.00
Case 2	70.00	66.67	73.33	83.33	73.33	93.33
Case 3	100.00	100.00	100.00	100.00	100.00	100.00
Case 4	100.00	100.00	100.00	100.00	100.00	100.00
Acc: accuracy, Sen: sensitivity, Spe: specificity						

Table 5.6 Performance measures of Spectral features of IA and temporal features of IA

Spectral features of IA 1 and temporal features of IA1						
AR order	AR(6)			AR(10)		
	Acc	Sen	Spe	Acc	Sen	Spe
Case 1	100.00	100.00	100.00	100.00	100.00	100.00
Case 2	96.67	100.00	93.33	96.67	100.00	93.33
Case 3	93.33	100.00	86.67	96.67	100.00	93.33
Case 4	96.67	100.00	93.33	86.67	100.00	73.33
Spectral features of IA 2 and temporal features of IA2						
	Acc	Sen	Spe	Acc	Sen	Spe
Case 1	100.00	100.00	100.00	100.00	100.00	100.00
Case 2	73.33	60.00	86.67	83.33	80.00	86.67
Case 3	100.00	100.00	100.00	96.67	100.00	93.33
Case 4	100.00	100.00	100.00	100.00	100.00	100.00
Acc: accuracy, Sen: sensitivity , Spe: specificity						

In Case 1, the total classification accuracy is 100% in the HHT1 and HHT2 types of signals. The spectral vector of IA and the temporal features of IF are successfully classified with higher rates of accuracy. Moreover, the classification accuracy is 100% in Case 3 for the classification between interictal and ictal classes. In Case 2, interictal and normal classification accuracy is only 83%. This finding is cross-verified in the statistical test. The ictal EEG signal is significant difference between the normal EEG and interictal EEG signals. The sensitivity and specificity of all cases in IA2 and IF2 are 100%, except in Case 2 ictal classification. In Case 2, specificity is 93.3% and sensitivity is only 73.3%. This finding is also confirmed in statistical analysis, that is the significant level in all of the cases is less than 0.001, except in Case 2, which clearly understood that normal EEG and interictal signals are correlated for some duration in an EEG signal. In Case 4, the normal and interictal EEG signals are combined with the ictal EEG signal to obtain a classification accuracy, specificity, and sensitivity of 100% in most types. Table 5.7 presents a comparison of ictal classification using AR modeling of EEG signal.

Table 5.7 Comparison with other AR modeling of EEG signal in the literature using the EEG data set

Authors	Methods	Classification Accuracy (%)
Martis <i>et al.</i> 2012	AR spectrum features of EMD with regression tree	95.33
Fu <i>et al.</i> 2015	HHT spectrum sub-band	95-100
Riaz <i>et al.</i> 2016	Temporal and Spectral EMD and SVM	96
Djemili <i>et al.</i> 2016	IMF features	97.7
Redelico <i>et al.</i> 2017	Permutation entropy for linear modeling	94.5
Jia <i>et al.</i> 2017	Ensemble EMD of phase space	98
Zhang <i>et al.</i> 2017	AR model in VMD and Random forest	97.35
Li <i>et al.</i> 2017	Dual tree complex wavelet transform	98.87
Proposed method	Spectral features of IA and Temporal features of IF with ANN	83-100%

5.6 INFERENCES

This chapter presents an analytical signal function of HHT, which is effective for the detection of different ictal stages in EEG signals. The proposed method emphasises on the spectral model based features of IA and temporal features of IA or IF. The AR Burg's method is the most suitable, model based method for spectral analysis of EEG. The selection of optimal order for Burg's AR modeling is affected by the performance of time series data. Here the performances of classification in AR (6) and AR (10) model based PSD are compared. The feature vector is set up as a combination of spectral features of IA and temporal features of IF. The performance is compared by another feature vector of combination of spectral features of IA and temporal features of IA. In both the conditions, IA and IF are calculated from IMF1 and IMF2. The effective classification of the different stages, namely, normal and ictal signal stage, normal and interictal stage, and interictal and ictal stages in EEG signal is done. The spectral features of IA and temporal features of IF are more apt for an ictal classification. The IA2 and IF2 yield better results than the IA1 and IF1 components in terms of classification performances respectively. The features of AR (10) order model shows better results in overall cases. In some cases, the performance of AR(6) and AR(10) are same as 100%.

CHAPTER 6

ICTAL EEG CLASSIFICATION BASED ON STATE SPACE MODELING OF IMF SIGNAL

This chapter deals with the ictal classification using nonlinear methods. Here IMF components of EEG signal are modeled in state space method. The EEG signal is subjected to empirical mode decomposition that yields a set of IMFs. Taking into account the nonlinear characteristics of the EEG signal, state space analysis of the IMFs is carried out. In order to accommodate the abrupt changes taking place within the EEG signal, a recursive estimation of the state values is done. Kalman filter is used for estimation of the state of the system. Several features are then extracted from the state estimations. Finally, a classification of the ictal EEG signal and healthy EEG is performed for the feature vectors of the state estimation.

6.1 INTRODUCTION

The non-linear methods of EEG analysis are found to be more efficient because it could describe the complex nature of the signal. A physical system described by differential equations in terms of inputs, outputs and state variables is called state space model (Sengupta *et al.* 2014). The state space model aims to ascertain information about the states as the new information from the given data. The potential to handle time varying attributes, missing data and the ability to incorporate changes makes state space model quite attractive (Cheung *et al.* 2010).

In a state space model, differential or difference equations of first order are used by the state variables to describe a system rather than using one or more nth order differential or difference equations. State variables are hidden and can't be obtained during the experiment, but can be rebuilt from the

obtained input-output data. A recursive estimation of the state vector improves adaptation to abrupt changes in the EEG signals (Wang *et al.* 2015). Kalman filter is one such method for recursive estimation, which enhances the epilepticform discharge spike (Oikonomou *et al.* 2007). Here in this chapter, state space estimation of different IMFs was obtained, which could reveal more information regarding the internal states of the system. The Kalman filter is used to estimate the state of the system. Then different features were extracted from the state vectors which will help to distinguish between ictal EEG and healthy EEG signals using a classifier.

6.2 METHODOLOGY

The Figure 6.1 shows the functional diagram of the proposed method. Initially, the EEG signal is made to undergo empirical mode decomposition. Then intrinsic mode functions are used for state space analysis. Kalman filter is incorporated to obtain the state values of the each IMF. Multiple features are extracted from the state values. These features are fed to a classifier, which will classify the signal as healthy EEG or ictal EEG.

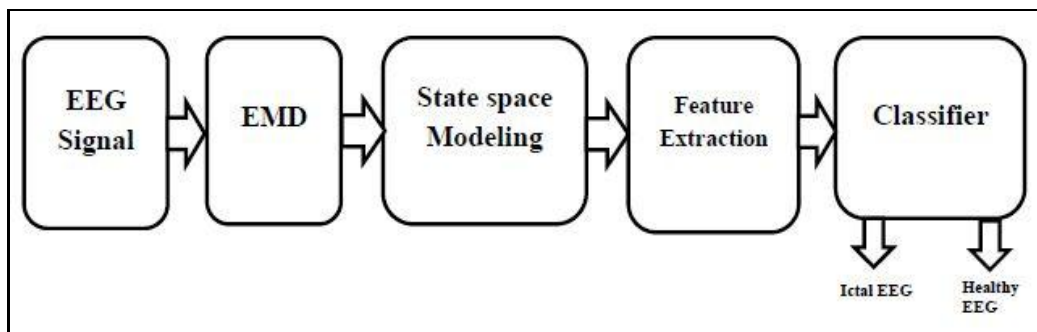


Fig. 6.1 Functional diagram of the proposed

6.3 ESTIMATION OF STATE SPACE MODEL

The Kalman filter is an efficient linear quadratic estimator which determines the internal state of a system from a set of noisy measurements over the time. It is a recursive algorithm for finding the state of a system

(Goshvarpour *et al.* 2014). It only requires the state estimation from the previous time step for estimating the current state value. The Kalman filter can be described as a combination of predict phase and update phase. In predict phase, the state estimation from previous time step is used to obtain the current state estimate. It is called a priori state estimate. In update phase, the state estimate at the current time step is combined with observation information to obtain the modified state estimation. It is called a posteriori state estimate.

The Kalman filter averages the predicted state and the measurement information by making use of a weighted average. The purpose of taking weights is that those values with better estimated ambiguity, which are trusted more. The ambiguity in state predictions is called covariance. The weights are computed from the covariance. It assures that the latest state estimate is in between the predicted and the observed state and has better estimated ambiguity than either of them considered separately. At every time step, the process is repeated with the covariance and new estimate enhancing the prediction in the subsequent iteration. Since certainty of measurements is difficult to calculate, the Kalman gain is formulated. It is a measure of the comparative uncertainty of measurements and it presents the state estimation. It can be modified to obtain the desired performance.

The Kalman filter is described by using the state space approach (Lacey 2019; Bishop and Greg, 2001). The state vector, x_k of the state of a discrete time controlled process is defined by the linear difference equations:

$$x_{k+1} = \Phi x_k + w_k \quad (6.1)$$

$$z_k = H x_k + v_k \quad (6.2)$$

Where z_k is measurement data, Φ is the state transition matrix, H is Observation matrix of the discrete time controlled process with measurement error, v_k and white noise, w_k . The w_k and v_k are independent, white random

variables which possess normal probability distributions, $p(w) \sim N(0, Q)$ and $p(v) \sim N(0, R)$.

$$Q = E[w_k w_{k+1}^T] \quad (6.3)$$

$$R = E[v_k v_{k+1}^T] \quad (6.4)$$

R is the state noise covariance and Q is the measurement error covariance.

The covariance matrix, P_k is defined from the mean square error as

$$P_k = E[e_k e_{k+1}^T] \quad (6.5)$$

$$P_k = E[(x_k - \hat{x}_k)(x_k - \hat{x}_k)^T] \quad (6.6)$$

Assume that prior estimate of state vector, \hat{x}_k is called \hat{x}_k^- .

The estimate of state vector, \hat{x}_k is update from prior estimate of state vector, \hat{x}_k^- , is measurement data, z_k and observation matrix, H .

$$\hat{x}_k = \hat{x}_k^- + K_k(z_k - H\hat{x}_k^-) \quad (6.7)$$

The $(z_k - H\hat{x}_k^-)$ is the measurement residual, r_k and K_k is the Kalman gain.

Substituting the Equ. (6.1) in Equ. (6.7)

$$\hat{x}_k = \hat{x}_k^- + K_k(Hx_k + v_k - H\hat{x}_k^-) \quad (6.8)$$

Substituting the Equ. (6.8) in Equ. (6.6)

$$P_k = E \left[\left((I - K_k H)(x_k - \hat{x}_k^-) - K_k v_k \right) \left((I - K_k H)(x_k - \hat{x}_k^-) - K_k v_k \right)^T \right] \quad (6.9)$$

The error of prior estimate, $(x_k - \hat{x}_k^-)$ is uncorrected with measurements noise, So the covariance matrix, P_k is reduce as

$$P_k = (I - K_k H) E \left[(x_k - \hat{x}_k^-)(x_k - \hat{x}_k^-)^T \right] + (I - K_k H)^T + K_k E[v_k v_k^T] K_k^T \quad (6.10)$$

Substituting the Equ. (6.4) and Equ. (6.6) in Equ. (6.10)

$$P_k = (I - K_k H) P_k^- (I - K_k H)^T + K_k R K_k^T \quad (6.11)$$

The P_k^- is the prior estimate P_k .

Rearrange the Equ. (6.11) as

$$P_k = P_k^- - K_k H P_k^- - P_k^- H^T K_k^T + K_k (H P_k^- H^T + R) K_k^T \quad (6.12)$$

The trace of the error covariance matrix, P_k is the sum of mean square error of diagonal element in the matrix.

$$T[P_k] = T[P_k^-] - 2T[K_k H P_k^-] + T[K_k (H P_k^- H^T + R) K_k^T] \quad (6.13)$$

Where $T[P_k]$ is the trace of the error covariance matrix, P_k

The trace of error or mean squared error should be minimized to obtain an optimal Kalman gain. So the trace of covariance matrix, P_k is differentiated with respect to K_k and equated to zero.

Differentiate the Equ. (6.13) with respect to K_k

$$\frac{dT[P_k]}{dK_k} = -2(H P_k^-)^T + 2K_k (H P_k^- H^T + R) = 0 \quad (6.14)$$

$$(H P_k^-)^T = K_k (H P_k^- H^T + R)$$

$$K_k = P_k^- H^T (H P_k^- H^T + R)^{-1} \quad (6.15)$$

Where K_k is the Kalman gain.

Rearrange the Equ. (6.15)

$$P_k = P_k^- - P_k^- H^T (H P_k^- H^T + R)^{-1} H P_k^- \quad (6.16)$$

Substituting the Equ. (6.15) in Equ. (6.12)

$$P_k = P_k^- - K_k H P_k^- = (I - K_k H) P_k^- \quad (6.17)$$

This updates the equation for the error covariance matrix, P_k with optimal gain.

The Equ. (6.8), Equ. (6.15) and Equ. (6.17) are used for estimate the state vector, x_k

The prior estimate of state vector, \hat{x}_k^- is by

$$\hat{x}_{k+1}^- = \Phi \hat{x}_k \quad (6.18)$$

Similarly, prior error in time k+1 is

$$e_k^- = (x_{k+1} - \hat{x}_{k+1}^-) \quad (6.19)$$

Substituting the Equ. (6.1) and Equ. (6.18) in Equ. (6.19)

$$e_{k+1}^- = (\Phi x_k + w_k) - \Phi \hat{x}_k = \Phi e_k + w_k \quad (6.20)$$

Similarly, prior covariance matrix, P_k in time k+1 is by substituting the Equ. (6.19) in Equ. (6.6)

$$P_{k+1} = E[(\Phi x_k + w_k)(\Phi x_k + w_k)^T] \quad (6.21)$$

The noise, w_k is accumulate in the interval k and $k+1$, where measurement error e_k , is buildup until the time k . So and e_k and w_k are perfectly have zero cross correlation.

There for the Equ. (6.21) is

$$P_{k+1} = E[\Phi e_k (\Phi e_k)^T] + E[w_k w_k^T] \quad (6.22)$$

Substituting the Equ. (6.3) and Equ. (6.5) in Equ. (6.22)

$$P_{k+1} = \Phi P_k \Phi^T + Q \quad (6.23)$$

The Equ (6.7) and (6.17) are update the state estimate and error covariance.

The Equ (6.18) and (6.23) are project into $k+1$ interval of state estimate and error covariance respectively are parameters in the Kalman filter recursive algorithm.

6.4 FEATURE EXTRACTION

In order to perform a successful ictal classification, different features are to be extracted. Features form the basis for detection and classification procedures in biomedical signal processing. A number of features can be obtained from the state estimations and feature reduction was carried out to obtain optimum features for effective classification. The extracted features are Mean Energy (ME), Mean Teager Energy (MTE), Approximate Entropy (ApEn), Sample Entropy (SpEn), Mean Autocorrelation (MA), Interquartile Range (IQR), Mean Absolute Deviation (MAD), Kurtosis (K_U), Variance (V) and Standard Deviation (STD). Table 6.1 shows the relevant mathematical expressions for computation of the different features in this analysis (Acharya *et al.* 2012; Gopan *et al.* 2012; Alam and Bhuiyan 2013).

The energy parameters, entropy parameters, interquartile range are explained in Section 4.4. The relevance of higher order statistics parameter, Kurtosis is explained in Section 5.3. The approximate entropy indicates the ambiguity of time series fluctuations in EEG. It describes the probability that additional replicas will not occur after identical observation patterns. The

healthy EEG often has a low value of approximate entropy with high regularity of data. However, the ictal EEG has high approximate entropy with random variations. Sample entropy is an adaptation of approximate entropy. It measures the complexity of physiological time series. Approximate entropy includes self matches when template matching is performed, which lowers the approximate entropy value. The ApEn is a biased estimator and it is lower than expected value. The sample entropy is a modification of ApEn, in which the self-comparison between vectors is avoided. So sample entropy performs better results in the measure of complexity in the time series signal. Autocorrelation of the signal is correlation between the signal in different times. The Mean Autocorrelation of a random process is the expectation of deviation of mean, \bar{x} and the time lag of the mean, \bar{x} .

The distinct of EEG signal are measured based on the IMFs and used it for epileptic signal classification (Pachori *et al.* 2015). The first four IMFs of EEG signals show better ictal classification results because of the larger information about the ictal EEG that is located in the initial four IMFs components (Sharma and Pachori, 2015; Oweis and Abdulhay, 2011). In this work, the features of coefficients of state space model of first four IMFs are considered for the ictal classification.

Table 6.1 Relevant mathematical expressions
of different features for computation.

Sl.No	Feature Parameter	Equation	remarks
1	Mean Energy (ME)	$ME = \log\left(\frac{1}{L} \sum_{n=1}^L (x(n))^2\right)$	
2	Mean Teager Energy (MTE)	$MTE = \log\left(\frac{1}{L} \sum_{n=1}^L (x(n)^2 - x(n+1)x(n) - 1)\right)$	
3	Approximate Entropy (ApEn)	$ApEn(N, m, r) = \Phi^m(r) - \Phi^{m+1}(r)$ $\Phi^m(r) = (N - (m - 1))^{-1} \sum_{i=1}^{N-m-1} \ln C_{m,i}(r)$	$C_{m,i}(r)$ is correlation integral, r, N, m integer
4	Sample Entropy (SpEn)	$SpEn(m, r, N) = \ln\left(\frac{C_{m+1}(r)}{C_m(r)}\right)$	
5	Mean Autocorrelation (MA)	$MA = \frac{E[(x - \bar{x})(x_\tau - \bar{x})]}{\sigma^2}$	
6	Interquartile Range (IQR)	$IQR = Q_3 - Q_1$	Q_3 is the third quartile and Q_1 is the first quartile
7	Mean Absolute Deviation (MAD)	$MAD = \frac{1}{L} \sum_{i=1}^n (x(i) - \bar{x})$	\bar{x} is the mean value of $x(n)$
8	Variance (V)	$V = \frac{1}{L} \sum_{i=1}^N x(i) - \bar{x})^2$	
9	Standard Deviation (STD)	$STD = \sqrt{\frac{1}{L} \sum_{i=1}^n (x(i) - \bar{x})^2}$	
10	Kurtosis (K_U)	$K_U = \frac{1}{L} \sum_{i=1}^L \frac{(x(i) - \bar{x})^4}{\sigma^4}$	

6.5 RESULTS AND DISCUSSION

Here only set A is considered for normal EEG signal and set E for ictal EEG signal as in the EEG database, discussed in Section 2.2. Each set is of 23 second duration with a length of 4096 samples. The first step in the analysis was to process EMD of the each of the set of EEG signals. The Figure 6.2 shows one of the EEG sample signal corresponding healthy EEG from the University of Bonn EEG database and its four IMFs in ascending order. The Figure 6.3 shows the one of the ictal EEG sample signal from the University of Bonn EEG database and its four IMFs in ascending order. The healthy EEG signal has less amplitude variations when compared to the ictal EEG signals. The EEG signals corresponding to ictal have sudden variations in amplitude, which can be observed in Figure 6.2 and Figure 6.4. The average computation time required for extracting IMFs from the EEG is 12.53 s per each category of the data set.

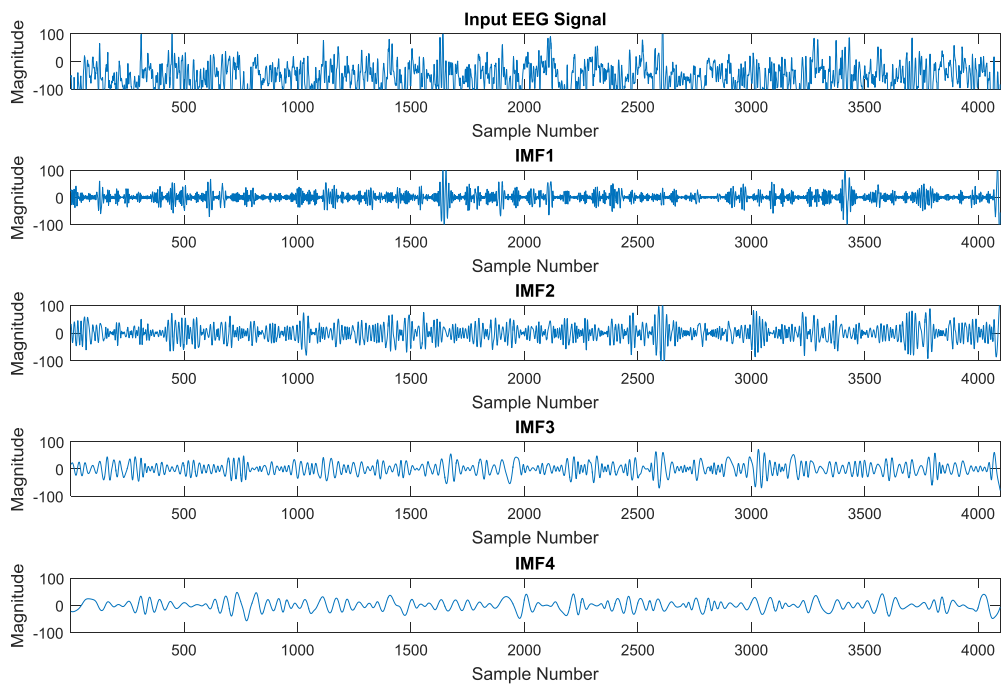


Fig. 6.2 Healthy EEG signal and its IMFs

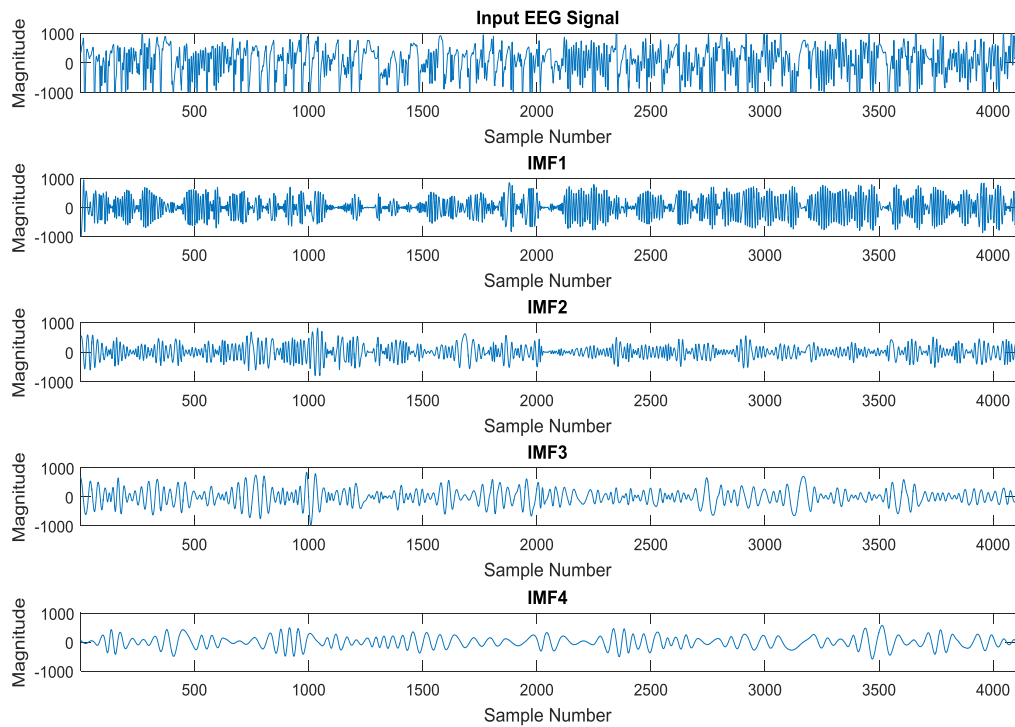


Fig. 6.3 Epileptic EEG signal and its IMFs

The process of decomposing the signal into IMFs causes specific frequency components to be separated out. The initial IMF has higher frequency components present in the EEG signal and in the lower IMFs, frequency components are gradually decreasing from high frequency. Also, the amplitudes of lower IMFs vary drastically when compared to higher IMFs. The amplitude variations in different IMF are shown in Figure 6.2 and Figure 6.3.

In this study, the features obtained from the first set of four IMFs are only considered to estimate the state space model. Then Kalman filter was used to obtain the state estimations of neural activity. Here Kalman filter estimate the 10th order state space model of the EEG data. So 10th order state vector is estimated from a set of 10th order recursion equations.. The different features are extracted from the state vector. The extracted features are mean energy, mean Teager energy, approximate entropy, sample entropy, mean autocorrelation, interquartile range, mean absolute deviation, Kurtosis, variance and standard deviation. The average computation time for the feature extraction of the state space model is 69.99 s per each IMF in each category of the data set. An analysis on the effect of mean Teager energy feature of the state estimations of different IMFs of seizure and healthy EEG datasets was also carried out. The comparison of mean Teager energy values of first four IMFs in healthy EEG and ictal EEG are shown in Figure 6.4 and Figure 6.5 respectively.

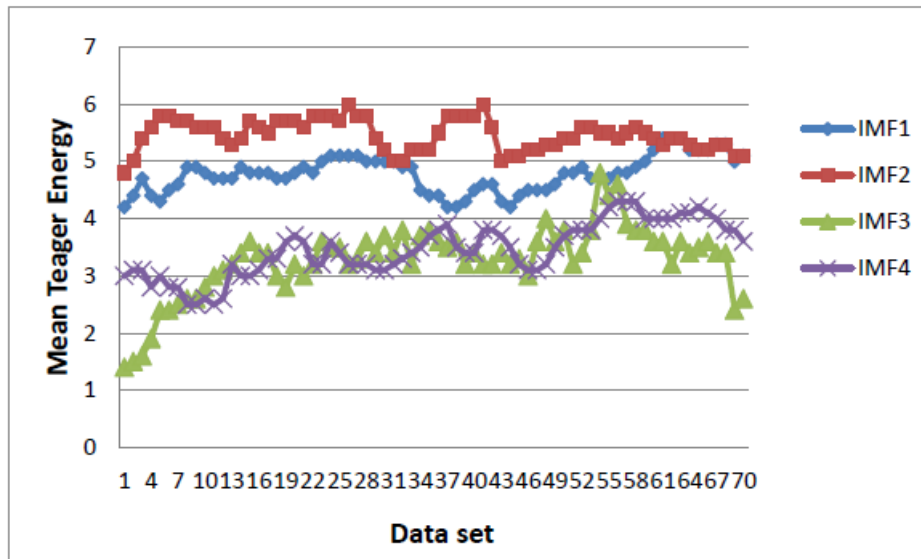


Fig. 6.4 Mean Teager energy of state values of healthy datasets for different IMFs

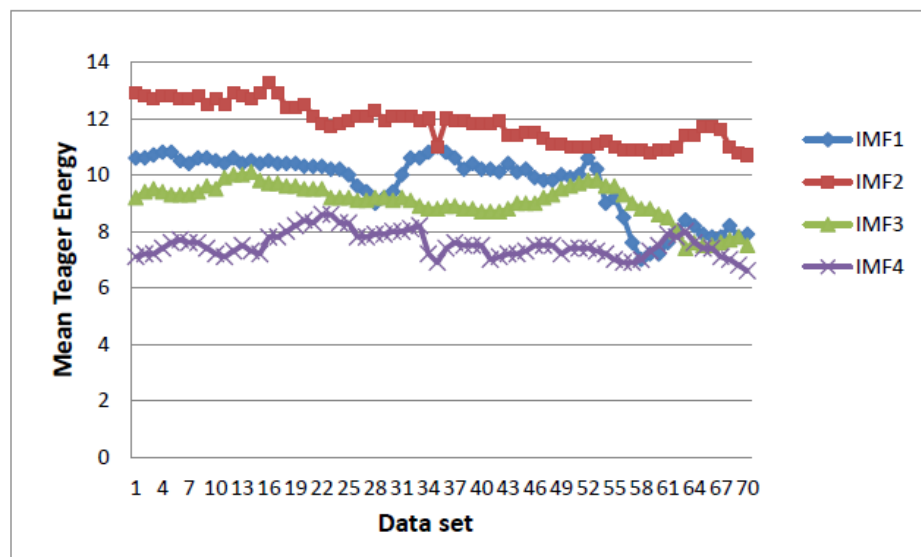


Fig. 6.5 Mean Teager energy of state values of ictal datasets for different IMFs

In the Figure 6.4 and 6.5, it is observed that mean Teager energy values of ictal EEG data are higher when compared to healthy EEG data. The ascending value of IMF is attributed to high frequency information in the original signal. The mean Teager energy of initial IMFs in the ictal EEG

shows highest values compared with the healthy EEG signals. Also among the mean Teager energy values of different IMFs, second IMF shows highest value for both healthy and ictal EEG signals. It was observed that second IMFs could capture relevant information of ictal EEG signals. Hence, it is highly efficient for spike detection, which is related to sudden appearance of high frequencies and rise in instantaneous energy.

The features of the state estimations of the IMF1, IMF2, IMF3 and IMF4 of ictal EEG and healthy EEG signals were fed to an ANN classifier. The total size of the population is 140 in each IMFs. So total sample size for feature classification is 560, which is enough as per Cochran's sample size formula for grouped data with 95% confidence level and margin of error as ± 0.05 . Approximately 70% of the samples are used for training out of 560 samples and 80 samples are used for testing the classifier performance. The ANN classifier yielded a successful classification of the given EEG data to ictal or healthy based on supervised learning. The back propagation algorithm is selected to train the three layer MLPNN. The gradient descent method was used to decrease the error rate in the network. The details of MLPNN structure used in the classification is explained in Section 5.5. The performance of the classifier was assessed in terms of three statistical parameters called sensitivity, specificity and accuracy. Table 6.2 shows the performance of the classifier for the proposed features for classification. The average computation time for the ANN classifier of each feature is 5.25 s. From the table, it shows that mean energy, mean Teager energy and Kurtosis shows better results in the classification of ictal EEG signals. Apart from the individual performance of each features, the classifier was assessed to a combination of selected features were fed as the inputs to the classifier.

Table 6.2 Classifier performance for different features

Feature	Sensitivity (%)	Specificity (%)	Accuracy (%)
Mean Energy	100	85	92
Mean Teager Energy	100	100	100
Approximate Entropy	80	50	65
Sample Entropy	80	80	80
Mean Autocorrelation	100	30	65
Interquartile Range	100	80	90
Mean Absolute Deviation	100	80	90
Standard Deviation	100	60	80
Variance	100	30	65
Kurtosis	100	85	92

The combination of features is due to energy features, entropy features and statistical features. The mean energy & mean Teager energy, approximate entropy & sample entropy, interquartile range & mean absolute deviation and Kurtosis & standard deviation are group together for the classification. In combined feature selection approximately 70% of the samples are used for training out of 1120 samples and 160 samples are used for testing the MLPNN classifier performance.

The performance of the classifier was assessed in terms of confusion matrix and Receiver Operating Characteristics (ROC) curve (Sonogo *et al.* 2018). The ROC curve is a plot between False Positive Rate (FPR) and True Positive Rate (TPR). The collection of all possible combinations of FPR and TPR is called ROC curve. TPR is equivalent to sensitivity and FPR is equivalent to specificity. The ideal point in ROC space corresponds to 100% sensitivity and specificity. This yields the coordinates (0, 1). This point indicates perfect classification. The interpretation of ROC curve is that, a curve closer to the ideal coordinates yields an accurate test. If a test has sensitivity and specificity of 50% then its ROC will be along the diagonal

specified by coordinates (0, 0) and coordinates (0, 1). A random guess yields point along this diagonal as per the theory. If a point estimated by a test falls into the upper half area relative to the diagonal, it represents good classification. Otherwise, classification will be bad. Figures 6.6 to 6.9 shows confusion matrix and ROC curve of ANN classifier with the combination of different features. Then sensitivity, specificity and accuracy were also obtained from the confusion matrix to evaluate the performance of the proposed method.

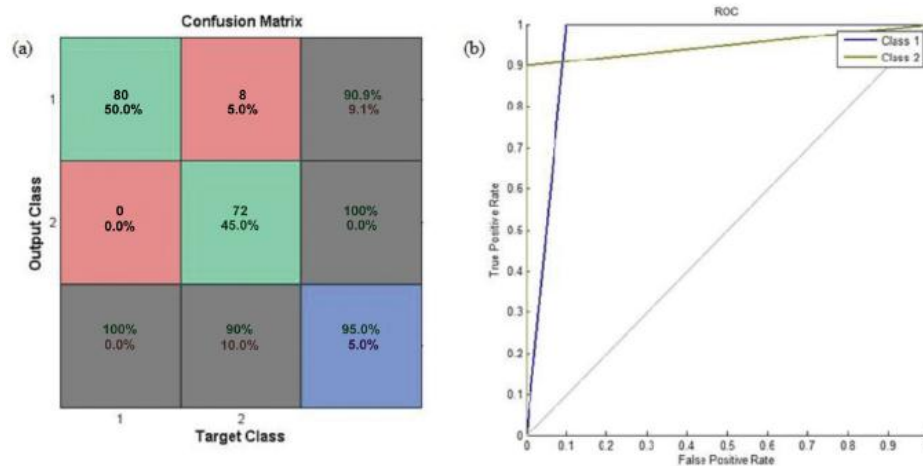


Fig. 6.6 Confusion matrix and ROC curve of ANN classifier with Kurtosis-standard deviation features.

Figure 6.6 shows the ROC curve for healthy dataset given by the blue line and the ROC curve for epileptic dataset given by the green line. Both ROC curves are above the diagonal line. The ROC curve of healthy signal approaches the ideal coordinates faster when compared to epileptic signal. Hence the classification for healthy signal is more accurate when compared to epileptic signal. The classification has a sensitivity of 100%, specificity of 90% and accuracy of 95%.

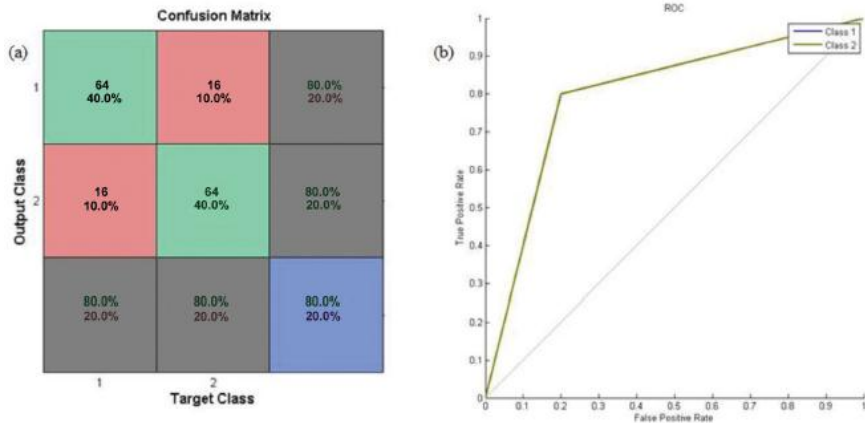


Fig. 6.7 Confusion matrix and ROC curve of ANN classifier with Approximate entropy-Sample entropy features.

The ROC curve for both healthy and epileptic datasets in Figure 6.7 shows that ROC curve of ANN classifier with approximate entropy and sample entropy feature has the same shape. The epileptic dataset's curve is superimposed on healthy dataset's curve. The ROC curve of epileptic dataset is shown by green line. Both ROC curves are above the diagonal line. Both ROC curves approaches the ideal coordinates at the same rate. The classification has a sensitivity of 80%, specificity of 80% and accuracy of 80%.

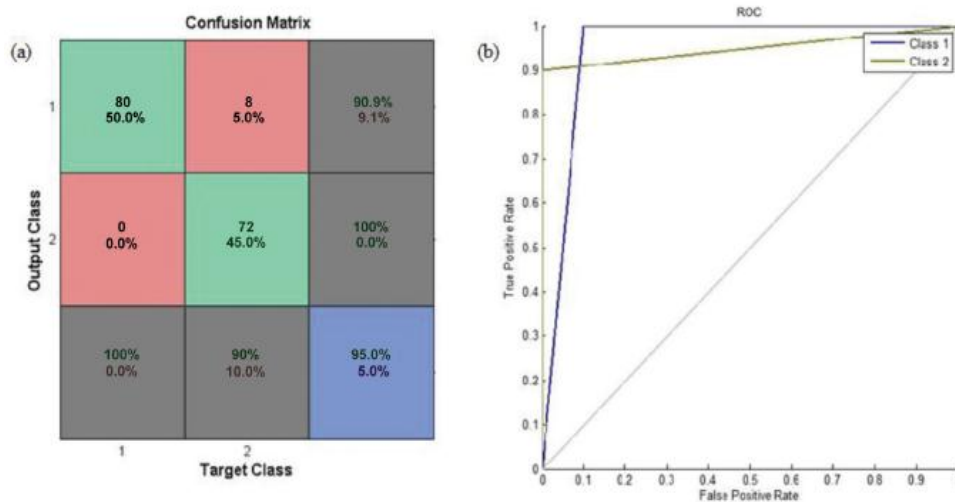


Fig. 6.8 Confusion matrix and ROC curve of ANN classifier with Interquartile range - Mean absolute deviation features.

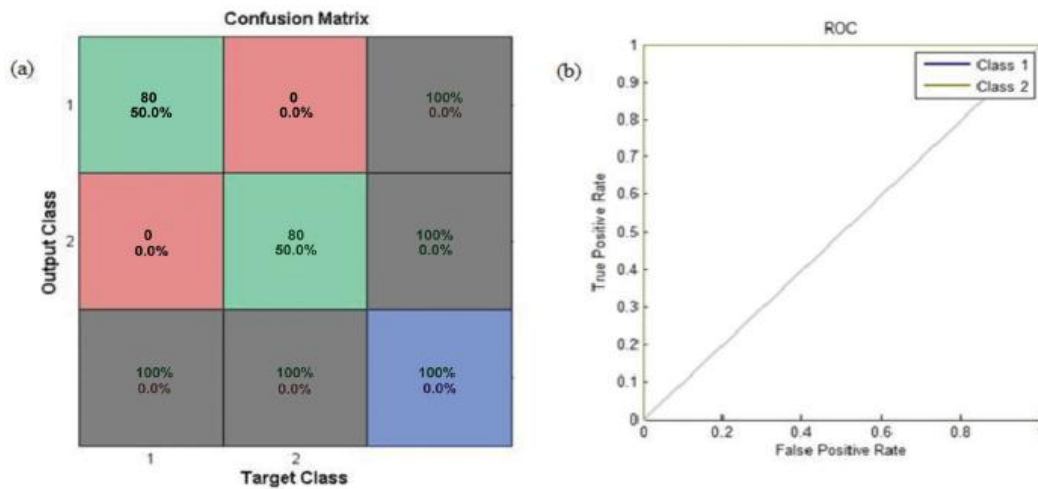


Fig. 6.9 Confusion matrix and ROC curve of ANN classifier with Mean energy - Mean Teager energy features.

Figure 6.8 shows the ROC curve of ANN classifier with interquartile range - mean absolute deviation feature. The performance of the classifier has a sensitivity of 100%, specificity of 90% and accuracy of 95%. Figure 6.9 shows confusion matrix and ROC curve of ANN classifier with Mean energy and Mean Teager energy features. In Figure 6.9, the ROC curves for both healthy and epileptic datasets are lines parallel to the x-axis with TPR value of 1. This indicates that the combination of Mean energy and Mean Teager energy features have achieved 100% classification accuracy. This combination also yields 100% performance in sensitivity and specificity.

Table 6.3 Classifier performance for different combination of features

Features	Sensitivity (%)	Specificity (%)	Accuracy (%)
Kurtosis & Standard Deviation	100	90	95
Approximate Entropy & Sample Entropy	80	80	80
Interquartile Range & Mean Absolute Deviation	100	90	95
Mean Energy & Mean Teager Energy	100	100	100

The sensitivity, specificity and accuracy of the combination of features are tabulated in Table 6.3. The average computation time for the ANN classifier of different combination of features is 6.05 s. The table shows that a combination of mean energy & mean Teager energy will serve as an appropriate feature set for classification of EEG signal into healthy and epileptic class. The combination of Kurtosis & standard deviation and interquartile range & mean absolute deviation features can also get good accuracy of about 95%. Table 6.4 shows the comparison of other non linear algorithms in the EEG classification using the EEG data set.

Table 6.4 Comparison with other algorithms
in the literature using the EEG data set

Authors	Methods employed	Classification Accuracy (%)
Riaz F <i>et al.</i> 2016	Temporal and Spectral EMD and SVM	96
Martis <i>et al.</i> 2015	Nonlinear features EEG sub-bands	96.33-98
Djemili <i>et al.</i> 2016	IMF features	97.7
Acharya <i>et al.</i> 2012	Entopies -Fuzzy classifier	98.1
Jia <i>et al.</i> 2017	Ensemble EMD of phase space	98
Sharma and Pachori, 2015	IMFs phase space	98.67
Bajaj and Pachori, 2012	EMD bandwidth LSSVM	99.5 - 100
Alam and Bhuiyan, 2013	Higher order statistics of IMFs and ANN	80-100
Goshvarpour <i>et al.</i> 2014	EEG Time series with state space model-RMS	98
Wang <i>et al.</i> 2015	Cauchy-Based State-Space and SVM	100
Proposed method	State space modelling of IMF-ME, MTE and ANN	100

6.6 INFERENCES

In this chapter, combination of empirical mode decomposition and state space model were used to analyze the EEG signal and to classify it as healthy EEG or ictal EEG. The EEG signal was decomposed into a set of IMFs that are band limited using EMD. With the aid of Kalman filter, estimation of the state matrix was obtained for the system. Multiple features were extracted from the state values and these were used for classification. The use of ANN helped fast computation in the classification of the EEG signals as epileptic or healthy. Here we used scaled conjugate gradient back-propagation algorithms for training. Only 140 EEG data are used for training, validation and testing sections. The method provided a successful means for classifying the ictal EEG signals. It was found that second IMFs could capture relevant underlying properties of EEG signals. Among the multiple features, the mean Teager energy served as an efficient and reliable feature in automatic seizure classification scenarios.

CHAPTER 7

CONCLUSIONS

The EEG is non-stationary and nonlinear in nature, which reflects the activity of the brain. The EEG measurements will help in diagnosing and treatment of many neurological disorders. Epilepsy is one of the most common neurological disorders other than stroke. In an EEG recording, the ictal is characterized by an acute epileptic seizure. The EMD is a well-accepted method for analyzing non-linear and non-stationary time series signal, which is more applicable for EEG signal. The EMD algorithm is a novel method for decomposing the signal into intrinsic mode function (IMF) and residue.

The combination of EMD with Hilbert transform analysis makes use of various parameters obtained from the instantaneous amplitude function and the instantaneous frequency function of EEG. Thus, we can explore the non-stationary and nonlinear EEG data in more detailed manner in comparison with other existing EEG analyzing methods. The EMD has lesser complexity. Variations in basic EMD approach have been able to reduce the mode-mixing problem.

7.1 CONTRIBUTION OF THE THESIS

The main objective of the thesis was to develop new methodology for ictal classification. Here we summarize the work carried out in this thesis to realize the goals identified in Chapter 1.

7.1.1 EEG analysis using wavelet packet transform for epileptic seizure detection

In this proposed method, the EEG signal is analyzed using Wavelet packet decomposition method. Here the pre-processed EEG is first decomposed into four levels using WPT method. The selected packets on each level of the WPT are

map to the sub-band of EEG signals. The different energy and entropy features of selected packets are obtained for normal EEG and epileptic EEG. The average training error of different sub-bands of EEG is compared. The lowest training error of all the feature parameters is in delta and theta sub-band. This shows the epileptic discharge not only affects the delta band, but its effects may propagate to theta sub-band also. The Mean Teager Energy feature shows a lowest training error in FIS training. Finally, mean Teager energy is taken in constructing the feature vector for ANFIS to classify the epileptic and normal EEG signals. To construct the feature vector of all mentioned energy-entropy features in the delta band is performed in the ANFIS classifier for seizure classification. The total classification accuracy of 97.5% is obtained. If the Mean Teager Energy in the delta band is taken as input to the classifier, 98.33% of total classification accuracy is achieved.

The proposed method is also tested in CHB-MIT scalp EEG database. Here the effect of seizure EEG signal is examined in T7-P7 and T8-P8 lobes. It shows that mean Teager energy has high significant difference in the delta band. The feature vector in channel T8-P8 is higher than the feature vector of channel T7-P7. It concludes that the selected data set (chb01) is a case of temporal lobe epilepsy. The main contribution of the chapter is that the mean Teager energy is the most weighted parameter of the EEG signal for classifying epileptic seizure.

7.1.2 Energy-Entropy feature extraction of the instantaneous amplitude function and statistical features of the instantaneous frequency function for ictal EEG classification

This work focuses on the ictal EEG classification strength of energy and entropy-based features using IMF components from EMD and their instantaneous amplitudes using HHT. The effect of ictal classification in different individual IMF features, feature vectors as multiple features with individual IMFs, and

feature vectors as individual features from multiple IMFs of both amplitude and frequency contour in HHT are tabulated. Therefore, to obtain an optimal single feature, we used the vector of features or vector of IMFs for better classification of ictal EEG and healthy EEG. To implement an embedded personal health care system, the number of features shall be minimized to reduce computation time and system complexity. The main contribution is to analyze the features individually in different Cases. These Cases are statistically evaluated by ANOVA test with feature ranking, in IA and IF functions. These features are concluded to possess a great discriminating power on the instantaneous amplitudes. By employing ANN and ANFIS classification, these features can be seen to perform well in the identification of seizure segments of EEG data. Compared with all IMFs, IMF2 and IMF1 has shown a good performance with 100% accuracy in the case of energy of an instantaneous amplitude. The standard deviation of frequency distribution also achieves 100% accuracy. These features are very much useful in representing the EEG data for an ictal detection.

7.1.3 Different types of ictal classification on spectral and temporal features of instantaneous amplitude -frequency components

In this methodology, the incoming EEG signals are pre-processed by the EMD method to obtain the IMFs, which represents a simple oscillatory mode as a counterpart to the simple harmonic function. Here only the first and second IMFs are extracted, which have relevant information about epileptic seizures. The different types of ictal EEG classification are tabulated using the spectral and temporal features of HHT. In this method, combining the features of the IA and IF functions of HHT is used as a feature vector to classify various ictal types. The spectral features of IA and temporal features of IF are more suitable for ictal classification. Four different Cases are framed for the classification. The different cases are Case 1 for healthy EEG with ictal EEG signal; Case 2 for healthy EEG with interictal EEG signal; Case 3, interictal EEG with ictal EEG signal; and Case

4 for combination of healthy EEG signal and interictal EEG signal with ictal EEG of HHT1 and HHT2 components respectively.

Spectral features of IA2 and temporal features of IF2 yield better results in terms of classification performances. The spectral feature of AR (10) order model shows better results when compared to all the Cases. The statistical validation are performed using the EEG datasets. There is significant different in Case1 and Case 3. The spectral features of IA2 and temporal features of IF2 of Case1, Case 3 and Case 4 achieve 100% classification accuracy.

7.1.4 Ictal EEG classification based on state space modeling of intrinsic mode function

In this work, the EEG signal is subjected to empirical mode decomposition, which yields a set of IMFs. Taking into account the nonlinear character of the EEG signal, state space analysis of the IMFs is carried out. In order to accommodate the abrupt changes taking place within the EEG signal, a recursive estimation of the state values is done. The Kalman filter is used for this purpose. Several features are then extracted from the state estimations. The artificial neural network is used to classify ictal EEG and healthy EEG status. The study shows mean Teager energy have 100% accuracy and Kurtosis and mean energy has 92% accuracy in ictal classification compared to other features. Finally, a classification of the EEG signal into a healthy and epileptic groups is performed. The combination of mean energy & mean Teager energy features shows a higher classification performance with 100% sensitivity, 100% specificity and 100% accuracy.

Novelty and originality of this research work is that an innovation methodology for ictal classification by employing an instantaneous amplitude-frequency contour of the IMFs of an EEG signal. The EMD is a method to decompose a nonlinear and non-stationary signal into a set components called,

IMFs. The main contribution of the thesis is that instantaneous frequency function and instantaneous amplitude function of IMF2 has better ictal classification accuracy than IMF1, which indicates that the ictal information is accumulated in IMF2. The IMF1 and IMF2 of instantaneous amplitude - frequency components show significant information about the ictal EEG compare to other IMFs. This indicate that the useful information for the discrimination between the healthy EEG and ictal EEG signals is mainly centred in the higher order IMFs. As reported in the literature survey that researchers are used features of all IMFs components for seizure detection. This will helps the researchers to concentrate the seizure detection problems in IMF1 and IMF2 components.

The second novelty of the thesis is to perform an ictal classification method, which combines spectral and temporal features of IA and IF, twin components of Hilbert- Huang Transform. Here spectral features are tabulated AR Burg's method, which is most suitable model based spectrum estimation for spectral analysis of EEG. The spectral features of IA and temporal features of IF is better ictal classification than spectral features of IA and temporal features of IA is all the cases discussed in section 5.4. The third novelty is to perform an ictal classification based on state space model on the IMFs. The state space analysis of the IMFs is carried out due to the non-linear characteristics of the EEG signal. The recursive estimation of the state values is done using Kalman filter.

The main contribution of the thesis is that instantaneous frequency function and instantaneous amplitude function of IMF2 has better ictal classification accuracy than IMF1, which indicates that the ictal information is accumulated in IMF2. In particular, IMF 2 has shown good performance with 100% accuracy of energy/entropy of amplitude distribution and the standard deviation of frequency distribution. The second contribution is the spectral features of IA and temporal features of IF is better ictal classification than spectral features of IA and temporal features of IA is all the cases discussed in section 5.4.

The features of AR (10) order model shows better results in overall cases. The third contribution is among the multiple features, the mean Teager energy served as an efficient and reliable feature in automatic seizure classification scenarios.

In current scenario, as mention in first paragraph of the motivations, accuracy and reliability of visual interpretation of the brain signal are limited. This lead patients visit normal physicians in multiple times. Later, the patients will end up to a specialist. Due to lack of exact features from EEG, the patients may be subject to wrong diagnosis, which will lead to wrong medication for antiepileptic medicine (AEM). These medicines, which are generally expensive. Moreover, wrong diagnosis will lead to social stigma that unemployment of the epileptic patients. The computer aided diagnosis system will reduce treatment costst for the patients. The computer aided diagnosis system for ictal classification does not intend to replace Neurologist, but facilitate to diagnosis proper causes of epilepsy. It also helps the Neurologist to ensure a second opinion of the observation of the complex EEG signal.

7.2 FUTURE SCOPE OF WORK

Seizure detection in long-term EEG data will be a tedious task for clinicians. In brief, most of the existing automated epilepsy detection methods are short segment EEG analysis for deducing the computational complexity. This will fail to tabulate the exact time of seizures occurrence. The conventional method to find the exact time of the seizure is to review from the EEG long data. However, this is time consuming and sometimes misidentifies the seizure pattern. The multivariate feature extraction of long term EEG using instantaneous amplitude function and instantaneous frequency function of HHT will give local information of epileptic seizure. Therefore, it shall focus on long-term EEG data for feature extraction by using Hilbert spectral analysis. It also focuses on complex features of long-term EEG signals, which

are directly extracted using deep learning classifier. Then one can select dominated features for the ictal classification, to reduce computational complexity. If it requires large computation, then computation time can be minimized by implementing cloud computing.

Real-time EEG processing can be possible with the Altium nanoboard 3000 FPGA development board to ensure the performance of the proposed algorithms. It can also be implemented in an embedded personal health care system with a wireless wearable sensor for a real-time seizure alert system.

Now days, medical diagnosis is efficiently possible due to telemetry biomedical data. In EEG telemetry applications, Neurologists required an efficient system, which provides more accurate, meaningful and timely information of reconstructed EEG data. This area of research is more challenging because of the large amount of data and randomness in the inherent behaviour of the EEG signal. For the efficient storage and/or transmission of EEG signals, the EEG telemetry system required a low error in reconstruction with high compression for more timely and accurate diagnosis. The intrinsic mode functions of EEG are possible solution in near-lossless compression method, which is capable to store and/or transmit the EEG signals for telemetry diagnosis.

REFERENCES

- [1] **Acharya, U. R., Fujita, H., Sudarshan, V. K., Bhat, S. and Koh, J. E.** (2015) Application of entropies for automated diagnosis of epilepsy using EEG signals: a review. *Knowledge-Based Systems*, **88**, 85-96.
- [2] **Acharya, U. R., Molinari, F., Sree, S. V., Chattopadhyay, S., Ng, K. H. and Suri, J. S.** (2012) Automated diagnosis of epileptic EEG using entropies. *Biomedical Signal Processing and Control*, **7(4)**, 401-408.
- [3] **Acharya, U. R., Sree, S. V. and Suri, J. S.** (2011) Automatic detection of epileptic EEG signals using higher order cumulant features. *International Journal of Neural Systems*, **21(05)**, 403-414.
- [4] **Acharya, U. R., Sree, S. V., Alvin, A. P. C. and Suri, J. S.** (2012) Use of principal component analysis for automatic classification of epileptic EEG activities in wavelet framework. *Expert Systems with Applications*, **39(10)**, 9072-9078.
- [5] **Acharya, U. R., Sree, S. V., Swapna, G., Martis, R. J. and Suri, J. S.** (2013) Automated EEG analysis of epilepsy: a review. *Knowledge-Based Systems*, **45**, 147-165.
- [6] **Acharya, U. R., Sudarshan, V. K., Adeli, H., Santhosh, J., Koh, J. E. and Adeli, A.** (2015) Computer-aided diagnosis of depression using EEG signals. *European Neurology*, **73(6)**, 329-336.
- [7] **Acharya, U. R., Yanti, R., Zheng, J. W., Krishnan, M. M. R., TAN, J. H., Martis, R. J. and Lim, C. M.** (2013) Automated diagnosis of epilepsy using CWT, HOS and texture parameters. *International Journal of Neural Systems*, **23(03)**, 1350009.
- [8] **Adamczak, S., Makiela, W. and Stępień, K.** (2010) Investigating advantages and disadvantages of the analysis of a geometrical surface structure with the use of Fourier and wavelet transform. *Metrology and Measurement Systems*, **17(2)**, 233-244.

- [9] **Adeli, H., Zhou, Z. and Dadmehr, N.** (2003) Analysis of EEG records in an epileptic patient using wavelet transform. *Journal of Neuroscience Methods*, **123(1)**, 69-87.
- [10] **Alam, S. S. and Bhuiyan, M. I. H.** (2013) Detection of seizure and epilepsy using higher order statistics in the EMD domain. *IEEE Journal of Biomedical and Health Informatics*, **17(2)**, 312-318.
- [11] **Alotaiby, T. N., Alshebeili, S. A., Alshawi, T., Ahmad, I. and El-Samie, F. E. A.** (2014) EEG seizure detection and prediction algorithms: a survey. *EURASIP Journal on Advances in Signal Processing*, **2014(1)**, 183.
- [12] **Altunay, S., Telatar, Z. and Eroglu, O.** (2010) Epileptic EEG detection using the linear prediction error energy. *Expert Systems with Applications*, **37(8)**, 5661-5665.
- [13] **Amaro, E. and Barker, G. J.** (2006) Study design in fMRI: basic principles. *Brain and Cognition*, **60(3)**, 220-232.
- [14] **Anderson, C. W., Stolz, E. A. and Shamsunder, S.** (1998) Multivariate autoregressive models for classification of spontaneous electroencephalographic signals during mental tasks. *IEEE Transactions on Biomedical Engineering*, **45(3)**, 277-286.
- [15] **Andrzejak, R.G., Lehnertz, K., Mormann, F., Rieke, C., David, P. and Elger, C.E.** (2001) Indications of nonlinear deterministic and finite-dimensional structures in time series of brain electrical activity: Dependence on recording region and brain state. *Physical Review E*, **64(6)**, 061907-1.
- [16] **Artameeyanant, P., Chiracharit, W. and Chamnongthai, K.** (2012) Spike and epileptic seizure detection using wavelet packet transform based on approximate entropy and energy with artificial neural network. *4th International Conference on Bioinformatics and Biomedical Engineering*, Chengdu, December, 1-4.

- [17] **Azami, H., Mohammadi, K. and Bozorgtabar, B.** (2012) An improved signal segmentation using moving average and Savitzky-Golay filter. *Journal of Signal and Information Processing*, **3(01)**, 39.
- [18] **Bairy, G. M., Niranjan, U. C., Oh, S. L., Koh, J. E., Sudarshan, V. K., Tan, J. H., Hagiwara, Y. and Ng, E. Y. K.** (2017) Alcoholic index using non-linear features Extracted from different frequency bands. *Journal of Mechanics in Medicine and Biology*, **17(07)**, 1740009.
- [19] **Bajaj, V. and Pachori, R. B.** (2012) Classification of seizure and nonseizure EEG signals using empirical mode decomposition. *IEEE Transactions on Information Technology in Biomedicine*, **16(6)**, 1135-1142.
- [20] **Bajaj, V. and Pachori, R. B.** (2013) Epileptic seizure detection based on the instantaneous area of analytic intrinsic mode functions of EEG signals. *Biomedical Engineering Letters*, **3(1)**, 17-21.
- [21] **Barlett, J. E. II, Kotrlik., J. W., and Higgins, C. C.** (2001) Organizational research: Determining appropriate sample size in survey research. *Information technology, learning and performance Journal*, **19(1)**, 43-50.
- [22] **Basheer, I. A. and Hajmeer, M.** (2000) Artificial neural networks: fundamentals, computing, design, and application. *Journal of Microbiological Methods*, **43(1)**, 3-31.
- [23] **Bedrosian, E.** *A Product Theorem for Hilbert Transforms*. Santa Monica, CA: RAND Corporation, 1962.
- [24] **Blej, M. and Azizi, M.** (2016) Comparison of Mamdani-Type and Sugeno-Type Fuzzy Inference Systems for Fuzzy Real Time Scheduling. *International Journal of Applied Engineering Research*, **11(22)**, 11071-11075.

- [25] **Bigan, C. and Woolfson, M. S.** (2000) Time-frequency analysis of short segments of biomedical data. *IEE Proceedings-Science, Measurement and Technology*, **147(6)**, 368-373.
- [26] **Biju, K. S., Hakkim, H. A. and Jibukumar, M. G.** (2017) Ictal EEG classification based on amplitude and frequency contours of IMFs. *Biocybernetics and Biomedical Engineering*, **37(1)**, 172-183.
- [27] **Bishop, G., and Greg W.** (2001) An introduction to the kalman filter. *Proc of SIGGRAPH*, 27599-23175, 41.
- [28] **Boashash, B., Azemi, G. and Khan, N. A.** (2015) Principles of time–frequency feature extraction for change detection in non-stationary signals: Applications to newborn EEG abnormality detection. *Pattern Recognition*, **48(3)**, 616-627.
- [29] **Brodu, N., Lotte, F. and Lécuyer, A.** (2012) Exploring two novel features for EEG-based brain–computer interfaces: Multifractal cumulants and predictive complexity. *Neurocomputing*, **79**, 87-94.
- [30] **Cao, D., Liu, C. and Wang, P.** (2010) Application of wavelet packet energy spectrum to extract the feature of the pulse signal. *4th International Conference on Bioinformatics and Biomedical Engineering*, Chengdu, June, 1-4.
- [31] **Casaubon, L., Pohlmann Eden, B., Khosravani, H., Carlen, P. L. and Wennberg, R.** (2003) VideoEEG evidence of lateralized clinical features in primary generalized epilepsy with tonic-clonic seizures. *Epileptic Disorders*, **5(3)**, 149-156.
- [32] **Chemali, J. J., Wong, K. K., Solt, K. and Brown, E. N.** (2011) A state-space model of the burst suppression ratio. *Annual International Conference of the IEEE Engineering in Medicine and Biology Society*, Boston, MA, August, 1431-1434.
- [33] **Chen, S. J., Peng, C. J., Chen, Y. C., Hwang, Y. R., Lai, Y. S., Fan, S. Z. and Jen, K. K.** (2016) Comparison of FFT and marginal spectra of EEG using empirical mode decomposition to monitor

- anesthesia. *Computer Methods and Programs in Biomedicine*, **137**, 77-85.
- [34] **Cheung, B. L. P., Riedner, B. A., Tononi, G. and Van Veen, B. D.** (2010) Estimation of cortical connectivity from EEG using state-space models. *IEEE Transactions on Biomedical Engineering*, **57(9)**, 2122-2134.
- [35] **Coifman, R. R., and Wickerhauser, M. V.** (1992) Entropy-based algorithms for best basis selection. *IEEE Transactions on Information Theory*, **38(2)**, 713-718.
- [36] **Collins, H.** *Collins English Dictionary*. 12e. HarperCollins Publishers, UK, 2014.
- [37] **Das, A. B. and Bhuiyan, M. I. H.** (2016) Discrimination and classification of focal and non-focal EEG signals using entropy-based features in the EMD-DWT domain. *Biomedical Signal Processing and Control*, **29**, 11-21.
- [38] **Das, A., Das, P. and Roy, A. B.** (2002) Applicability of Lyapunov exponent in EEG data analysis. *Complexity International*, **9(01)**, 1-8.
- [39] **Dash, B. and Jounious, A. M. M.** *Handbook of Ayurveda*. Concept Publishing Company, NewDelhi, 1997.
- [40] **Deivasigamani, S., Senthilpari, C. and Yong, W. H.** (2016) Classification of focal and nonfocal EEG signals using ANFIS classifier for epilepsy detection. *International Journal of Imaging Systems and Technology*, **26(4)**, 277-283.
- [41] **Diez, P. F., Mut, V., Laciari, E., Torres, A. and Avila, E.** (2009). Application of the empirical mode decomposition to the extraction of features from EEG signals for mental task classification. *Annual international conference of the IEEE engineering in medicine and biology society*, September, 2579-2582.
- [42] **Dingle, A. A., Jones, R. D., Carroll, G. J. and Fright, W. R.** (1993) A multistage system to detect epileptiform activity in the EEG. *IEEE*

Transactions on Biomedical Engineering, **40(12)**, 1260-1268.

- [43] **Djemili, R., Bourouba, H. and Korba, M. A.** (2016) Application of empirical mode decomposition and artificial neural network for the classification of normal and epileptic EEG signals. *Biocybernetics and Biomedical Engineering*, **36(1)**, 285-291.
- [44] **Dumermuth, G., Huber, P., Kleiner, B. and Gasser, T.** (1970) Numerical analysis of electroencephalographic data. *IEEE Transactions on Audio and Electroacoustics*, **18(4)**, 404-411.
- [45] **Duun-Henriksen, J., Kjaer, T. W., Madsen, R. E., Remvig, L. S., Thomsen, C. E. and Sorensen, H. B. D.** (2012) Channel selection for automatic seizure detection. *Clinical Neurophysiology*, **123(1)**, 84-92.
- [46] **Fatma, T., Farooq, O., Khan, Y. U., Tripathi, M. and Sharma, P.** (2016) Automatic detection of non-convulsive seizures: A reduced complexity approach. *Journal of King Saud University-Computer and Information Sciences*, **28(4)**, 407-415.
- [47] **Faust, O., Acharya, U. R., Adeli, H. and Adeli, A.** (2015) Wavelet-based EEG processing for computer-aided seizure detection and epilepsy diagnosis. *Seizure*, **26**, 56-64.
- [48] **Faust, O., Yu, W. and Kadri, N. A.** (2013) Computer-based identification of normal and alcoholic EEG signals using wavelet packets and energy measures. *Journal of Mechanics in Medicine and Biology*, **13(03)**, 1350033.
- [49] **Finotello, F., Scarpa, F. and Zanon, M.** (2015) EEG signal features extraction based on fractal dimension. *37th Annual International Conference of the IEEE Engineering in Medicine and Biology Society (EMBC)*, Milan, August, 4154-4157.
- [50] **Fu, K., Qu, J., Chai, Y. and Zou, T.** (2015) Hilbert marginal spectrum analysis for automatic seizure detection in EEG signals. *Biomedical Signal Processing and Control*, **18**, 179-185.

- [51] **Gao, R. X. and Yan, R.** *Wavelets: Theory and Applications for Manufacturing*. International Publishing, Berlin, 2010.
- [52] **Garrett, D. D., Samanez-Larkin, G. R., MacDonald, S. W., Lindenberger, U., McIntosh, A. R. and Grady, C. L.** (2013) Moment-to-moment brain signal variability: A next frontier in human brain mapping?. *Neuroscience & Biobehavioral Reviews*, **37(4)**, 610-624.
- [53] **Gevins, A. S., Yeager, C. L., Diamond, S. L., Spire, J., Zeitlin, G. M. and Gevins, A. H.** (1975) Automated analysis of the electrical activity of the human brain (EEG): A progress report. *Proceedings of the IEEE*, **63(10)**, 1382-1399.
- [54] **Gigola, S., Ortiz, F., D'attellis, C. E., Silva, W. and Kochen, S.** (2004) Prediction of epileptic seizures using accumulated energy in a multiresolution framework. *Journal of Neuroscience Methods*, **138(1)**, 107-111.
- [55] **Goldberger A. L., Amaral LAN, Glass L., Hausdorff J. M., Ivanov P. Ch., Mark R. G., Mietus J. E., Moody G. B., Peng C. K., Stanley H. E.** (2000) PhysioBank, PhysioToolkit, and PhysioNet: Components of a New Research Resource for Complex Physiologic Signals. *Circulation*, **101(23)**, e215-e220
- [56] **Gopan, K. G., Harsha, A., Joseph, L. A., and Kollialil, E. S.** (2013) Adaptive neuro-fuzzy classifier for 'Petit Mal'epilepsy detection using Mean Teager Energy. *International Conference on Advances in Computing, Communications and Informatics (ICACCI)*, Mysore, August, 752-757.
- [57] **Goshvarpour, A., Goshvarpour, A. and Shamsi, M.** (2014) Modeling Epileptic EEG Time Series by State Space Model and Kalman Filtering Algorithm. *International Journal of Intelligent Systems and Applications*, **6(3)**, 26.
- [58] **Grossmann, A., Kronland-Martinet, R. and Morlet, J.** Reading and

- Understanding Continuous Wavelet Transforms. pp. 2-20. In **Combes, J., M., Grossmann, A. and Tchamitchian, P.**, (eds) *Wavelets. Inverse Problems and Theoretical Imaging*. Springer International Publishing, Berlin, 1990.
- [59] **Güler, I. and Übeyli, E. D. (2005)** Adaptive neuro-fuzzy inference system for classification of EEG signals using wavelet coefficients. *Journal of Neuroscience Methods*, **148(2)**, 113-121.
- [60] **Hassan, A. R. and Subasi, A. (2016)** Automatic identification of epileptic seizures from EEG signals using linear programming boosting. *Computer Methods and Programs in Biomedicine*, **136**, 65-77.
- [61] **Hassanien, A. E., Moftah, H. M., Azar, A. T. and Shoman, M. (2014)** MRI breast cancer diagnosis hybrid approach using adaptive ant-based segmentation and multilayer perceptron neural networks classifier. *Applied Soft Computing*, **14**, 62-71.
- [62] **Hassanpour, H., Mesbah, M. and Boashash, B. (2003)** SVD-based newborn EEG seizure detection in the time-frequency domain. *IFAC Proceedings Volumes*, **36(15)**, 329-333.
- [63] **Huang, N. E., Shen, Z. and Long, S. R. (1999)** A new view of nonlinear water waves: the Hilbert spectrum. *Annual Review of Fluid Mechanics*, **31(1)**, 417-457.
- [64] **Huang, N. E., Shen, Z., Long, S. R., Wu, M. C., Shih, H. H., Zheng, Q., Yen, N., Tung, C.C. and Liu, H. H. (1998)** The empirical mode decomposition and the Hilbert spectrum for nonlinear and non-stationary time series analysis. *In Proceedings of the Royal Society of London A: Mathematical, Physical and Engineering Sciences*, **454(1971)**, 903-995. The Royal Society.
- [65] **Irie, J., Yamaguchi, T., Omori, K. and Inoue, K. (2010)** Feature extraction of visual evoked potentials using state-space model. *Proceedings of SICE Annual Conference 2010*, Taipei, August 54-57.

- [66] **Islam, M. K., Rastegarnia, A. and Yang, Z.** (2016). Methods for artifact detection and removal from scalp EEG: A review. *Neurophysiologie Clinique/Clinical Neurophysiology*, **46(4-5)**, 287-305.
- [67] **Isler, Y.** (2016) Discrimination of systolic and diastolic dysfunctions using multi-layer perceptron in heart rate variability analysis. *Computers in Biology and Medicine*, **76**, 113-119.
- [68] **Jaakko, M. and Robert, P.** *Bioelectromagnetism - Principles and Applications of Bioelectric and Biomagnetic Fields*, Oxford University Press, 1995
- [69] **Janati, A. B., ALGhasab, N. S., Alshammari, R. A., ALGhasab, A. S. and AL-Aslami, Y. F.** (2016) Sharp slow waves in the EEG. *The Neurodiagnostic Journal*, **56(2)**, 83-94.
- [70] **Jang, J. S.** (1993) ANFIS: adaptive-network-based fuzzy inference system. *IEEE Transactions on Systems, Man, and Cybernetics*, **23(3)**, 665-685.
- [71] **Jansen, B. H., Bourne, J. R. and Ward, J. W.** (1981) Autoregressive estimation of short segment spectra for computerized EEG analysis. *IEEE Transactions on Biomedical Engineering*, **9**, 630-638.
- [72] **Jasper, H. H.** *Jasper's Basic Mechanisms of the Epilepsies* (80) Oxford University Press, USA, 2012.
- [73] **Jia, J., Goparaju, B., Song, J., Zhang, R. and Westover, M. B.** (2017) Automated identification of epileptic seizures in EEG signals based on phase space representation and statistical features in the CEEMD domain. *Biomedical Signal Processing and Control*, **38**, 148-157.
- [74] **Jiang, X., Bian, G. B. and Tian, Z.** (2019). Removal of artifacts from EEG signals: a review. *Sensors*, **19(5)**, 987.
- [75] **Joshi, V., Pachori, R. B. and Vijesh, A.** (2014) Classification of ictal and seizure-free EEG signals using fractional linear

- prediction. *Biomedical Signal Processing and Control*, **9**, 1-5.
- [76] **Kaiser, J.F.** (1990). On a simple algorithm to calculate the 'energy' of a signal. *IEEE International Conference on in Acoustics, Speech, and Signal Processing*, New Mexico, 381-384.
- [77] **Kamath, C.** (2011) ECG beat classification using features extracted from Teager energy functions in time and frequency domains. *IET Signal processing*, **5(6)**, 575-581.
- [78] **Kannathal, N., Choo, M. L., Acharya, U. R. and Sadasivan, P. K.** (2005) Entropies for detection of epilepsy in EEG. *Computer Methods and Programs in Biomedicine*, **80(3)**, 187-194.
- [79] **Kasper, D., Fauci, A., Hauser, S., Longo, D., Jameson, J. and Loscalzo, J.** *Harrison's Principles of Internal Medicine*, 19e. USA, 2015.
- [80] **Khamis, H., Mohamed, A. and Simpson, S.** (2009) Seizure state detection of temporal lobe seizures by autoregressive spectral analysis of scalp EEG. *Clinical Neurophysiology*, **120(8)**, 1479-1488.
- [81] **Khan, Y. U. and Gotman, J.** (2003) Wavelet based automatic seizure detection in intracerebral electroencephalogram. *Clinical Neurophysiology*, **114(5)**, 898-908.
- [82] **Kıymık, M. K., Güler, I., Dizibüyük, A. and Akın, M.** (2005) Comparison of STFT and wavelet transform methods in determining epileptic seizure activity in EEG signals for real-time application. *Computers in Biology and Medicine*, **35(7)**, 603-616.
- [83] **Klein, F. F.** (1976) A waveform analyzer applied to the human EEG. *IEEE Transactions on Biomedical Engineering*, **3**, 246-252.
- [84] **Klem, G. H., Lüders, H. O., Jasper, H. H. and Elger, C.** (1999) The ten-twenty electrode system of the International Federation. *Electroencephalography and Clinical neurophysiology*, **52(3)**, 3-6.
- [85] **Krstacic, G., Krstacic, A., Martinis, M., Vargovic, E., Knezevic, A., Smalcelj, A., Jembrek-Gostovic, M., Gamberger, D., and Smuc, T.**

- (2002) Non-linear analysis of heart rate variability in patients with coronary heart disease. *Computers in Cardiology*, 673-675.
- [86] **Ktonas, P. Y., Luoh, W. M., Kejariwal, M. L., Reilly, E. L. and Seward, M. A.** (1981) Computer-aided quantification of EEG spike and sharp wave characteristics. *Electroencephalography and Clinical Neurophysiology*, **51(3)**, 237-243.
- [87] **Kumar, Y., Dewal, M. L. and Anand, R. S.** (2014) Epileptic seizure detection using DWT based fuzzy approximate entropy and support vector machine. *Neurocomputing*, **133**, 271-279.
- [88] **Lacey, T. (2019)** Tutorial: The kalman filter. *Georgia Institute of Technology*.
- [89] **Lachaux, J. P., Rudrauf, D. and Kahane, P.** (2003) Intracranial EEG and human brain mapping. *Journal of Physiology-Paris*, **97(4)**, 613-628.
- [90] **Lawhern, V., Hairston, W. D., McDowell, K., Westerfield, M. and Robbins, K.** (2012) Detection and classification of subject-generated artifacts in EEG signals using autoregressive models. *Journal of Neuroscience Methods*, **208(2)**, 181-189.
- [91] **Li, M., Chen, W. and Zhang, T.** (2017) Classification of epilepsy EEG signals using DWT-based envelope analysis and neural network ensemble. *Biomedical Signal Processing and Control*, **31**, 357-365.
- [92] **Li, X., Li, D., Liang, Z., Voss, L. J. and Sleight, J. W.** (2008) Analysis of depth of anesthesia with Hilbert–Huang spectral entropy. *Clinical Neurophysiology*, **119(11)**, 2465-2475.
- [93] **Li, S., Zhou, W., Yuan, Q., Geng, S. and Cai, D.** (2013) Feature extraction and recognition of ictal EEG using EMD and SVM. *Computers in Biology and Medicine*, **43(7)**, 807-816.
- [94] **Liang, S. F., Wang, H. C. and Chang, W. L.** (2010) Combination of EEG complexity and spectral analysis for epilepsy diagnosis and seizure detection. *EURASIP Journal on Advances in Signal*

Processing, **2010(1)**, 853434.

- [95] **Liu, D. and Pang, Z.** (2008) Epileptic seizures predicted by modified particle filters. *IEEE International Conference on Networking, Sensing and Control*, Sanya, April, 351-356.
- [96] **Liu, Y., Zhou, W., Yuan, Q. and Chen, S.** (2012) Automatic seizure detection using wavelet transform and SVM in long-term intracranial EEG. *IEEE Transactions on Neural Systems and Rehabilitation Engineering*, **20(6)**, 749-755.
- [97] **Mahapatra, A. G., and Horio, K.** (2018) Classification of ictal and interictal EEG using RMS frequency, dominant frequency, root mean instantaneous frequency square and their parameters ratio. *Biomedical Signal Processing and Control*, **44**, 168-180.
- [98] **Mallat, S. G.** (1989) A theory for multiresolution signal decomposition: the wavelet representation. *IEEE Transactions on Pattern Analysis and Machine Intelligence*, **11(7)**, 674-693.
- [99] **Martis, R. J., Acharya, U. R., Prasad, H., Chua, C. K., Lim, C. M. and Suri, J. S.** (2013) Application of higher order statistics for atrial arrhythmia classification. *Biomedical Signal Processing and Control*, **8(6)**, 888-900.
- [100] **Martis, R. J., Acharya, U. R., Tan, J. H., Petznick, A., Yanti, R., Chua, C. K., Ng, E. K. and Tong, L.** (2012) Application of empirical mode decomposition (EMD) for automated detection of epilepsy using EEG signals. *International Journal of Neural Systems*, **22(06)**, 1250027.
- [101] **Martis, R. J., Tan, J. H., Chua, C. K., Loon, T. C., YEO, S. W. J. and Tong, L.** (2015) Epileptic EEG classification using nonlinear parameters on different frequency bands. *Journal of Mechanics in Medicine and Biology*, **15(03)**, 1550040.
- [102] **Megiddo, I., Colson, A., Chisholm, D., Dua, T., Nandi, A. and Laxminarayan, R.** (2016) Health and economic benefits of public

- financing of epilepsy treatment in India: An agent-based simulation model. *Epilepsia*, **57(3)**, 464-474.
- [103] **Mertins, A.** *Signal Analysis: Wavelets, Filter Banks, Time-Frequency Transforms and Applications*, J. Wiley and sons, 1999.
- [104] **Møller, M. F.** (1993). A scaled conjugate gradient algorithm for fast supervised learning. *Neural Networks*, **6(4)**, 525-533.
- [105] **Mula, M. and Monaco, F.** (2011) Ictal and peri-ictal psychopathology. *Behavioural Neurology*, **24(1)**, 21-25.
- [106] **Musselman, M. and Djurdjanovic, D.** (2012) Time–frequency distributions in the classification of epilepsy from EEG signals. *Expert Systems with Applications*, **39(13)**, 11413-11422.
- [107] **Ocak, H.** (2009) Automatic detection of epileptic seizures in EEG using discrete wavelet transform and approximate entropy. *Expert Systems with Applications*, **36(2)**, 2027-2036.
- [108] **Oikonomou, V. P., Tzallas, A. T. and Fotiadis, D. I.** (2007) A Kalman filter based methodology for EEG spike enhancement. *Computer Methods and Programs in Biomedicine*, **85(2)**, 101-108.
- [109] **Orosco, L., Correa, A. G. and Leber, E. L.** (2011). Epileptic seizures detection based on empirical mode decomposition of EEG signals. *In Management of Epilepsy-Research, Results and Treatment*, IntechOpen, 1-20.
- [110] **Oweis, R. J. and Abdulhay, E. W.** (2011) Seizure classification in EEG signals utilizing Hilbert-Huang transform. *Biomedical Engineering Online*, **10(1)**, 38.
- [111] **Pachori, R. B., Sharma, R. and Patidar, S.** Classification of normal and epileptic seizure EEG signals based on empirical mode decomposition. pp. 367-388, In **Zhu Q. and Azar A.** (eds) *Complex System Modelling and Control Through Intelligent Soft Computations Studies in Fuzziness and Soft Computing*, **319**, Springer International Publishing, Berlin. 2015.

- [112] **Parvez, M. Z. and Paul, M.** (2014) Epileptic seizure detection by analyzing EEG signals using different transformation techniques. *Neurocomputing*, **145**, 190-200.
- [113] **Patnaik, L. M. and Manyam, O. K.** (2008) Epileptic EEG detection using neural networks and post-classification. *Computer methods and programs in biomedicine*, **91(2)**, 100-109.
- [114] **Picinbono, B.** (1997) On instantaneous amplitude and phase of signals. *IEEE Transactions on Signal Processing*, **45(3)**, 552-560.
- [115] **Polat, K. and Güneş, S.** (2007) Classification of epileptiform EEG using a hybrid system based on decision tree classifier and fast Fourier transform. *Applied Mathematics and Computation*, **187(2)**, 1017-1026.
- [116] **Qazi, K. I., Lam, H. K., Xiao, B., Ouyang, G. and Yin, X.** (2016) Classification of epilepsy using computational intelligence techniques. *CAAI Transactions on Intelligence Technology*, **1(2)**, 137-149.
- [117] **Rabbi, A. F., Azinfar, L. and Fazel-Rezai, R.** (2013) Seizure prediction using adaptive neuro-fuzzy inference system. *35th Annual International Conference of the IEEE Engineering in Medicine and Biology Society (EMBC)*, Osaka, July, 2100-2103.
- [118] **Raghu, S. and Sriraam, N.** (2017) Optimal configuration of multilayer perceptron neural network classifier for recognition of intracranial epileptic seizures. *Expert Systems With Applications*, **89**, 205-221.
- [119] **Rangaprakash, D.** (2014) Connectivity analysis of multichannel EEG signals using recurrence based phase synchronization technique. *Computers in Biology and Medicine*, **46**, 11-21.
- [120] **Redelico, F. O., Traversaro, F., García, M. D. C., Silva, W., Rosso, O. A. and Risk, M.** (2017) Classification of Normal and Pre-Ictal EEG Signals Using Permutation Entropies and a Generalized Linear Model as a Classifier. *Entropy*, **19(2)**, 72.
- [121] **Riaz, F., Hassan, A., Rehman, S., Niazi, I. K. and Dremstrup, K.**

- (2016) EMD-based temporal and spectral features for the classification of EEG signals using supervised learning. *IEEE Transactions on Neural Systems and Rehabilitation Engineering*, **24(1)**, 28-35.
- [122] **Rodríguez-Bermúdez, G., García-Laencina, P. J., Roca-González, J. and Roca-Dorda, J.** (2013) Efficient feature selection and linear discrimination of EEG signals. *Neurocomputing*, **115**, 161-165.
- [123] **Saidatul, A., Paulraj, M. P., Yaacob, S. and Yusnita, M. A.** (2011) Analysis of EEG signals during relaxation and mental stress condition using AR modeling techniques. *IEEE International Conference on Control System, Computing and Engineering*. Penang, Malaysia, November 477-481.
- [124] **Santhosh, N. S., Sinha, S. and Satishchandra, P.** (2014) Epilepsy: Indian perspective. *Annals of Indian Academy of Neurology*, **17(1)**, S3.
- [125] **Sengupta, A., Datta, S., Kar, S. and Routray, A.** (2014) Analysis of fatigue using EEG state-space analysis. *Annual IEEE India Conference (INDICON)*, Pune, December, 1-6.
- [126] **Sharanya, B., Murali, L. and Manigandan, T.** (2014) Adaptive filtering of EEG and epilepsy detection using Recurrence Quantification Analysis. *IEEE International Conference on Advanced Communications, Control and Computing Technologies*, Ramanathapuram, May, 1316-1320.
- [127] **Sharif, B. and Jafari, A. H.** (2017) Prediction of epileptic seizures from EEG using analysis of ictal rules on Poincaré plane. *Computer Methods and Programs in Biomedicine*, **145**, 11-22.
- [128] **Sharma, M., Pachori, R. B. and Acharya, U. R.** (2017) A new approach to characterize epileptic seizures using analytic time-frequency flexible wavelet transform and fractal dimension. *Pattern Recognition Letters*, **94**, 172–179.
- [129] **Sharma, R. and Pachori, R. B.** (2015) Classification of epileptic seizures in EEG signals based on phase space representation of

- intrinsic mode functions. *Expert Systems with Applications*, **42(3)**, 1106-1117.
- [130] **Sharmila, A. and Geethanjali, P.** (2016) DWT based detection of epileptic seizure from EEG signals using naive Bayes and k-NN classifiers. *IEEE Access*, **4**, 7716-7727.
- [131] **Shayegh, F., Sadri, S., Amirfattahi, R. and Ansari-Asl, K.** (2014) A model-based method for computation of correlation dimension, Lyapunov exponents and synchronization from depth-EEG signals. *Computer Methods and Programs in Biomedicine*, **113(1)**, 323-337.
- [132] **Siuly, S. and Li, Y.** (2015) Designing a robust feature extraction method based on optimum allocation and principal component analysis for epileptic EEG signal classification. *Computer Methods and Programs in Biomedicine*, **119(1)**, 29-42.
- [133] **Sonego, P., Kocsor, A. and Pongor, S.** (2008) ROC analysis: applications to the classification of biological sequences and 3D structures. *Briefings in bioinformatics*, **9(3)**, 198-209.
- [134] **Sood, M. and Bhooshan, S. V.** (2014) Modular based dynamic analysis of EEG signals using non-linear feature. *IEEE International Conference on Parallel, Distributed and Grid Computing*, Solan, December, 186-190.
- [135] **Subasi, A., Alkan, A., Koklukaya, E. and Kiymik, M. K.** (2005) Wavelet neural network classification of EEG signals by using AR model with MLE preprocessing. *Neural Networks*, **18(7)**, 985-997.
- [136] **Subha, D. P., Joseph, P. K., Acharya, R. and Lim, C. M.** (2010) EEG signal analysis: A survey. *Journal of Medical Systems*, **34(2)**, 195-212.
- [137] **Subramaniyam, N. P. and Hyttinen, J.** (2013) Analysis of nonlinear dynamics of healthy and epileptic eeg signals using recurrence based complex network approach. *6th International IEEE/EMBS Conference*

- on *Neural Engineering (NER)*, San Diego, CA, November, 605-608.
- [138] **Tawfik, N. S., Youssef, S. M. and Kholief, M.** (2016) A hybrid automated detection of epileptic seizures in EEG records. *Computers & Electrical Engineering*, **53**, 177-190.
- [139] **Teager, H.** (1980). Some observations on oral air flow during phonation. *IEEE Transactions on Acoustics, Speech, and Signal Processing*, **28(5)**, 599-601.
- [140] **Tu, J. V.** (1996) Advantages and disadvantages of using artificial neural networks versus logistic regression for predicting medical outcomes. *Journal of clinical epidemiology*, **49(11)**, 1225-1231.
- [141] **Tudor, M., Tudor, L. and Tudor, K. I.** (2005) Hans Berger (1873-1941) the history of electroencephalography. *Acta Medica Croatica: Casopis Hrvatske Akademije Medicinskih Znanosti*, **59(4)**, 307-313.
- [142] **Tzallas, A. T., Tsipouras, M. G. and Fotiadis, D. I.** (2009) Epileptic seizure detection in EEGs using time–frequency analysis. *IEEE Transactions on Information Technology in Biomedicine*, **13(5)**, 703-710.
- [143] **Tzallas, A. T., Tsipouras, M. G., Tsalikakis, D. G., Karvounis, E. C., Astrakas, L., Konitsiotis, S. and Tzaphlidou, M.** Automated epileptic seizure detection methods: a review study. pp. 75-98. In **Dejan, S., Ivana, T., and Tanja, N.**, (eds) *Epilepsy-Histological, Electroencephalographic and Psychological Aspects*. InTechOpen 2012.
- [144] **Übeyli, E. D.** (2010) Lyapunov exponents/probabilistic neural networks for analysis of EEG signals. *Expert Systems with Applications*, **37(2)**, 985-992.
- [145] **Übeyli, E. D., Cvetkovic, D., Holland, G. and Cosic, I.** (2010) Analysis of sleep EEG activity during hypopnoea episodes by least squares support vector machine employing AR coefficients. *Expert*

Systems with Applications, **37(6)**, 4463-4467.

- [146] **Upadhyay, R., Padhy, P. K. and Kankar, P. K.** (2016) A comparative study of feature ranking techniques for epileptic seizure detection using wavelet transform. *Computers & Electrical Engineering*, **53**, 163-176.
- [147] **Uthayakumar, R.** Fractal dimension in Epileptic EEG signal analysis. pp. 103-157. In **Abarbanel, H.D.I., Braha, D., Érdi, P., Friston, K.J., Haken, H., Jirsa, V., Kacprzyk, J., Kaneko, K., Kelso, S., Kirkilionis, M., Kurths, J., Menezes, R., Nowak, A., Qudrat-Ullah, H., Reichl, L., Schuster, P., Schweitzer, F., Sornette, D. and Thurner, S.** (eds.) *Applications of Chaos and Nonlinear Dynamics in Science and Engineering -Understanding Complex Systems Vol. 3.* Springer International Publishing, Berlin. 2013.
- [148] **Van Vugt, M. K., Sederberg, P. B. and Kahana, M. J.** (2007) Comparison of spectral analysis methods for characterizing brain oscillations. *Journal of Neuroscience Methods*, **162(1)**, 49-63.
- [149] **Van, S. K. J., Stel, V. S., Reitsma, J. B., Dekker, F. W., Zoccali, C. and Jager, K. J.** (2009) Diagnostic methods I: sensitivity, specificity, and other measures of accuracy. *Kidney international*, **75(12)**, 1257-1263.
- [150] **Vogl, T. P., Mangis, J. K., Rigler, A. K., Zink, W. T. and Alkon, D. L.** (1988) Accelerating the convergence of the back-propagation method. *Biological Cybernetics*, **59(4)**, 257-263.
- [151] **Walker, B. R. and Colledge, N. R.** *Davidson's Principles and Practice of Medicine E-Book.* Elsevier Health Sciences, 22e. Amsterdam, 2013.
- [152] **Wang, Y., Qi, Y., Zhu, J., Zhang, J., Wang, Y., Zheng, X. and Wu, Z.** (2015) A cauchy-based state-space model for seizure detection in eeg monitoring systems. *IEEE Intelligent Systems*, **30(1)**, 6-12.
- [153] **Yang, Z., Wang, Y. and Ouyang, G.** (2014) Adaptive neuro-fuzzy

- inference system for classification of background EEG signals from ESES patients and controls. *The Scientific World Journal*, **2014**,1-8.
- [154] **Yildiz, A., Akin, M., Poyraz, M. and Kirbas, G.** (2009) Application of adaptive neuro-fuzzy inference system for vigilance level estimation by using wavelet-entropy feature extraction. *Expert Systems with Applications*, **36(4)**, 7390-7399.
- [155] **Wong, K. F. K., Galka, A., Yamashita, O. and Ozaki, T.** (2006) Modelling non-stationary variance in EEG time series by state space GARCH model. *Computers in Biology and Medicine*, **36(12)**, 1327-1335.
- [156] **Xia, Y., Zhou, W., Li, C., Yuan, Q. and Geng, S.** (2015) Seizure detection approach using S-transform and singular value decomposition. *Epilepsy & Behavior*, **52**, 187-193.
- [157] **Xiong, Z., Ramchandran, K. and Orchard, M. T.** (1998) Wavelet packet image coding using space-frequency quantization. *IEEE Transactions on Image Processing*, **7(6)**, 892-898.
- [158] **Xue, L. Y. and Ritaccio, A. L.** (2006) Reflex seizures and reflex epilepsy. *American Journal of Electroneurodiagnostic Technology*, **46(1)**, 39-48.
- [159] **Yusaf, M., Nawaz, R. and Iqbal, J.** (2016) Robust seizure detection in EEG using 2D DWT of time-frequency distributions. *Electronics Letters*, **52(11)**, 902-903.
- [160] **Zamir, Z. R.** (2016) Detection of epileptic seizure in EEG signals using linear least squares preprocessing. *Computer Methods and Programs in Biomedicine*, **133**, 95-109.
- [161] **Zandi, A. S., Javidan, M., Dumont, G. A. and Tafreshi, R.** (2010) Automated real-time epileptic seizure detection in scalp EEG recordings using an algorithm based on wavelet packet transform. *IEEE Transactions on Biomedical Engineering*, **57(7)**, 1639-1651.

- [162] **Zappasodi, F., Olejarczyk, E., Marzetti, L., Assenza, G., Pizzella, V. and Tecchio, F.** (2014) Fractal dimension of EEG activity senses neuronal impairment in acute stroke. *PLoS One*, **9(6)**, e100199.
- [163] **Zhang, T., Chen, W. and Li, M.** (2017) AR based quadratic feature extraction in the VMD domain for the automated seizure detection of EEG using random forest classifier. *Biomedical Signal Processing and Control*, **31**, 550-559.
- [164] **Zhang, Y., Guo, Z., Wang, W., He, S., Lee, T. and Loew, M.** (2003) A comparison of the wavelet and short-time Fourier transforms for Doppler spectral analysis. *Medical Engineering & Physics*, **25(7)**, 547-557.
- [165] **“CHB-MIT Scalp EEG database”**, (2014) [online]. Available: <https://www.physionet.org/pn6/chbmit/> [accessed: 1-Aug-2014]
- [166] **“EEG Time series data”** (2015) [Online]. Available: http://epileptologie-bonn.de/cms/front_content.php?idcat=193&lang=3. [accessed: 10-Jun-2015]
- [167] **“WHO-media centre on Epilepsy”** (2012) [Online]. Available: <http://www.who.int/mediacentre/factsheets/fs999/en/>. [accessed: 08-Sep-2012].

LIST OF PUBLICATIONS BASED ON THESIS

Refereed Journals

1. **Biju, K. S., Hakkim, H. A. and Jibukumar, M. G.** (2017) Ictal EEG classification based on amplitude and frequency contours of IMFs. *Biocybernetics and Biomedical Engineering*, **37(1)**, 272-283, ISSN 0208-5216. (Impact factor 2.159)
2. **Biju, K. S. and Jibukumar, M. G.** (2018) Classification of Ictal EEG Using modeling based spectral and temporal features on Instantaneous Amplitude–Frequency Components of IMFs. *Biomedical Engineering: Applications, Basis and Communications*, **30(6)**, 18500421-11, ISSN1016-2372. (Indexed in ESCI)

Book Chapter

3. **Biju, K. S., Jibukumar, M. G. and Rajasekharan, C.** EEG analysis using wavelet packet transforms on mean energy and mean Teager energy with artificial neuro-fuzzy system. pp. 627-635. In **Aloui, F. and Dincer, I.** (eds.) *Exergy for A Better Environment and Improved Sustainability 2. Green Energy and Technology*. Springer, Cham. 2018. ISBN 978-3-319-62574-4. (Proceeding of 7th International Exergy, Energy and Environment Symposium, University of Valenciennes, France, May, 2015). (Scopus)

International Conference

4. **Biju, K. S. and Jibukumar, M. G.** (2017) Ictal EEG Classification based on State Space Modeling of Intrinsic Mode Function. *Proceeding of 6th International Conference on Smart Computing and Communications*, NIT Kurukshetra, India. December, 2018. (Published in Elsevier Procedia Computer Science-**125 (2018)**: 468-475. ISSN 1877

CURRICULUM VITAE

1. **Name** : BIJU K. S.
2. **Date of Birth** : 14-08-1971
3. **Gender** : Male
4. **Name of Father** : G. Sivathanu

Educational Qualification :

1993 Bachelor of Technology. (B. Tech.)

- Institution : College of Engineering Thiruvananthapuram.
Branch : Applied Electronics and Instrumentation Engg.

1998 Master of Technology (M. Tech.)

- Institution : College of Engineering Thiruvananthapuram.
Branch : Electronics and Communication Engg.
Specialization : Applied Electronics and Instrumentation

Doctor of Philosophy (Ph. D)

- Institution : Cochin University of Science & Technology
Registration date : 28.11.2011 (Part-time)

